Development of Laser Doping at Room Temperature for Crystalline Silicon Solar Cell Fabrication Process

（結晶シリコン太陽電池作製プロセスに向けた室温レーザードーピングの開発）

Kenji Hirata

平田　憲司

March 2012

Graduate School of Materials Science

Nara Institute of Science and Technology

Acknowledgements

This work has been done at the Microelectronic Device Science Laboratory, Graduate School of Materials Science, Nara Institute of Science and Technology (NAIST), under the direction of Professor Takashi Fuyuki. This study was partially supported by New Energy and Industrial Technology Development Organization (NEDO) as part of the Ultimate Crystalline Silicon Solar Cells R&D Program.

The author would like to express his deepest appreciation and gratitude to Professor Takashi Fuyuki for his kind advices, continuous supporting, valuable suggestions and encouragements to this study as well as critical reading of this thesis. He is also grateful to his supervisors at NAIST; Professor Hiroshi Daimon, Professor Yukiharu Uraoka, and Associate Professor Teruki Sugiyama, for their valuable discussions and critical comments for this thesis.

The author sincerely acknowledges to Dr. Pere Roca i Cabarrocas and Dr. Erik Johnson at Laboratory of Physics of Interfaces and Thin Films (LPICM), Ecole Polytechnique for his international supervision, the collaboration work and giving the chance of oversea study to the author at LPICM. The author also acknowledges to Dr. Samir Kasouit at Total Gas & Power, for teaching the deposition technique of micro crystalline silicon with ATOS, fruitful discussion and giving the mind of engineer. The author would like to acknowledge to Dr. Linwei Yu, Mr. Benedict O’Donnell, Mr. Jinyoun Cho, Mr. Alfonso Torres, Dr. Laurent Kroely, Dr. Pavel Bulkin, Dr. Martin Labrune, Mr. Ka-Hyun Kim, and all members in LPICM, for the acceptance and guidance for author’s stay with useful discussions.

The author is grateful to Associate Professor Yasuaki Ishikawa at NAIST, Associate

Professor Kensuke Nishioka at Miyazaki University, Associate Professor Takashi Minemoto at Ritsumeikan University, Dr. Keisuke Ohdaira at Japan Advanced Institute of Science and Technology, Dr. Dhamrin Marwan and Mr. Shuhei Yoshiba at Tokyo University of Agriculture and Technology, for their fruitful advices and discussions.

The author wishes to thank to Dr. Tomohiro Machida and Mr. Hidenori Yashiki at SHARP Coporation, Dr. Makoto Tanaka, Dr. Eiji Maruyama, Dr. Mikio Taguchi, Mr. Hitoshi Sakata, and Mr. Takashi Nakashima at Panasonic Corporation (SANYO Electronic Co., Ltd.), and Mr. Mitsuo Saitoh and Dr. Hisao Nagai at Panasonic Corporation, for useful discussions.

The author is indebted to the staffs and researchers in Microelectronic Device Science Laboratory; Dr. Tomoaki Hatayama, Dr. Hiroshi Yano, Dr. Atsushi Miura, Ms. Ayumi Tani, Ms. Yuko Tanaka, Ms. Kumi Hora, Ms. Masami Tsuji, and Ms. Kaori Araki, for their experimental and clerical helps, useful advices and heartfelt encouragements.

The author sincerely acknowledges to those who belonged or belongs to PV group in the Microelectronic Device Science Laboratory; Dr. Yu Takahashi (now at SHARP Corporation), Dr. Akiyoshi Ogane (now at Panasonic Corporation), Ms. Yuki Kishiyama (now at Daihatsu Motor Co., Ltd.), Mr. Koyo Horiuchi (now at Panasonic Corporation), Mr. Takashi Saitoh (now at Babcock-Hitachi K.K.), Mr. Masakazu Nakatani (now at Clean Venture 21 Corporation), Mr. Tomohiro Funatani (now at Panasonic Corporation), Mr. Mitsuhiro Hasegawa (now at DENSO), Mr. Tamaki Takayama (now at Fujikura Ltd.), Mr. Shinichiro Tsujii (now at Panasonic Corporation), Ms. Emi Sugimura, Mr. Hideki Nishimura, Mr. Takuya Katagiri, Mr. Sohichiro Takamoto, Mr. Shota Morisaki, Mr. Shigeaki Tanaka, Mr. Shingo Yumoto, for their valuable discussions, continuous encouragements, kind helps and excellent time of working together. The author also wishes to thank to Dr. Athapol Kitiyanan, the Ph. D. researcher in PV group, Dr. Marie Buffière, the internship from Universite de

Poitiers (now at IMEC) for having useful discussions and good days.

The author would like to thank to Dr. Kazunori Ichikawa (now at Kobe City College of Technology), Dr. Yuta Sugawara (now at Panasonic), Dr. Yoshinori Iwasaki (now at ROHM CO., Ltd.), Dr. Dai Okamoto (now at AIST), and all other members in Microelectronic Device Science Laboratory for sharing good time of research work. In particular, the author would like to thank to his friends, Mr. Hidenori Koketsu at Microelectronic Device Science Laboratory, Mr. Kouske Ohara, Mr. Yosuke Ohara, and Ms. Mami Fujii at Information Device Science Laboratory, Mr. Keiichi Ikeda at Synthetic Organic Chemistry Laboratory, Ms. Hisako Nakagawa at Laboratory for Photonic Molecular Science, Ms. Mami Segawa at Theoretical Condensed Matter Physics Laboratory, and Mr. Arata Nakajima at Photonic Device Science Laboratory for sharing good time of research work and daily life.

The author is grateful to President Jun Kyokane at Akashi National College of Technology for his understanding, supporting and heartfelt encouragement.

The author would like to extend his great appreciation to his father, Professor Yoshinori Hirata at Osaka University for the valuable discussions, advices and teaching the mind of Ph D.

Finally, the author really thanks his parents and his brother for their understanding, continuous support and heartfelt encouragement.

March, 2012

Kenji Hirata

Abstract

The purpose of this thesis is the development of laser doping (LD) technique at room temperature for crystalline silicon (c-Si) solar cell fabrication process and realizing a fabrication of high-conversion-efficiency c-Si solar cells. In order to achieve this purpose, firstly, the mechanism of LD technique is revealed by investigation of doping profile on a variety of laser irradiation conditions, and a relationship between dopant film and laser irradiation. Secondly, LD technique is applied to a pn junction formation at room temperature as an alternative to conventional thermal diffusion in the c-Si solar cell fabrication process. Finally, in order to realize the fabrication of low-cost and high-conversion-efficiency c-Si solar cells, LD technique is applied to a selective emitter formation at room temperature without any treatments.

In Chapter 2, in order to reveal the mechanism of LD, a dependency of laser irradiation condition for the doping profile was investigated in detail. It was found out that the laser irradiation conditions influenced to not only the doping profile, but also the surface appearance after laser irradiation. The doping depth was able to control depending on laser output power, focus condition and scanning speed. Furthermore, LD mechanism was discussed to reveal the principle of LD. From a point of view of a doping layer formation, LD is very fast compared with conventional thermal diffusion, since the diffusivity in liquid

silicon is up to 10 orders of magnitude greater than that in solid silicon.

In Chapter 3, phosphorous silicate glass (PSG) film as a dopant precursor of LD was investigated for optimization of LD. In particular, the investigation was focused on reflectance of PSG film. A new method using the sputtering for the formation of PSG film was proposed. A calculation of reflectance of PSG film at the used laser wavelength indicated that the reflectance of PSG film depends on PSG film thickness. The reflectance of PSG film formed by sputtering method agreed well with calculations in the margin of error within 1.5 %. This indicated that various reflectance of PSG film can be formed and controlled by the sputtering method. The results indicated that the doping profiles strongly depended on the reflectance of PSG film.

In Chapter 4, LD was applied to the fabrication of c-Si solar cells at room temperature and in air ambience. The conditions of laser irradiation in LD were optimized for the c-Si solar cell emitters. The obtained results demonstrated that c-Si solar cells fabricated by LD in condition of optimum laser irradiation gave relatively similar photovoltaic properties to one fabricated by the conventional method. Furthermore, the results of internal quantum efficiency (IQE) indicated that laser-doped c-Si solar cells formed deeper pn junction than that of thermal diffused. Finally, electroluminescence (EL) revealed that laser-doped c-Si solar cells emitted the inhomogeneous EL in 2 dimensions. The efficiency of laser-doped c-Si solar cells deposited with SiN_x film as antireflective coating (ARC) eventually resulted in 7.3 %.

In Chapter 5, LD applied to form and optimize the selective emitter. It was confirmed that a selective emitter formed by LD at room temperature and in air ambient was realized to fabricate the high-conversion-efficiency of c-Si solar cells. Furthermore, it was found that the laser-doped emitter gave the improvement of the series resistance, eventually F.F. improved up to 1%. Obtained results showed the potential of LD at room temperature for fabricating low-cost and high-conversion-efficiency c-Si solar cells.

Contents

Chapter 1

Introduction

1.1 Background

A vital energy source of human life is fossil fuels. The most of fossil fuels, in particular, oils are important for human life such as power generator, plant, transportation, and so on. However, the oils have issues for human life and the earth. One of the issues is a shortage of resources. A research team predicted this issue to be lost completely until 2048.1) Anther of the issues is gases such as CO_2, NO_x, and/or SO_x exhausted by the fire of fossil fuels. These gases cause the acid rain, air pollution, and climate change. In order to prevent these issues, energy sources without fossil fuels has been developing and already established.

The most important thing for human life is electric power. In order to un-use fossil fuels, nuclear plant has been developing and established in Japan as an alternative of coal and/or oil fired plant. The nuclear plant is the highest conversion efficiency of the electric power generation, no air pollution, and the cheapest electric power generation than the others.2) However, on March 11th 2011 in Japan, the earthquake and tsunami hit. The Fukushima Daiich nuclear plant which is one of the big nuclear plants in Japan was hit, and damaged by this disaster. Finally, the radioactivity is exhausted to the atmosphere. This is still exhausting around Fukushima Daiichi nuclear plant now. In addition, the radioactive waste treatment has issues for the future of human life in Japan. People on the earth are praying "Never Fukushima", and thus the new energy sources are more and more required.

As new energy sources, fuel cell, wind, and solar cells are greatly expected for the solutions to the above problems. In particular, solar cells are much strongly expected. The solar cells can convert sunlight to electric power directly by the photoelectric effect, without any pollution including radioactivity to the earth environment. In addition, sunlight is a virtually unlimited energy resource about 1.8×10^{14} kW. Thus, the solar cells are the most important energy resource for human life.

Recently, solar cell production and installation has been exponentially increasing all over the world. The total production of solar cells exceeded 20 GW in 2010 as shown in Fig. 1.1.3) This growth can be predicted to continue more, and the production of solar cells would exceed 1,000 GW by 2020.* Actually, the nuclear plant can generate electric power within 1 GW. The nuclear plant in the world sets 432 plants, and the sum of their capacity of generation is about 39 GW.4) Thus, solar cells have a potential of the next primary power generation. However, in spite of such growth in recent, the power generating cost is higher than that of other conventional electric power generators as shown in Table 1.1.2) The cost of generation in solar cells is 46 yen/kWh. To become the primary power generation as an alternative to conventional electric power generators, it should be reduction to under 7

*Predicted by eye guide line shown in Fig.1.1.

yen/kWh by 2050, which was raised in “PV Roadmap 2030$^+$ (PV2030$^+$)” by New Energy and Industrial Development Organization (NEDO).5) In order to reduce the cost of generation of solar cells, the technological developments are necessary.

1.2 Laser Processing for Crystalline Silicon Solar Cells

The solar cells have been researching and developing using much kind of materials. In the production level, the main solar cells over 80 % in the ratio of all solar cells consist of wafer-based mono- or multi-crystalline silicon (c-Si) as shown in Fig. 1.2.3) Because, this base material, namely silicon is abundant materials available on the earth.6) Moreover, wafer based c-Si solar cells has a long history of development that the first experiment of wafer-based c-Si solar cells was reported by D. M. Chapin et al. in 1954.7) As being a long history of development over 60 years, the solar cells based on c-Si should be also the primary solar cells in production in the future. However, they mainly suffer from the high material cost of c-Si, which is in the range of 60 % of total solar cell cost. The remaining 40 % are dominated by fabrication process, especially diffusion to form a pn junction, etching, and edge isolation process.8) In order to reduce total solar cell cost, it is necessary to be the reduction of c-Si wafer-thickness and develop the fabrication process. From the point of view in the reduction of c-Si wafer-thickness, a thin c-Si wafer (< 100 μm) is achieved. However, recent technologies in c-Si solar cell fabrication process are unsuitable for such a thin wafer. The fabrication of c-Si solar cells usually needs metallization, lithography with wet chemical etching and high temperature annealing in furnaces processes. If their processes apply to thinner c-Si wafer, it cannot stand the mechanical or thermal stress, resulting in deterioration of fabrication yield. Thus, the establishment of new processes suitable for thinner silicon solar cell is necessary. Laser processing is one alternative to the conventional c-Si solar cell process because it can be performed at room temperature in air ambient and form a selective structure easily. Several techniques using laser such as Laser Fired Contact9), Laser Texturing10), Laser Grooved Buried Contact11), Laser Drilling12), and dielectric layer removal13) have been proposed and developed. In addition, an essential structure in solar cell, namely pn junction is formed by conventional thermal diffusion which uses temperature in the range of 900°C. Therefore, this processing step is one of the most costly ones during the entire c-Si solar cell fabrication.8) Replacement of diffusion method using a laser for pn junction formation could reduce the process cost in principle. Laser doping (LD) technique is the promising laser process in fabrication of c-Si solar cells. To clarify these lasers process applying to c-Si solar cell, Fig.1.3 was illustrated.

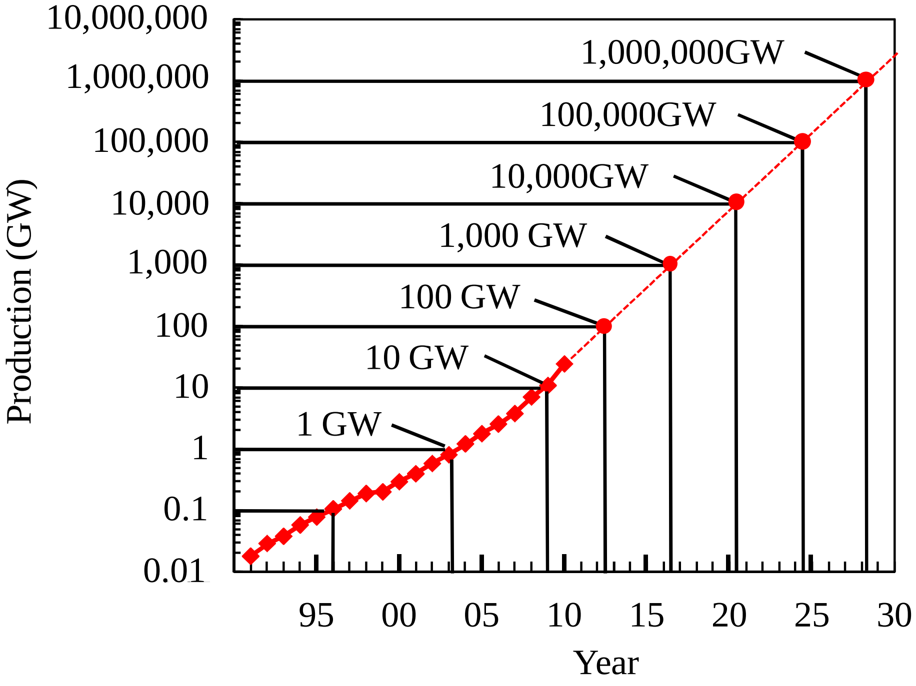

Figure 1.1: Annual production of solar cells in the world.[3)]

Table 1.1: Power generation cost of different energy source.[2)]

Energy source	Power generation cost (yen/kWh)
Oil	10.0 ~ 17.3
Coal	5.0 ~ 6.5
LNG	5.8 ~ 7.1
Water	8.2 ~ 13.3
Nuclear	4.8 ~ 6.2
Solar	46
Wind	10 ~ 14

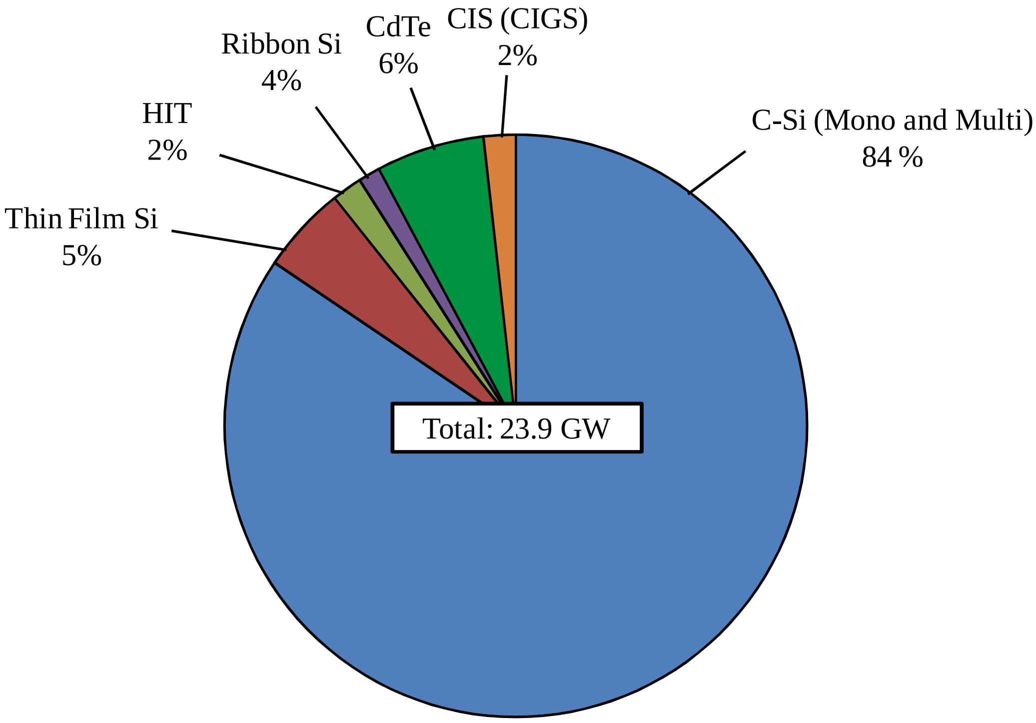

Figure 1.2: The annual production ratio of solar cell.3)

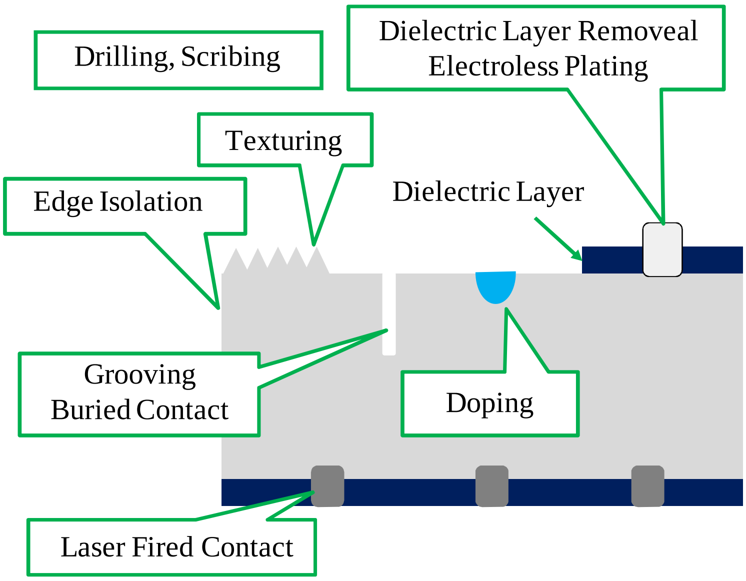

Figure 1.3: Application of laser processing to c-Si solar cell structure/fabrication process.

1.3 Laser Doping Technique for Crystalline Silicon Solar Cells

LD technique was developed by J. M. Fairfield and G. H. Schwuttke who were the first to form a doping layer with a laser in 1968.14) And then, LD technique has been widely studied with a wide variety of dopant sources to create a pn junction such as dopant gas atmosphere15), liquid dopant16), deposited dopant17), discharge implantation and excimer laser annealing18, 19). Although such LD techniques for the formation of a doping layer in gate metal oxide transistors (MOS) or solar cells had been studied and developed for a long time, they have not been applied into semiconductor device fabrication process due to the high cost of laser source, low stability of laser beam quality, and large size of laser equipment. Therefore, they are not suitable for low-cost processing of such semiconductor devices. Moreover, many defects were created by laser irradiation in silicon.

By recent progresses, the laser sources have developed dramatically for a low-cost and high stability of laser beam quality. One of the laser sources, diode pumped solid state (DPSS) laser achieved low-cost, high stability of laser beam quality, and minimization of laser source. In addition, this laser can irradiate high intensity of power. Therefore, the LD technique returned to attract much attention as an alternative for low-cost processing of semiconductors, in particular c-Si solar cells, to conventional doping layer formation.

1.4 Purpose and Outline of This Thesis

Recently, c-Si solar cells require not only cost reduction but also high conversion efficiency. In order to realize these requirements, the LD technique is an attractive method as an alternative to conventional doping layer formation, namely thermal diffusion. Because it can be performed at room temperature in air ambient and form a selective structure easily without any lithography steps. A selective area doping for the selective emitter in c-Si solar cells is very important for increasing conversion efficiency η.20) Typical processes for selective emitter require extra diffusion in the furnace and photolithography.21) C-Si solar cells require many treatments at these process steps; for example, diffusion barrier, wafer cleaning, and thermal diffusion. C-Si solar cells are subjected to stress at each process step. These steps are time-consuming and result in additional costs. Instead of the conventional selective area doping, LD technique is more attractive as an alternative. Thus, this is a simple and easy method for fabrication of low-cost and high-conversion-efficiency c-Si solar cells. In addition, these advantages can improve the fabrication yield, especially in the case of silicon substrates of less than 100 μm thickness, which leads to low-cost and high-conversion-efficiency c-Si solar cells.

The purpose of this thesis is the development of LD technique at room temperature for c-Si solar cell fabrication process and realizing the fabrication of high-conversion-efficiency c-Si solar cells. The formation of dopant source in this thesis is performed by spin coating. This method can form a dopant source easily using dopant contained liquid. Moreover, a solid state dopant source can be obtained at quite low temperature around 150 ºC.

In this thesis, firstly, the principle of LD technique is discussed by investigation of doping profile on a variety of laser irradiation conditions and relationship between dopant film and laser irradiation. Secondly, LD technique is applied to a pn junction formation at room temperature as an alternative to conventional thermal diffusion in c-Si solar cell fabrication process. Finally, in order to realize the fabrication of low-cost and high-conversion-efficiency c-Si solar cells, LD technique is applied to a selective emitter formation at room temperature without any treatments. This thesis is consisted of 6 chapters as below.

In Chapter 1, the introduction of this research is described about the background, purpose and contents.

In Chapter 2, the fundamental principle of LD is discussed by investigation of doping profile with vary conditions of laser irradiation. In conditions of laser irradiation, three parameters are chosen. Furthermore, the dependence of doping profile and surface appearance change on vary conditions of laser irradiation are investigated and discussed to reveal the LD mechanisms.

In Chapter 3, the further investigation of LD is carried out to reveal the relationship between dopant film and LD. A new technique of dopant film formation is introduced in this chapter. The influence of dopant film to the doping profile in LD is revealed and discussed.

In Chapter 4, LD technique is applied to a pn junction formation at room temperature as an alternative to conventional thermal diffusion in c-Si solar cell fabrication process. The LD for the fabrication of c-Si solar cells is optimized in this chapter. Furthermore, the LD with optimum conditions of laser irradiation applying to the formation of pn junctions and fabrication of c-Si solar cells is characterized for electrical properties. Obtained characteristics are suggested to the realization of high-conversion-efficiency c-Si solar cells.

In Chapter 5, the LD technique is applied to selective emitter formation for realization of high-conversion-efficiency c-Si solar cells. The selective emitter is formed at room temperature into furnace diffused emitter. The selective emitter formed by LD is optimized and discussed about correlation between emitter and selective emitter. Furthermore, c-Si solar cells with selective emitter are fabricated only by LD at room temperature. This chapter reveals feasibility for the fabrication of high-conversion-efficiency c-Si solar cells.

In Chapter 6, conclusions of this research are summarized. Outlooks of this research are also described.

References of Chapter 1.

1) N. Malyshkina, and D. Niemeier: Environ. Sci. Technol. (2010) 44 9134.

2) Agency for Natural Resources and Energy: “White book of Energy 2008” (2008) (in Japanese)

3) RTS Corporation: “*Information of Solar Power Generation, Inter- and intra-national current about solar power generation*”, Vol.21, No.5, (2011) p.4 (in Japanese)

4) Japan Atomic Industrial Forum Inc.: “JAIF Press Release 2010” (2010), http://www.jaif.or.jp/ (in Japanese)

5) New Energy and Industrial Development Organization (NEDO): “Roadmap of PV 2030$^+$” (2009), http://www.nedo.go.jp/index.html (in Japanese)

6) V. Petrova-Koch, R. Hezel, and A. Goetzberger: *High-Efficient Low-Cost Photovoltaics Recent Developments* (Springer, Berlin, 2009), p. 46.

7) D. M. Chapin, S. Fuller, and G. L. Pearson: J. Appl. Phys. **25** (1954) 676.

8) R. Preu, R. Lüdemann, G. Emanuel, W. Wettling, W. Eversheim, G. Güthenke, D. United, and G. Schweizer: Proc. of 16th European Photovoltaic Solar Energy Conf., 2000, p.1451.

9) E. Schneiderlöchner, R. Preu, R. Lüdemann, and S. W. Glunz: Prog. Photovoltaics: Res Appl., **10** (2002) 29.

10) J. Rentsch , F. Bamberg, E. Schneiderlöchner, and R. Preu: Proc. of 20th European Photovoltaic Solar Energy Conf., 2005, p.1321.

11) T. M. Bruton, N. B. Mason, S. Roberts, O. Nast-Hartley, S. Gledhill, J. Fernandez, R. Russell, G. Willeke, W. Warta, S. W. Glunz, and O. Schultz: Proc. of 3rd World Conf. on Photovoltaic Energy Conversion, 2003, p.899.

12) N. Mingirulli, A. Grohe, A. Dohrn, M. Hofmann, M. Schubert, T. Roth, D. Biro, and R. Preu: Proc. of 22nd European Photovoltaic Solar Energy Conf., 2007, p.1415.

13) P. Engelhart, S. Hermann, T. Neubert, H. Plagwitz, R. Grischke, R. Meyer, U. Klug, A, Schoonderbeek, U. Stute, R. Brendel: Prog. Photovoltaics: Res. Appl.,**15** (2007) 521.

14) J. Fairfield, and G.H. Schwuttke: Solid State Electronics **11** (1968) 1175.

15) G.B. Turner, D. Tarrant, G. Pollock, R. Pressley, R. Press: Appl. Phys. Lett. **39** (1981) 967.

16) R. Stuck, E. Fogarassy, J.C. Muller, M. Hodeau, A. Wattiaux, and P. Siffert: Appl. Phys. Lett. **38** (1981) 715.

17) E. Fogarassy, R. Stuck, J. J. Grob, and P. Siffert: J. Appl. Phys. **52** (1981) 1076.

18) R. T. Young, G. A. van der Leeden, R. L. Sandstrom, R. F. Wood, and R. D. Westbrook: Appl. Phys. Lett. **43** (1983) 666.

19) T. Sameshima, S. Usui, and M. Sekiya: J. Appl. Phys. **62** (1987) 711

20) J. Szlufcik, S. Sivoththaman, J. Nijs, R. P. Mertens, and R. Van Overstraeten: in *Practical Handbook of Photovoltaics: Fundamentals and Applications*, ed. T. Markvart and L. Castañer (Elsevier, Oxford, 2003), p. 137.

21) A. W. Blakers, A. Wang, A. M. Milne, J. Zhao, and M. A. Green: Appl. Phys. Lett. **55**

(1989) 1363.

Chapter 2

Principle of Laser Doping

2.1 Introduction

C-Si solar cells need a doping layer, namely pn junction, to generate electric power. A usual method for formation of pn junction in c-Si solar cells is a thermal diffusion.$^{1)}$ The conventional thermal diffusion in c-Si solar cell fabrication process achieves an impurity doping at a high temperature around 900 ºC, in N_2 ambience to avoid the other impurity diffusion which reduces device performance.$^{2)}$ However, the conventional method is unsuitable for low-cost processing of c-Si solar cells, especially in the case of silicon substrates of less than 100 µm thickness. This is because silicon substrates are subject to stress induced by high temperature. LD is an alternative to the conventional c-Si solar cell fabrication process because it can be operated at room temperature and in air ambience.

In this chapter, the doping profile, which is doped by LD at room temperature and in air ambience, is investigated to reveal the principle of LD. The conditions of laser irradiation for investigation of LD are determined by controllable parameter in the laser system. Moreover, surface morphology after laser irradiation is investigated to reveal a dependence on the conditions of laser irradiation. Obtained results in this chapter are very important in order to apply LD to the silicon solar cell fabrication process, also optimize LD for the fabrication of c-Si solar cells.

2.2 System for Laser Doping Experiments

Fig. 2.1 illustrated photograph of the laser system used in this research. This system consists of $Nd^{3+}:YVO_4$ Continuous Wave (CW) laser with 532 nm wavelength (Coherent, Verdi/V-5), mechanical shutter, reflective mirrors, collective lens (Nicon, CF Plan, 5×/0.35, Work Distance: 20.5 mm), x-y stage for scanning of samples, x-y stage controller unit (SHOT T-202, SIGMA KOKI), shutter controller (Model F116, SURUGA SEIKI) and personal computer for controlling of x-y stage automatically. The laser spot shape and distribution are circle and Gaussian (TEM_{00}-mode), respectively.3)

2.3 Experiment of Laser Doping

As the silicon substrates, 0.1-2 Ωcm 300-µm-thick, p-type, Czochrralski (Cz), (100)-oriented substrate was used. The 2 inch silicon wafer was cut into $1.0 \times 1.0\ \mathrm{cm}^2$ size and RCA cleaning was performed to clean the samples. The RCA cleaning procedure is summarized in Table 2.1. After RCA cleaning, the dopant contained liquid (Tokyo Ohka

Kogyo co.,ltd, OCD T-1) was spin-coated onto the polished surface using spin-coater (KYOWARIKEN.inc, K-359 S-1). The phosphorus contained liquid was used to form n^+ doped layer in p-type substrates. They were subsequently dried on a hotplate at 100°C for 15 min to obtain the solid phase precursor film, namely phosphorus silicate glass (PSG) film. Then, the laser was irradiated on the full-surface area of the PSG film coated sample at room temperature and in air ambience to form a doping layer as shown in Fig. 2.2. Doped area was accomplished by moving the stage on which a sample was mounted during laser irradiation; a xy-translation stage moved in x-direction from edge to edge of the sample then shifted in y-direction and this cycle was repeated in whole sample surface. The laser spot diameter on the sample surface and the stage shifted pitch were approximately 6.0 µm at the focal point of the collective lens and 6.0 µm, respectively. The spot diameter was determined by using the following equations.$^{4)}$

$$r_0{}^2 = \frac{\left\{\frac{r^2 \times f^2}{Zr^2}\right\}}{\left\{1+\left(\frac{f}{Zr}\right)^2\right\}} \tag{2.1}$$

$$Zr = \frac{\pi \times r^2 \times n}{M2 \times \lambda} \tag{2.2}$$

M2 is the value of M^2, *f* is the focal point distance of lens, *n* is the refractive index, *r* is the initial beam diameter of laser head. In the case of this laser system, these parameters are as followings.⁵⁾

$$M2 = 1.1\ (M^2)$$

$$f = 20.5\ \mathrm{mm}$$

$$n \approx 1\ \text{(in air)}$$

$$r = 2.25\ \mathrm{mm}$$

The calculated spot diameter on the sample surface is approximately 6.0 μm (Gaussian distribution at $\frac{1}{e^2}$).

For the investigation of doping concentration and depth, the secondary ion mass spectrometry (SIMS, Physical Electronics, ADEPT 1010 Quadrupole SIMS) measurement was performed. The concentration and depth profiles in SIMS data was calculated to change the value from mass counts (data obtained at SIMS measurement) to concentration by reference sample which has been measured for the amount of dose impurity in silicon material and to change the value from time (data obtained at SIMS measurement) to the depth by etching rate, respectively. The etching rate of SIMS was measured by uneven measurement.

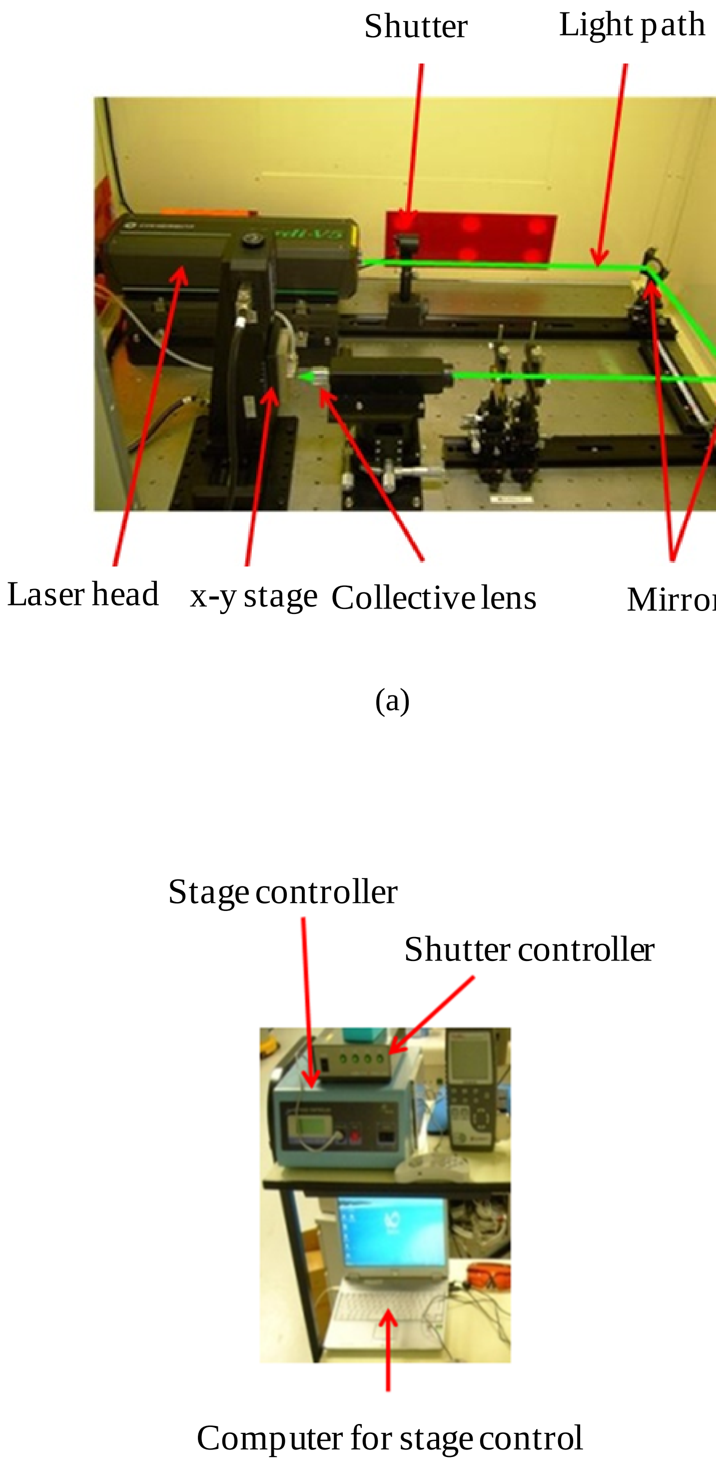

(a)

(b)

Figure 2.1: Laser system of laser doping.
(a) Overview of laser system for doping,
(b) Stage control system

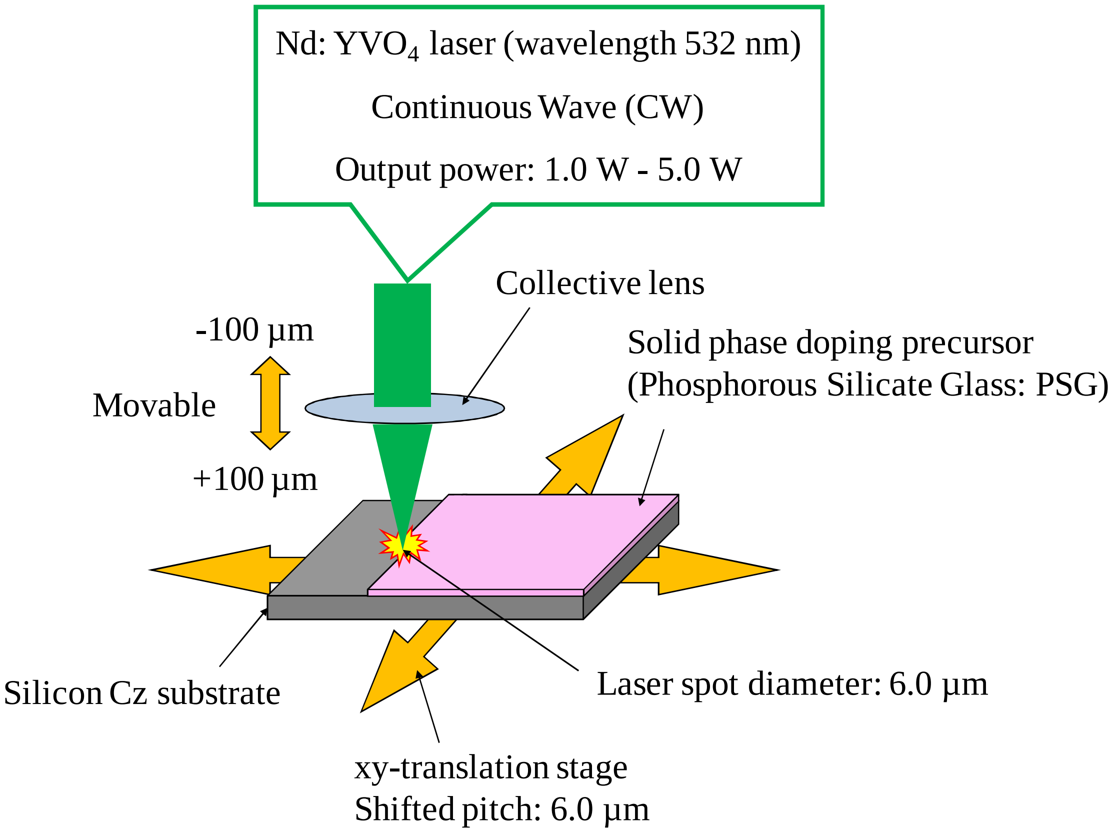

Figure 2.2: Schematic model of LD.

Table 2.1: RCA cleaning procedures.

No.	Process	Chemicals	Conditions
1	SPM	H_2SO_4 (97%) → 1:1 = H_2SO_4(97%):H_2O_2 (30%)	15 min at 80ºC → 10 min at 80ºC
2	Rinse	Deionized H_2O (18 MΩ•cm^2)	1 min at 20ºC
3	HF	HF (5%)	3 min at 25ºC
4	Rinse	Deionized H_2O (18 MΩ•cm^2)	1 min at 20ºC
5	RCA-1 (SC-1)	1:5:1 = NH_3(27%):H_2O:H_2O_2	15 min at 80ºC
6	Rinse	Deionized H_2O (18 MΩ•cm^2)	1 min at 20ºC
7	HF	HF (5%)	3 min at 25ºC
8	RCA-2 (SC-2)	1:5:1 = HCl (27%):H_2O:H_2O_2 (30%)	15 min at 80ºC
9	Rinse	Deionized H_2O (18 MΩ•cm^2)	1 min at 20ºC
10	HF	HF (5%)	3 min at 25ºC
11	Rinse	Deionized H_2O (18 MΩ•cm^2)	1 min at 20ºC
12	Dry	N_2 gas	N_2 gun blow

2.4 Laser Doping Dependence on Irradiation Condition

In this section, the doping profiles which doped on different conditions of laser irradiation were investigated. The controllable parameters of the laser system are laser output power controlled by laser power adjuster, scanning stage speed controlled by stage controller, laser focus condition controlled by micro meter attached lens holder.

The laser output power was changed in range from 1.0 W to 5.0 W. The laser focus condition can be controlled in range from - 100.0 μm to + 100.0 μm which is defined as shown in Fig. 2.3. The laser scanning speed was controlled in range from 1.0 cm/s to 10.0 cm/s.

2.4.1 Laser Output Power

The SIMS result which indicates the concentration of phosphorous atoms doped into p-type silicon substrate was shown in Fig. 2.4. In this experiment, the laser scanning speed and focus during laser irradiation were 6.0 cm/s and about +-10.0 μm, respectively. The irradiation time at laser spot is 0.1 ms. The doping depth was completely controlled by changing the laser output power. In the case of laser output power at 4.0 W and at 5.0 W, the doping depth over 2.0 μm and the doping concentration of 10^{21} cm^{-3} at the surface were obtained. On the other hand, in the case of laser output power from 1.0 W to 3.0 W, the doping depth under 2.0 µm and doping concentration at 10^{19} cm^{-3} were obtained. It was clearly shown that laser output power between 3.0 W and 4.0 W is a threshold of doping depth and concentration. This would be explained by the LD mechanism as follows. Laser irradiation causes the melting of silicon and simultaneously creates dopant atoms by photolysis or pyrolysis of the solid phase doping precursor.6) Then, dopant atoms are incorporated into the molten silicon region by the liquid-phase diffusion during the liquid-phase re-crystallization of silicon.6, 7) At the same time, the activated dopant atoms by laser would diffuse deeper into silicon substrate. The depth of silicon melting and energy given to dopant atoms strongly depends on the laser output power and penetration depth of light into silicon substrate. The penetration depth at the wavelength of 532 nm is around 1 µm as shown in Fig. 2.5.8)

Fig. 2.6 shows the surface morphology after the laser irradiation on changing the laser output power. Many holes were observed at higher laser output power conditions (4.0 W and 5.0 W). However, in the case of lower output power, the smooth surface after the laser irradiation observed. These results indicated that surface morphology would be related to the doping depth by LD.

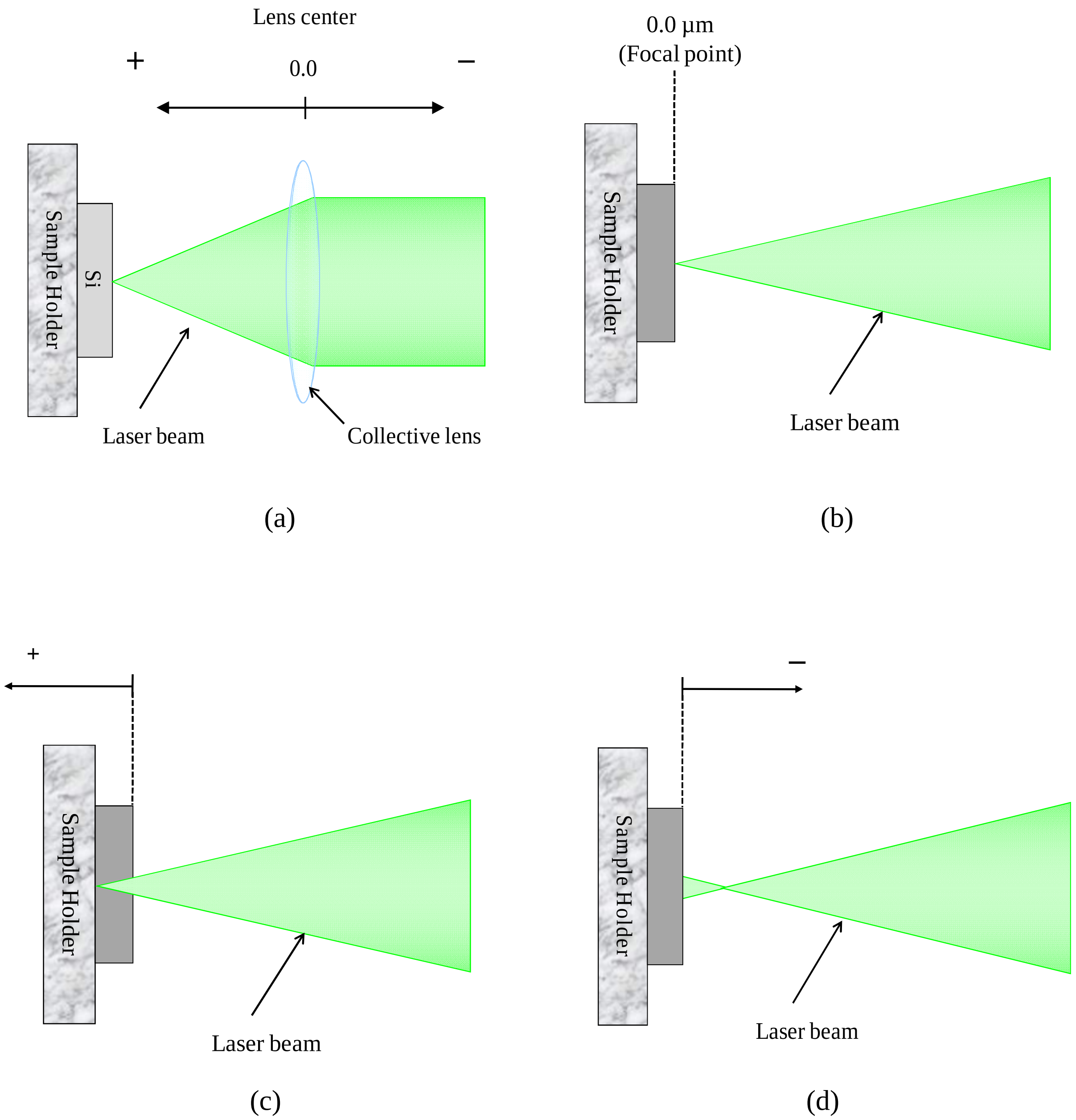

Fig. 2.3: Definition of focus distance and direction.
(a) Lens condition, (b) at focal point,
(c) at defocus inside substrate, (d) at defocus outside substrate

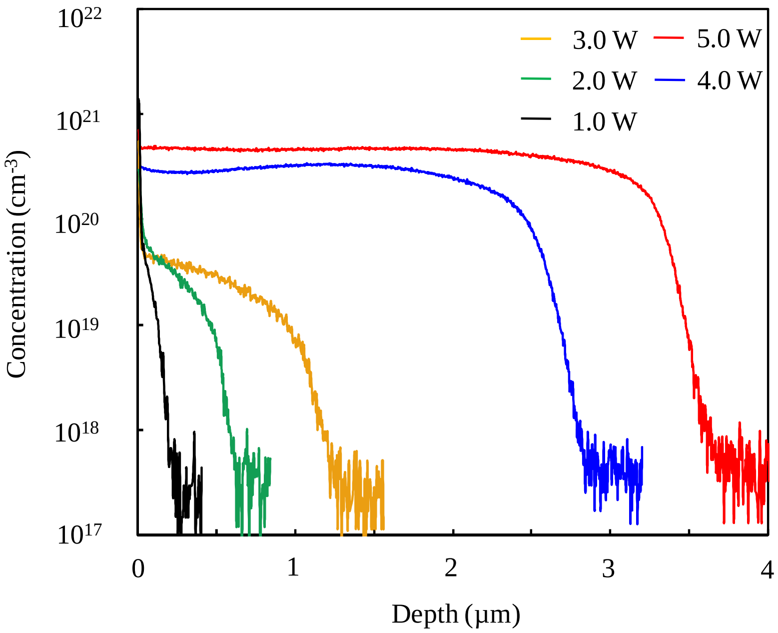

Figure 2.4: Doping dependence on laser output power.

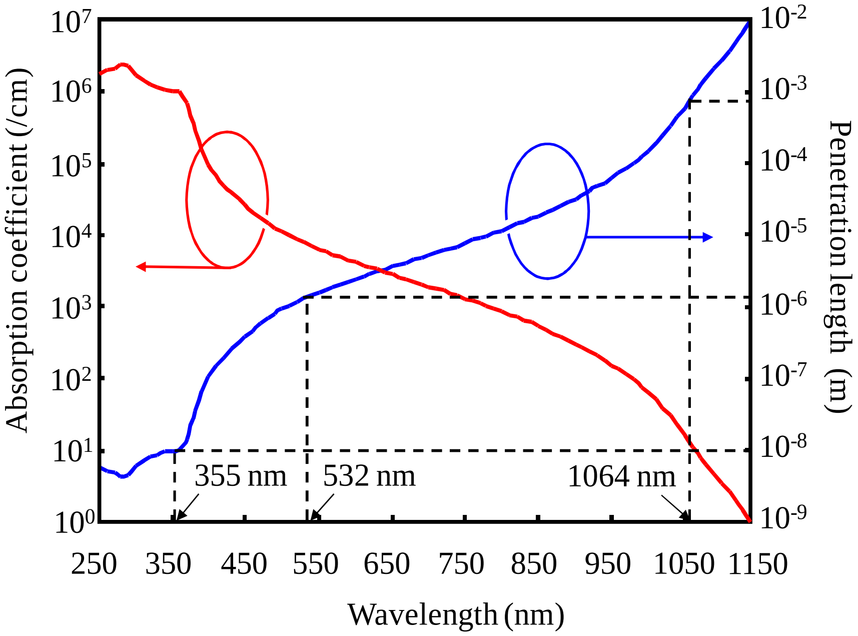

Figure 2.5: Penetration depth of wavelength into silicon at 300K.[8)]

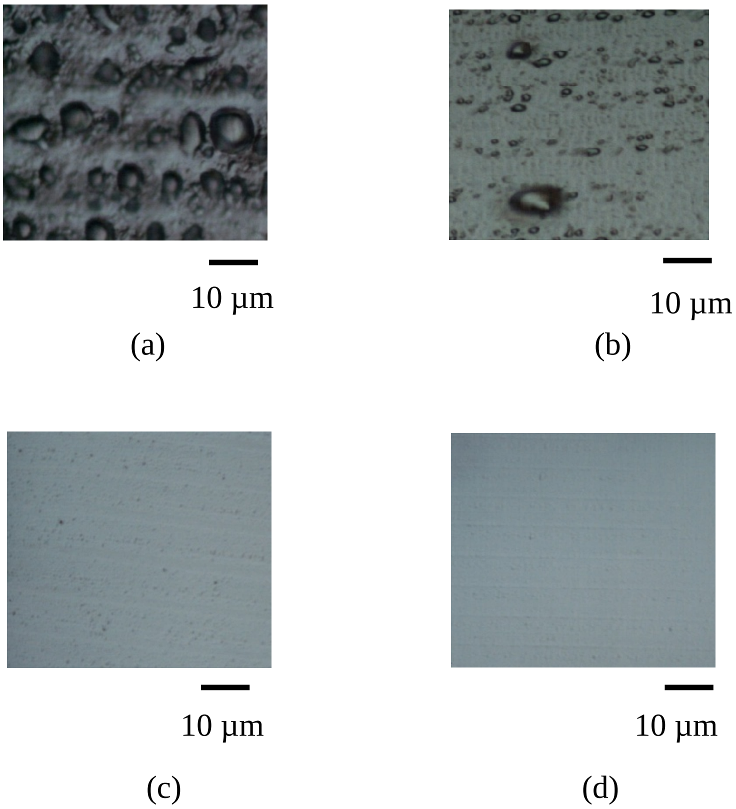

Figure 2.6: Surface morphology after laser irradiation when the laser output power changed. (a) 5.0 W, (b) 4.0 W, (c) 3.0 W, (d) 2.0 W

2.4.2 Laser Focus

Fig. 2.7 shows the depth profile of phosphorous atoms doped into p-type wafer with the different laser focus conditions. In this experiment, the laser output power and scanning speed during laser irradiation were 5.0 W and 6.0 cm/s, respectively. The irradiation time at laser spot is 0.1 ms. The focal point of the collective lens is 0.0 µm as a definition of laser focus condition (shown in Fig. 2.3). The doping depth was over 3.0 µm on the focal point condition as shown in Fig. 2.7. However, the doping depth was under 3.0 µm at defocus condition over 50.0 µm. Thus, the doping depth profile depended on the laser focus condition. Moreover, the different concentration of dopant atoms was confirmed depending on the laser focus condition. This difference is probably due to the reduction of supplied energy density from laser to dopant atom on defocus condition. The supplied energy density at 0.0 µm, +- 50.0 µm, +- 80.0 µm, +- 90.0 µm and +- 100.0 µm were 1768.4 J/cm^2, 1762.5 J/cm^2, 1756.7 J/cm^2, 1750.8 J/cm^2 and 1750.8 J/cm^2, respectively.

Fig. 2.8 shows the surface morphology after the laser irradiation on the different focus conditions. The focal point created the rough like grooved surface as shown in Fig. 2.8 (a).9, 10) By contrast, the defocus condition created the smooth like re-crystallized surface as shown in Fig. 2.8 (b), (c).11) Fig. 2.9 shows the cross sectional image of laser irradiated area using the scanning electron microscope (SEM) observation. Many defects were observed in laser irradiated area by the cross sectional image on focal condition as shown in Fig. 2.9 (a).

On the other hand, at defocus condition, the cross sectional image observed no defects in laser irradiated area as shown in Fig. 2.9 (b), (c). These results would be explained as followings. In the case of focal condition, the silicon was ablated by high laser energy irradiation when the silicon was melted during laser irradiation. By contrast, in the case of defocus condition, the silicon was not ablated due to low laser energy density.

For the focus direction, when the defocus direction was from the surface to outside of substrate, the doping profiles depended on the focus distance from the focal point as shown in Fig. 2.10. While, when the defocus direction was moved from the surface to inside of substrate, the same doping profiles on focus condition of 0.0 µm and 50.0 µm were formed as shown in Fig. 2.10. Moreover, the morphology was formed like grooved surface at inside focus condition as shown in Fig. 2.11 (b), and also the cross sectional SEM image observed the damage near surface as shown in Fig. 2.12 (b). Thus, the focus direction at inside from focal condition would influence to not only the doping depth profile, but also morphology formation after laser irradiation.

These obtained results revealed that the doping depth profile and morphology after the laser irradiation strongly depend on and relate to the laser focus condition.

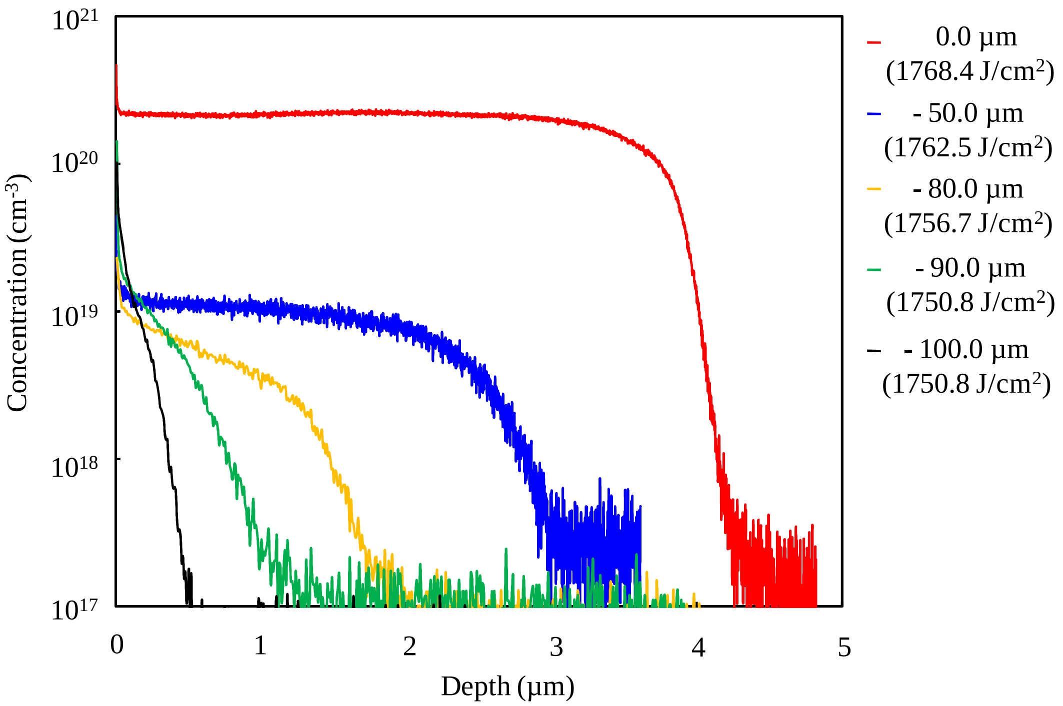

Figure 2.7: Doping dependence on focus condition from focal point to outside substrate.

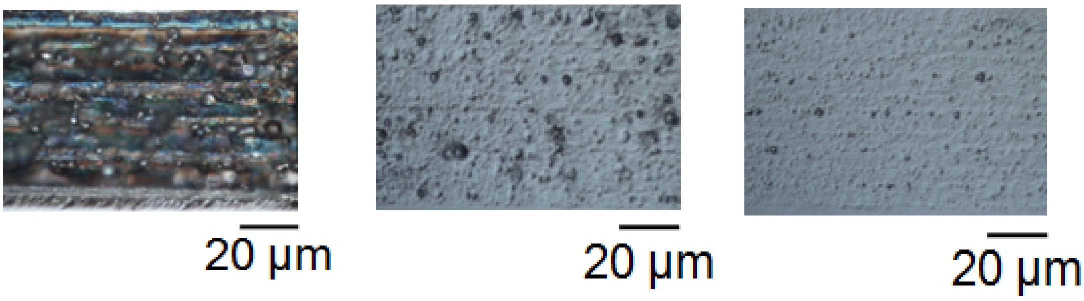

(a) (b) (c)

Figure 2.8: Surface morphology after laser irradiation with different focus conditions.

(a) Focal point (0.0 µm) (Energy density: 1768.4 J/cm^2),

(b) Defocus at – 40.0 µm (Energy density: 1762.5 J/cm^2),

(c) Defocus at – 100.0 µm (Energy density: 1750.8 J/cm^2)

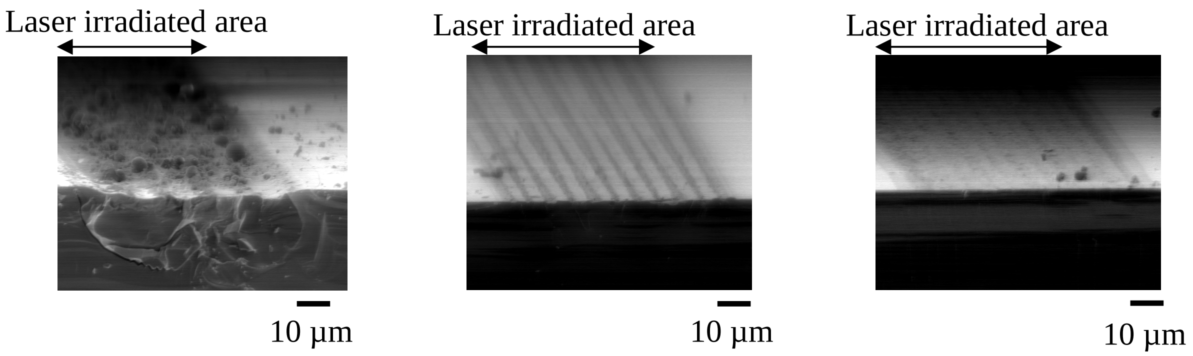

(a) (b) (c)

Figure 2.9: Cross sectional images at laser irradiated area with different focus conditions.
(a) Focal point (0.0 µm) (Energy density: 1768.4 J/cm^2),
(b) Defocus at – 40.0 µm (Energy density: 1762.5 J/cm^2),
(c) Defocus at – 100.0 µm (Energy density: 1750.8 J/cm^2)

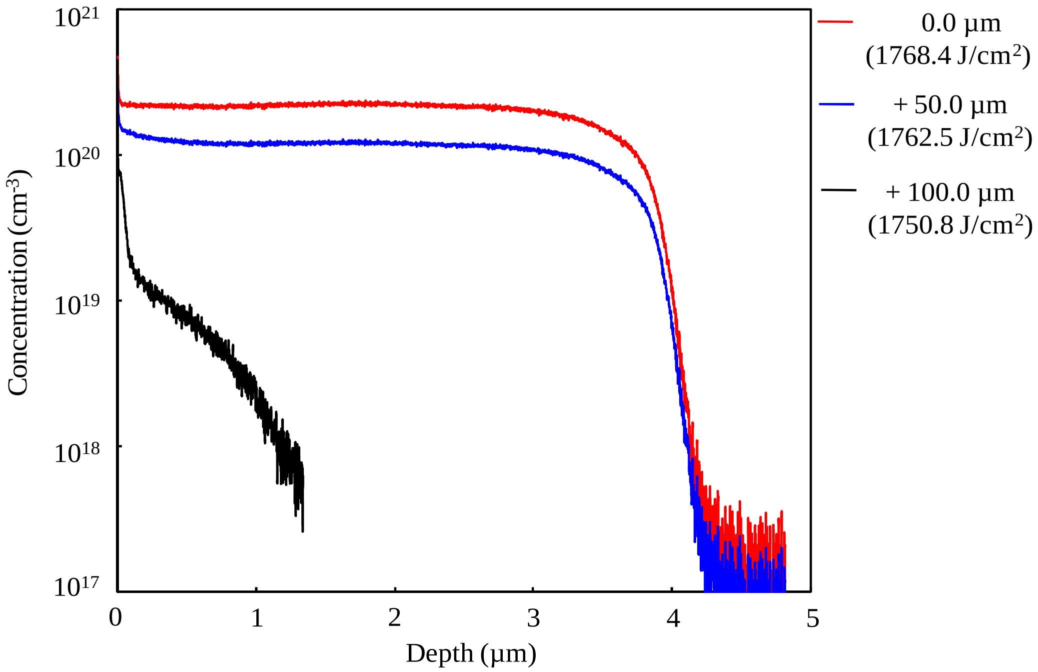

Figure 2.10: Doping profiles when defocus direction was from focal point to inside substrate.

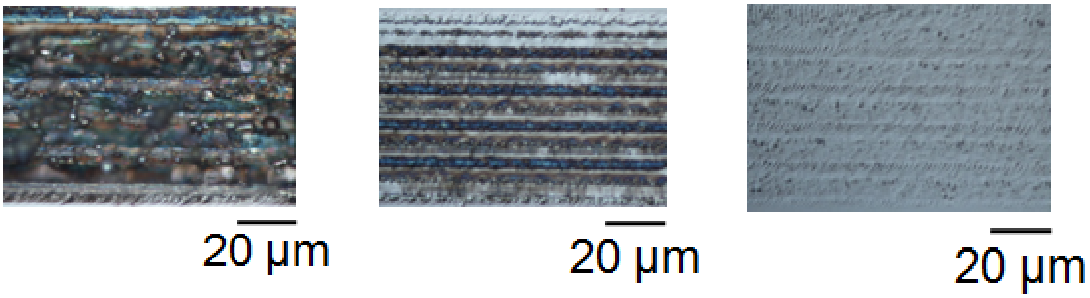

(a) (b) (c)

Figure 2.11: Surface morphology after laser irradiation with different focus conditions.
(a) Focal point (0.0 µm) (Energy density: 1768.4 J/cm^2),
(b) Defocus at + 40.0 µm (Energy density: 1762.5 J/cm^2),
(c) Defocus at + 100.0 µm (Energy density: 1750.8 J/cm^2)

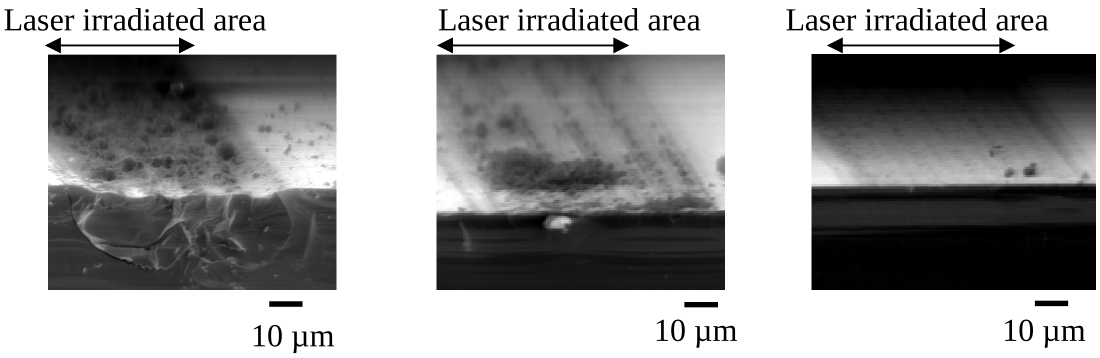

(a) (b) (c)

Figure 2.12: Cross sectional images at laser irradiated area with different focus conditions.
(a) Focal point (0.0 µm) (Energy density: 1768.4 J/cm^2),
(b) Defocus at + 40.0 µm (Energy density: 1762.5 J/cm^2),
(c) Defocus at + 100.0 µm (Energy density: 1750.8 J/cm^2)

2.4.3 Laser Scanning Speed

Fig. 2.13 shows the depth profile of phosphorous atoms doped into p-type wafer on the different scanning speeds. In this experiment, the laser output power and focus during laser irradiation were 5.0 W and approximately – 90.0 µm, respectively. The irradiation time at the laser spot was 0.6 ms at 1.0 cm/s, 0.1 ms at 6.0 cm/s, and 0.06 ms at 10.0 cm/s. The results showed that the doping depth depends on scanning speed. It is considered that doping depth would relate to scanning speed, namely time of laser irradiation.

Fig. 2.14 shows the surface morphology after the laser irradiation with the different scanning speeds. The rough surface was observed at the slower scanning speed, while the smooth surface was observed at the faster scanning speed. This morphology formation strongly depended on time of laser irradiation.

Obtained results indicated that the doping depth and surface morphology formed by LD depends on time of laser irradiation.

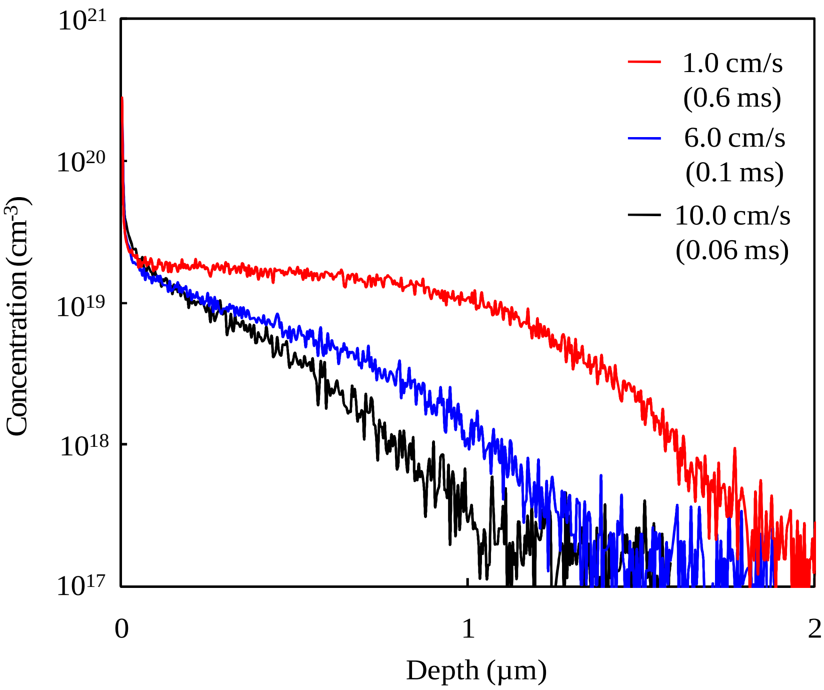

Figure 2.13: Doping profiles dependence on scanning speed.

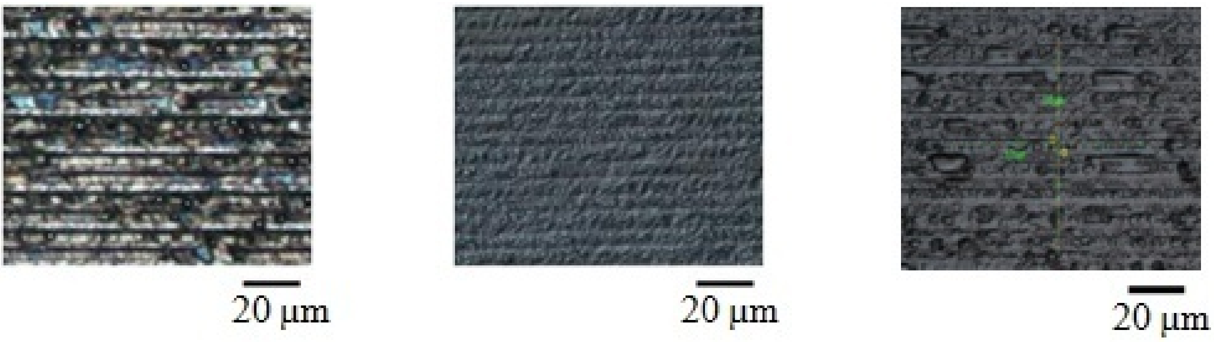

(a) (b) (c)

Figure 2.14: Surface morphology after laser irradiation with different scanning speeds.
(a) 1.0 cm/s (0.6 ms),
(b) 6.0 cm/s (0.1 ms),
(c) 10.0 cm/s (0.01 ms)

2.5 Discussion of Laser Doping Mechanism

The doping mechanism of LD is different from the solid phase diffusion of impurities like a conventional thermal diffusion over 800 ºC with long diffusing time into silicon. LD induces silicon melting, namely liquid phase diffusion of impurity, and then incorporates impurity during re-crystallization.[6, 7)] In addition, LD can form a doping layer in short time within a few second. In this section, doping depth, concentration and cavity creation by LD were discussed in order to reveal the doping mechanism of LD.

2.5.1 Doping Depth and Concentration

The impurity diffusion process can be approximated by two kinds of functions.[12)] In the case of limited source concentration, the impurity diffusion is given by the Gaussian function,

$$\mathrm{C}(\mathrm{x},\mathrm{t}) = \frac{\mathrm{S}}{\sqrt{\pi \mathrm{Dt}}}\exp\left(-\frac{\mathrm{x}^2}{4\mathrm{Dt}}\right) \tag{2.1}$$

where C [/cm^3], D [cm^2/s], S [/cm^3], t [s], and x [nm] are the impurity concentration, the diffusion coefficient, the total amount of impurities in diffusion source, diffusion time, and doping depth, respectively. In the case of constant surface concentration, the impurity diffusion is given by the complementary error function,

$$\mathrm{C(x,t)} = \mathrm{C_s}\,\mathrm{erfc}\left(-\frac{\mathrm{X}}{2\sqrt{\mathrm{Dt}}}\right) \tag{2.2}$$

where C_s [/cm^3] is a surface concentration.

The investigation of LD profile was approximated by two functions (equation 2.1, 2.2) with LD profile as shown in Fig. 2.7. Assuming the limited doping source in the doping precursor (PSG film) of LD, LD profile should be approximated by Gaussian function. The parameters of approximation were S, and D. The diffusion time of impurity t = 0.1 ms was laser irradiation time at laser spot (6.0 μm). The results of approximation data using experimental data from Fig. 2.7 were shown in Fig. 2.14. As shown in Fig. 2.14, the all experimental data curves agreed well with approximated data curves. However, the experimental data curves of laser output power from 2.0 W to 5.0 W did not agree with approximated data curves using Gaussian function. To fit with approximation curves, the experimental curves were separated at a depth where the doping concentration decreased. That calls “Tail region” in this thesis. Moreover, the tail region was approximated by the complementary error function. As well as the first approximation, the diffusion time of impurity t was 0.1 ms. The results of the tail region of approximation data were shown in Fig. 2.15. The obtained values of S and D from approximations were summarized in Table. 2.2. At the first approximation by Gaussian function, the diffusivity of 5.0 W and 4.0 W was 5.1×10^{-4}

cm^2/s. The diffusivity of phosphorous in the liquid silicon is around 5.1×10^{-4} cm^2/s.13) Thus, LD at 5.0 W and 4.0 W formed a doping layer in liquid phase diffusion. By contrast, the diffusivities of from 3.0 W to 1.0 W were 2.0×10^{-5} cm^2/s, 3.0×10^{-6} cm^2/s, and 2.0×10^{-7} cm^2/s, respectively. However, the diffusivity of phosphorous in solid silicon at melting point of silicon around 1410°C is 1.0×10^{-10} cm^2/s.12) The diffusivity in solid silicon were summarized in Table. 2.3. Thus, LD at from 3.0 W to 1.0 W induced the melting of silicon. Although the diffusivities of from 3.0 W to 1.0 W over that of melting point of silicon, they were lower than that of liquid silicon. It is considered that the solidification of silicon relates to the diffusivity. Moreover, in the second approximation for the tail region, the diffusivities were between 1.5×10^{-6} cm^2/s and 1.1×10^{-7} cm^2/s. It is considered in the tail region that the solidification of silicon strongly influenced the diffusivity.

LD profile was obtained large different concentration between 4.0 W and 3.0 W as shown in Fig 2.4. This can be also discussed by approximations. The values of impurity concentration obtained from approximations were summarized in Table. 2.4. The difference of impurity concentration existed between 4.0 W and 3.0 W as shown in Table. 2.4. Taking account into the diffusivity, the difference of impurity concentration related to solidification of silicon. Thus, it is considered that the impurity concentration relates to segregation of impurity.

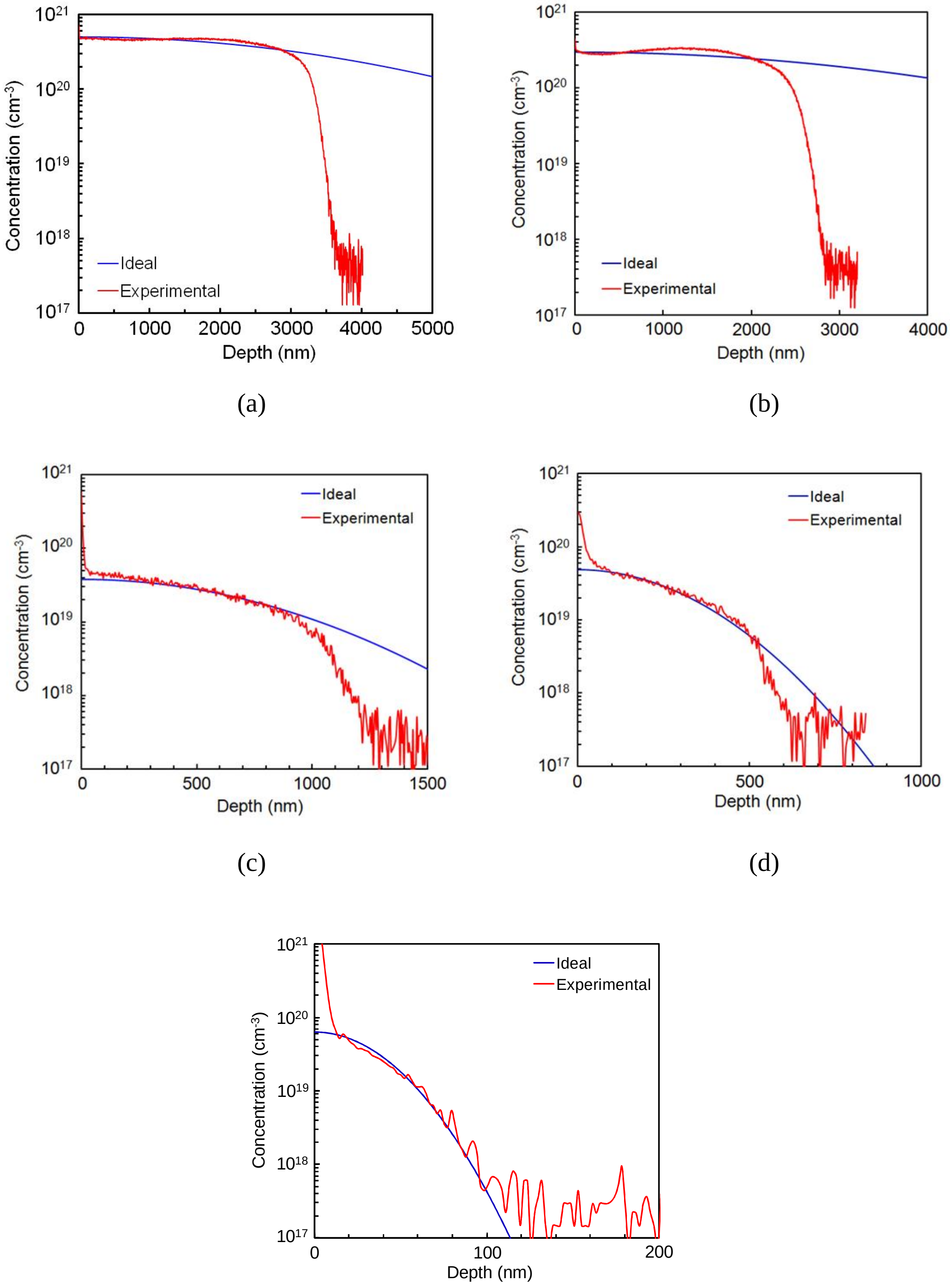

(a)

(b)

(c)

(d)

(e)

Figure 2.14: Doping profile of laser output power approximated by the Gaussian function. (a) 5.0 W, (b) 4.0 W, (c) 3.0 W, (d) 2.0 W, (e) 1.0 W

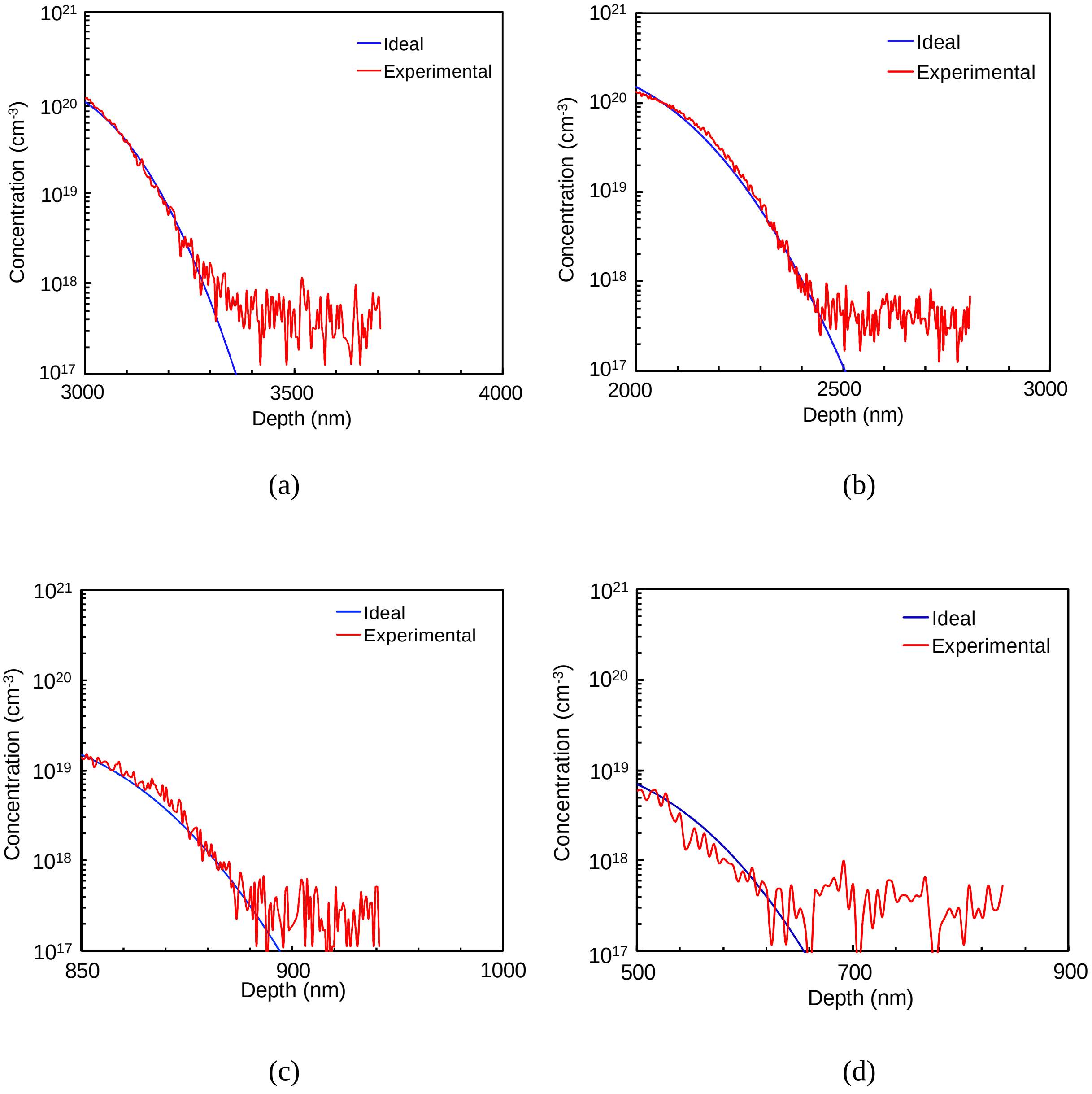

(a)

(b)

(c)

(d)

Figure 2.15: Tail region of doping profile on laser output power approximated by the complementary error function.
(a) 5.0 W, (b) 4.0 W, (c) 3.0 W, (d) 2.0 W

Table. 2.2: The diffusivity *D* of phosphorous of LD from experimental curves in doping profile and tail region.

	Doping profile	Tail region
Laser output power	D (cm^2/s)	D (cm^2/s)
5.0 W	5.1×10^{-4}	6.0×10^{-7}
4.0 W	5.1×10^{-4}	1.1×10^{-7}
3.0 W	2.0×10^{-5}	1.5×10^{-6}
2.0 W	3.0×10^{-6}	2.0×10^{-7}
1.0 W	2.0×10^{-7}	

Table. 2.3: The diffusivity of phosphorous in solid silicon.$^{12)}$

Temperature	D (cm^2/s)
1410 °C (Melting point)	1.0×10^{-10}
1000 °C	1.0×10^{-14}
900 °C	1.0×10^{-15}

Table. 2.4: The impurity concentration obtained from approximations

Laser output power	S (/cm^3)	C_s (/cm^3)
5.0 W	2.0×10^{17}	1.0×10^{20}
4.0 W	2.0×10^{17}	1.0×10^{20}
3.0 W	3.0×10^{15}	1.5×10^{19}
2.0 W	1.5×10^{15}	7.0×10^{18}
1.0 W	1.5×10^{15}	

LD profile was obtained a large different depth between 3.0 W and 4.0 W as shown in Fig 2.5. This is considered as following mechanisms. The laser has the two kinds of melting mode. One is the thermal diffusion mode, and another is the deep melting mode. In the case of thermal diffusion mode, this mode occurs at irradiated laser power density under 10^5 W/cm^2. 14) In this mode, thermal induced by laser diffuses to wide area from irradiated to other area, and throughout material. By contrast, in the case of deep melting mode, this melting mode occurs at the irradiated laser power density over 10^5 W/cm^2.14) In this melting mode, the molten pool is created at the laser irradiation area. The laser irradiated surface is ablated during molten pool creation. The surface of the molten pool generates waves induced by ablated materials. These waves induce a hole in the molten pool. The laser beam gets into deep depth through this hole. These mechanisms usually occur in the case of weld of stainless using CO_2 or YAG laser with infrared wavelength.14) Moreover, all laser output powers in this study are over 10^5 W/cm^2. Thus, this should be considered to relating to optical absorption into silicon. The schematic model of these mechanisms was shown in Fig. 2.16.

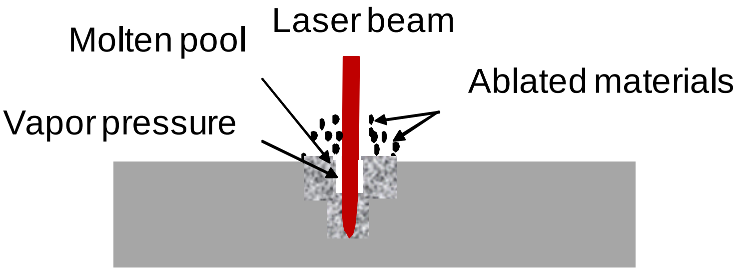

(a)

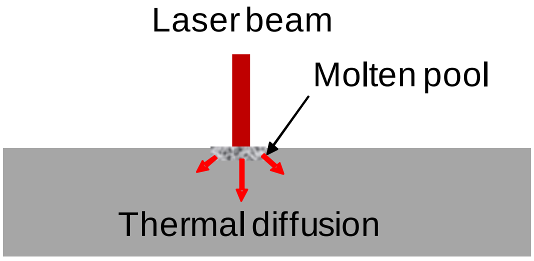

(b)

Figure 2.16: Schematic model of laser melting mode.13)
(a) Melting at Deep melting mode,
(b) Melting at thermal diffusion mode

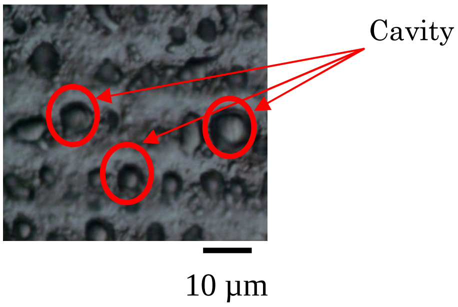

Figure 2.17: Cavities creation at 5.0 W.

2.5.2 Cavity Creation

It was verified that the cavity created after laser irradiation at 5.0 W as shown in Fig. 2.17. This is considered that the ablated materials from laser irradiated area attached on molten pool, and then the molten pool created air bubbles. These bubbles were broken by surface tension. The broken bubbles solidified when removed laser irradiation. In particular, in the case of 5.0 W, the doping depth is the deepest than that of other laser output powers. The deepest melting condition would be a much easier creation of cavity due to a lot of ablated materials. Fig. 2.18 shows the laser trace after one scan at scanning speed of 6.0 cm/s and the focal point. Higher laser output power observed a lot of ablated materials around the laser scanned area (Fig. 2.18 (a)). By contrast, lower laser output power observed no ablated materials (Fig. 2.18 (b)). These figures are a proof of the creation of cavity after laser irradiation at high output power. A model of cavity creation was illustrated in Fig. 2.19.

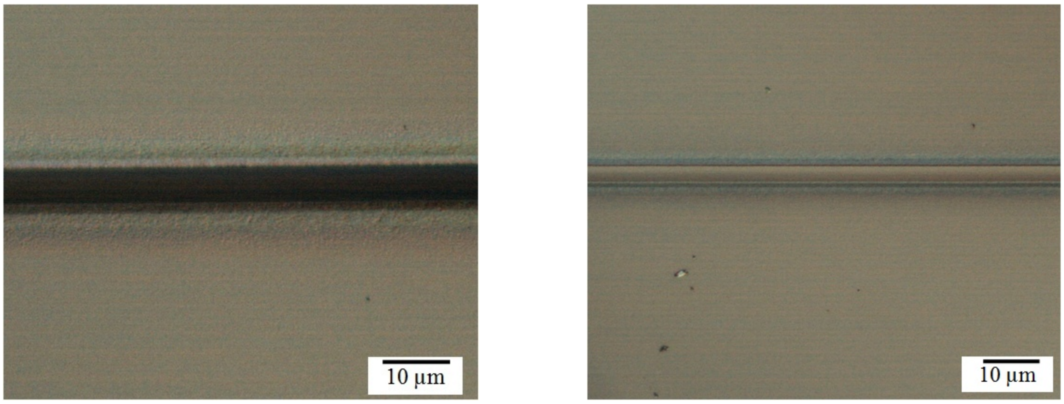

(a) (b)

Figure 2.18: Laser trace after one scan on surface with higher and lower laser output power. (a) 5.0 W, (b) 3.0 W

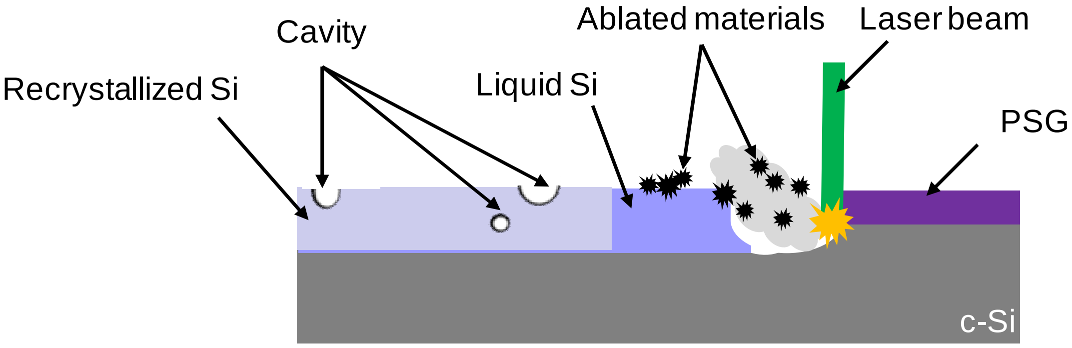

Figure 2.19: Model of cavity creation by laser irradiation.15)

2.6 Summary

In order to reveal the principle of LD, a dependence of laser irradiation condition for the doping profile was investigated in detail. It was found out that the laser irradiation conditions influenced not only the doping profile, but also the morphology after laser irradiation. The doping depth could control depending on laser output power, focus condition and scanning speed. In particular, laser output power could control the doping depth in range from 1.0 µm to 5.0 µm.

Laser focus could control the doping depth. However, it is unstable the doping profile depending on focus direction. The focus from the surface to outside of substrate could obtain as changed from rough to smooth surface. Furthermore, the cross sectional image was observed that defects were created by laser irradiation at the focal point. At the focus from the surface to outside of substrate, no defect was observed by SEM in the cross sectional image.

Laser scanning speed could control the doping depth in range of from 1.0 µm to 2.0 µm. The morphology formation strongly depended on the scanning speed, thus time of laser irradiation related to this dependence.

The LD mechanism was discussed with doping depth and cavity creation. To reveal the LD mechanism, the approximations were introduced. The LD induces the silicon melting, and then the impurity doping into silicon during solidification of silicon. Thus, the LD has the transient mechanism related to melting and solidification of silicon. From a point of view of the diffusivity, in the solid silicon, the diffusivity of phosphorous is around 1.0×10^{-14} cm^2/s at 900 ºC, and 1.0×10^{-10} cm^{-2}/s at melting point of silicon.12) By contrast, the diffusivity of LD is over 1.0×10^{-7}. Furthermore, the maximum diffusivity of LD is around 5.1×10^{-4} cm^2/s. Thus, LD induces the melting of silicon and forms a doping layer in a short time, since the diffusivity of LD is higher than that in solid silicon.

References of Chapter 2.

1) M. A. Green: *SILICON SOLAR CELLS Operating Principles, Technology and System Applications* (University of New South Wales, Sydney, 1995), p.108.
2) S. M. Sze: *Physics of Semiconductor Devices* (Wiley, New York, 1981) 2nd ed., p.64.
3) Operator's Manual, Verdi $^{\mathrm{TM}}$V-2/V-5/V-6 Diode-Pumped-Lasers (Coherent, USA, 2002)
4) A. E. Siegman, and S. W. Townsend, IEEE Journal of Quantum Electronics, 1993, Vol.29, No.4.
5) Dictionary of Physical Science (Baifuukan, Tokyo, 1996) Editorial committee of dictionary of physical science.
6) A. Ogane, K. Hirata, K. Horiuchi, Y. Nishihara, Y. Takahashi, A. Kitiyanan, and T. Fuyuki: Jpn. J. Appl. Phys. **48** (2009) 071201.
7) T. Sameshima, S. Usui and M. Sekiya: J. Appl. Phys. **62(2)** (1987) 711.
8) M. A. Green: *SILICON SOLAR CELLS Advanced Principles & Practice* (University of New South Wales, Sydney, 1995), p. 334.
9) L. Pirozzi, G. Arabito, F. Artuso, V. Barbarossa, U. Besi-Vetrella, S. Loreti, P. Mangiapane, E. Salza: Sol. Energy Mater. Sol. Cells **65** (2001) 287.
10) D. Kray, A. Fell, S. Hopman, K. Mayer, M. Mesec, S. W. Glunz, G. P. Willeke: Proc. of 22nd European Photovoltaic Solar Energy Conf., 2007, p. 1227.
11) A. Esturo-Breton, M. Ametowobla, C. Carlsson, J. Köhler, and J. H. Werner: Proc. 21st of European Photovoltaic Solar Energy Conf., 2006, p. 1247.

12) S. M. Sze: *Physics of Semiconductor Devices* (Wiley, New York, 1981) 2nd ed., p. 68

13) H. Kodera: Jpn. J. Appl. Phys. **2** (1963) 212.

14) T. Arai: *Fundamental Engineering Science for Laser Materials Processing* (Maruzen, Tokyo, 2007) p. 114. (in Japanese)

15) Y. Kawahito, N. Matsumoto, Y. Abe, and S. Katayama: Proc. of 71st Laser Materials Processing Conf., 2008, p. 9.

Chapter 3

Investigation of Dopant Films for Laser Doping

3.1 Introduction

LD induces the melting and recrystallization of silicon to form a pn junction.1) The conditions of laser irradiation gave the dependence of the doping profile which revealed in chapter 2. However, LD for the formation of a doping layer to form a pn junction needs a dopant precursor. Forming a pn junction in c-Si solar cells, a dopant contained film or solution is generally utilized.2-7) Thus, it is important for optimization of LD that the efficiency of light absorption in a dopant precursor is investigated because the laser emits a specific wavelength.8) An investigation of dopant precursor for LD has not yet revealed so far.

In this chapter, the dopant precursor was investigated for optimization of LD. A phosphorous silicate glass (PSG) film was used as the dopant precursor in this study. The optimization of LD not only for the fabrication of c-Si solar cells but also high effiency c-Si solar cells would depend strongly on the optical properties of PSG film.The PSG film was formed by the spin-coating method in this thesis. However, this method forms ununiform film on the sample surface. In addition, it is difficult to control the film thickness less than 200 nm.

Therefore, a sputtering for the formation of PSG film on the sample surface as a new method is proposed. This method can form a uniform film on whole sample surface.[9, 10] Moreover, this method can control the film thickness easily by changing the deposition time of film, RF power, and the distance between a sputtering target and substrate.[11] By this method, the optical properties of PSG film; in particular, the reflectance can be controlled. In this study, only the film reflectance was focused in order to reveal the correlation between the LD and dopant precursor.

3.2 Preparation of Dopant Films using Sputtering Method

The sputtering is one of the film deposition methods. This method can be deposited the film from the target sputtered by accelerated ions of ambient gas in the sputtering chamber. The ambient gas is dissolved by plasma.

The sputtering equipment used in this study is the radiofrequency (RF: 13.56 MHz) magnetron ternary sputtering (Eiko). Fig. 3.1 shows the diagram of sputtering equipment. The film was deposited on a substrate held on sample holder. The film was formed by sputtering of a target where was attached at the bottom part of equipment as shown in Fig. 3.1. The target was sputtered by Ar ions (ambient gas).

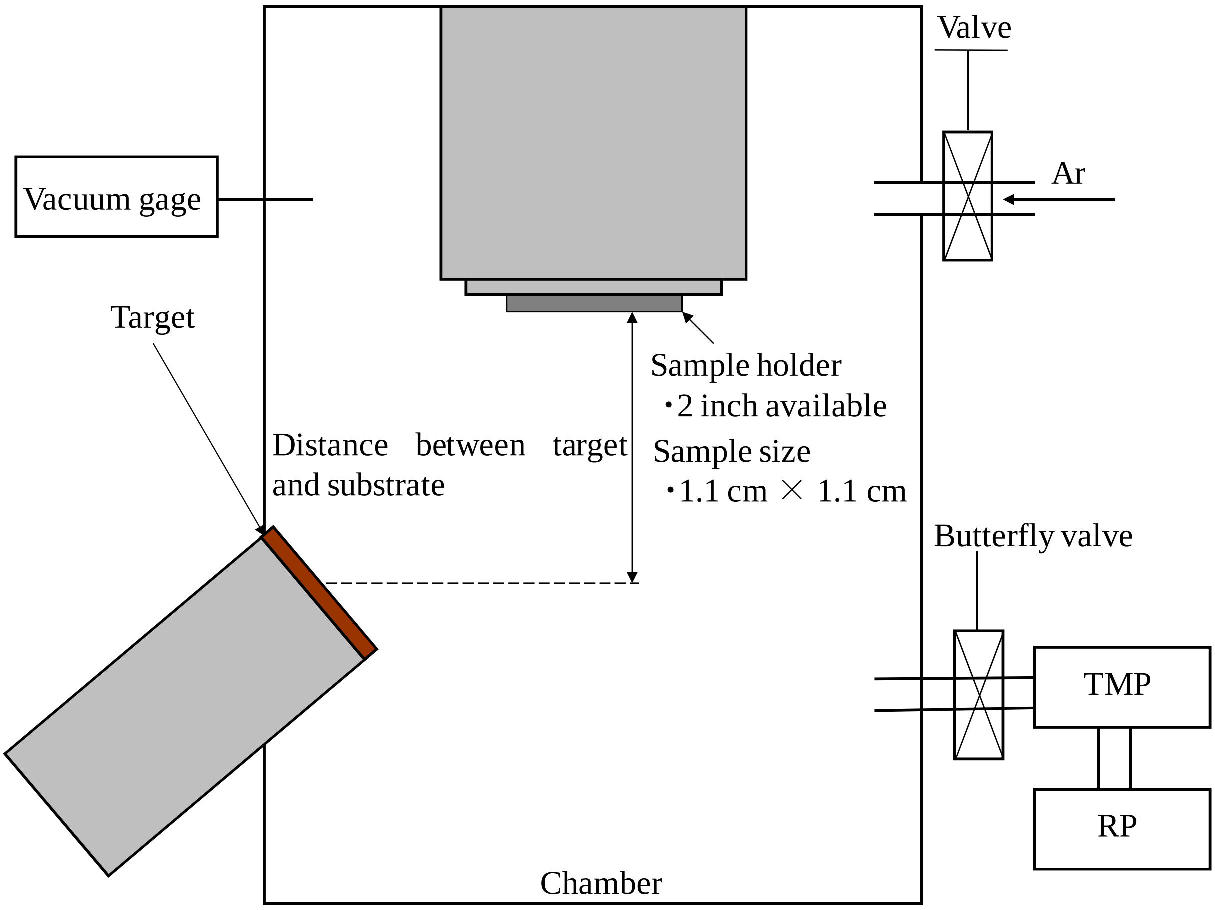

TMP: Turbo molecular pump
RP: Rotary pump

Figure 3.1: Diagram of used sputtering equipment.

3.3 Experiment

As the substrate, 0.1-2 Ωcm 300-μm-thick, p-type, Cz, (100)-oriented Si was used. To obtain the dopant precursor, the PSG film was formed by sputtering PSG target. In condition of sputtering for formation of PSG film, the vacuum inside the chamber, RF power, and the distance between the target and sample holder were in range from 1.5×10^{-4} Pa to 7.5×10^{-5} Pa, 100 W, and 10 cm, respectively. The deposition rate of PSG film in this condition was in range from 1.9 - 4.2 nm/s.12) The deposited PSG film thickness was measured by ellipsometer (HORIBA JOBIN YVON). The used target of PSG for the formation of PSG film on the substrate consists of SiO_2 (95 %) and P_2O_5 (5%). The reflectance of PSG film was measured by ultraviolet-visible-near infrared spectral photometer (JASCO: V-570).

Fig. 3.2 shows the schematic model of LD in this study. In order to investigate the influence of PSG film reflectance to LD, two types of laser were used. One of lasers was Nd^{3+}: YAG pulsed-laser with 355 nm wavelength (Coherent: AVIA Ultla 355-350). This laser can dope the dopant atoms into the silicon depth of around 300 nm.13) Another laser was Nd^{3+}: YVO_4 CW laser with 532 nm wavelength (Coherent: Verdi/V-5). This laser can dope the dopant atoms into the silicon depth of around 1 μm as revealed in chapter 2.

The laser was irradiated on the full-surface area of the sample with deposited PSG film at room temperature and in air ambience. The conditions of laser irradiation were summarized in Table 3.1.

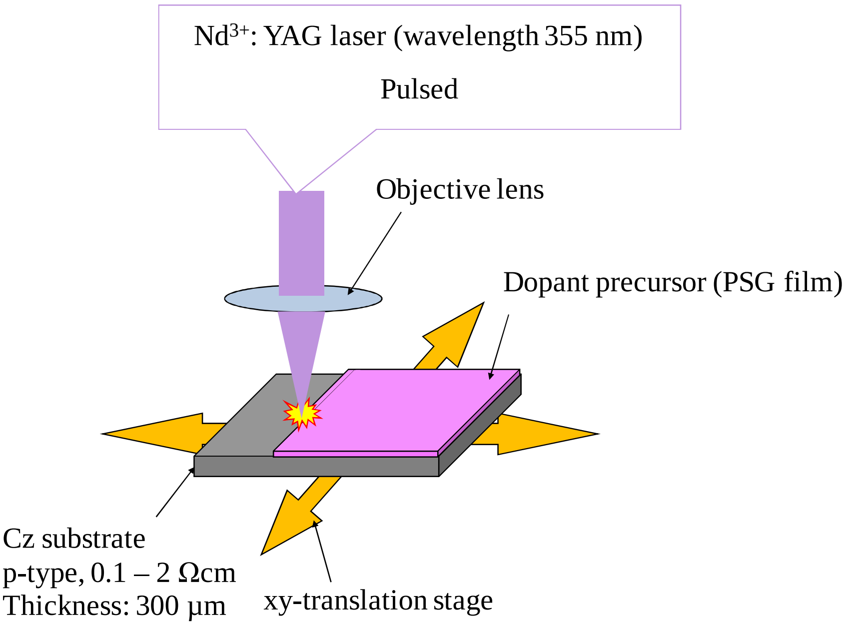

(a)

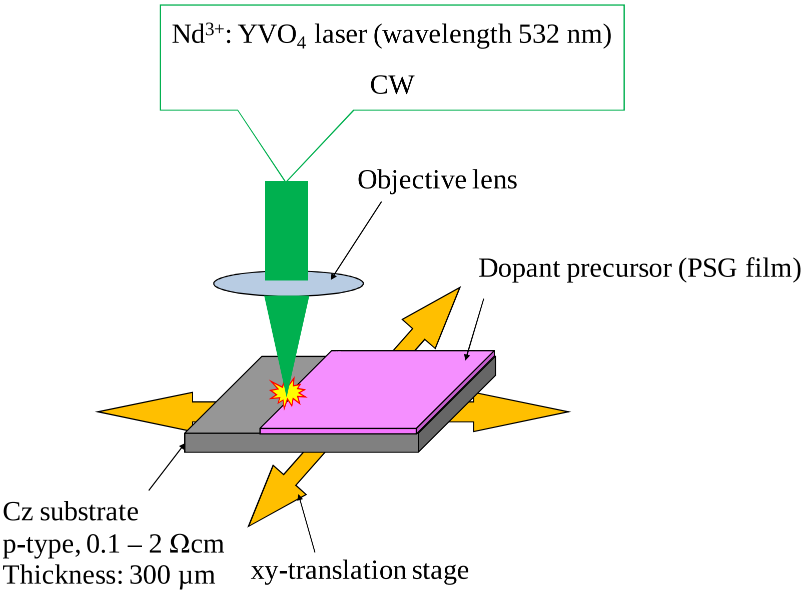

(b)

Figure 3.2: Schematic model of LD in this study.

Table 3.1: The conditions of laser irradiation for LD in this study.

Laser	Output power	Scanning speed	Spot diameter	Shifted pitch
Nd^{3+}: YAG Pulsed-laser (Wavelength: 355 nm)	0.5W	1.0 cm/s	50 µm	25 µm
Nd^{3+}: YVO_4 CW-laser (Wavelength: 532 nm)	5.0W	6.0 cm/s	6 µm	6 µm

3.4 Reflectance Dependence on Thickness of Dopant Film

Absorption efficiency of incident light is generally given by the ratio between reflection and transmission of incident light. As a silicon base substrate, 300 μm-thick was used in this study. The wavelengths of used lasers in this study were 355 nm and 532 nm, respectively. The penetration depth of incident light into silicon depends on the wavelength of light.14) Taking into account the wavelengths of used lasers, the penetration depths of their wavelength are within 10 nm and approximately 1 μm, respectively.15) Thus, only reflectance can be considered for investigation of influence of film in LD since incident light does not transmit the whole depth area of base substrate.

Fig.3.3 shows the reflectance of PSG film of 330 nm-thickness fitted with calculated reflectance. Calculated reflectance was evaluated by equations as shown in Appendix A. The results showed that the experimental reflectance agrees well with calculations. The margin of error between experimental and calculated reflectance was within 1.5 %. In addition, at the specific wavelength, namely laser wavelength at 355 nm and 532 nm, the reflectance of PSG films with various film thicknesses agrees well with calculations as shown in Fig. 3.4. These results indicated that the reflectance of PSG film depends on the film thickness. In addition, it is possible that sputtering method for formation of PSG film control its reflectance.

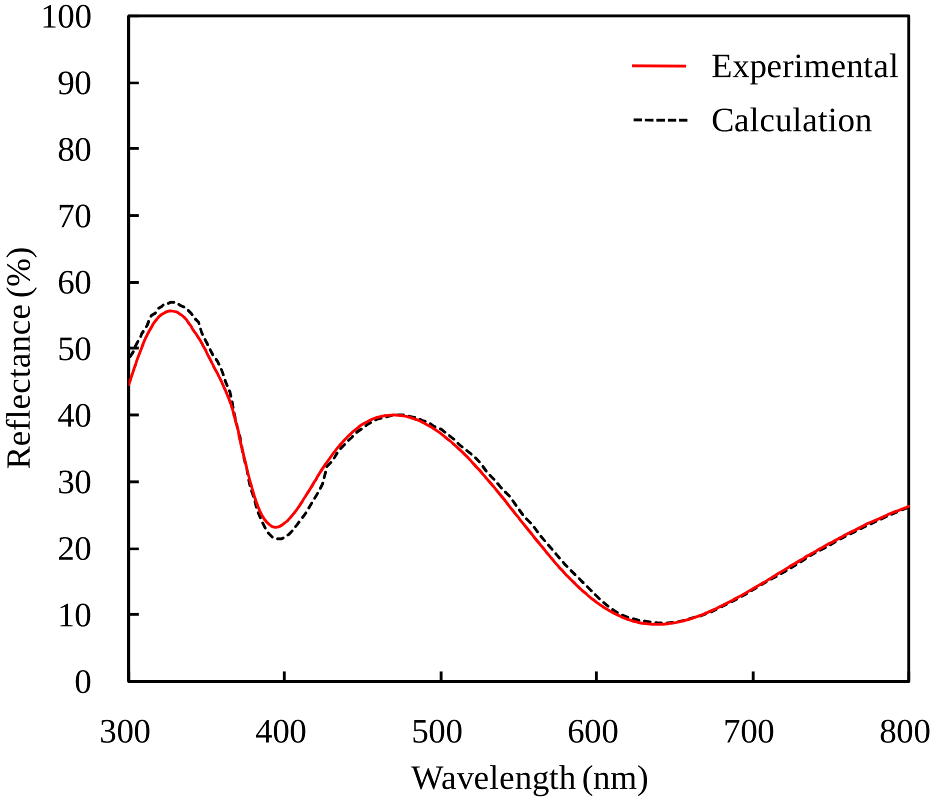

Figure 3.3: The reflectance of PSG film of 330 nm-thickness fitted with calculated reflectance.

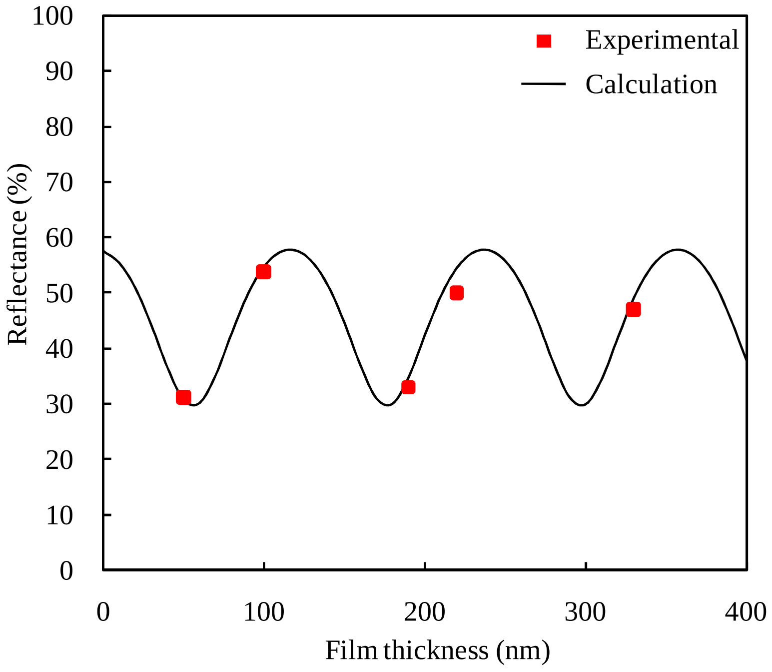

(a)

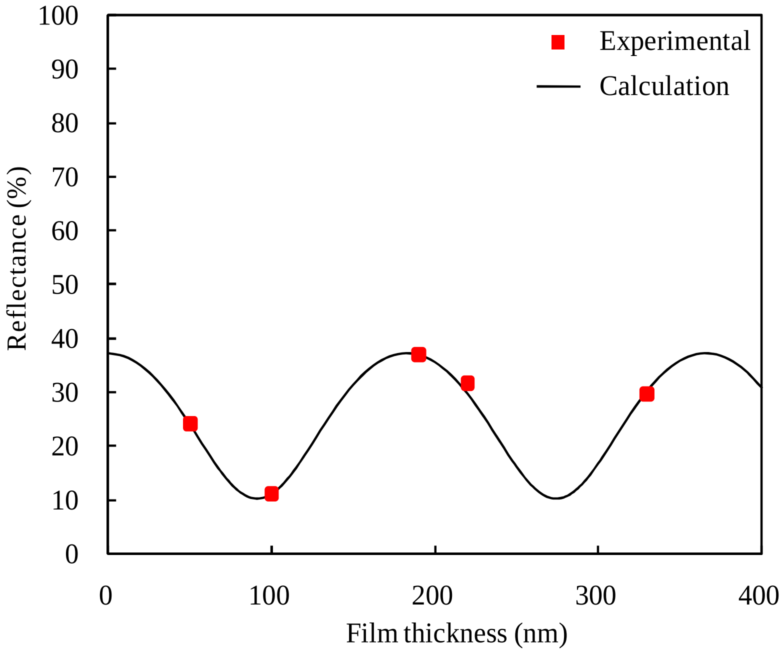

(b)

Figure 3.4: The reflectance of various PSG film thicknesses fitted with calculated reflectance. (a) at 355 nm, (b) at 532 nm

3.5 Influence of Doping Profile with Different Reflectance of Dopant Films

3.5.1 Pulsed Laser with 355 nm Wavelength

Fig. 3.5 shows the surface image after pulsed-laser with 355 nm wavelength irradiation to different reflectance of PSG film. Fig. 3.5 (a) and (b) show the surface morphology after LD at the reflectance of 58.0 % with 240 nm-thickness and 30.0 % with 180 nm-thickness at 355 nm wavelength, respectively. Comparing these images, in the case of highest reflectance of PSG film (58.0 %), laser trace was observed. The laser trace is usually created by ablation of materials occurred in condition of high laser fluence.16) In other words, laser fluence was increased due to lower reflectance of PSG film. By contrast, in the case of lowest reflectance of PSG film (30.0 %), no laser trace was observed. This is considered that the laser fluence was reduced by higher reflectance of PSG film. Thus, the reflectance of PSG film impacts on surface morphology after LD.

Fig. 3.6 shows the doping profile of after LD with different reflectance of PSG films. As comparison of LD results, in the case of lower reflectance of PSG film, the dopant atoms were doped at a depth of 400 nm. By contrast, in the case of higher reflectance of PSG film, the dopant atoms were doped at a depth of 250 nm. This difference can be explained by LD mechanism.1) LD induces the silicon melting and incorporates the dopant during recrystallization. Thus, the deeper doping depth in the case of lower reflectance of PSG film than that of higher reflectance was formed by deep melting depth which was induced by high laser fluence. In addition, the concentration of dopant atoms was higher in the case of lower reflectance of PSG film than that of the higher reflectance. This is considered that the dopant materials ablated by high laser fluence re-attached to the PSG surface, and then laser scanned on PSG with the re-attached dopant materials.17) Consequently, the amount of dopant atoms of PSG film was increased. Thus, the high concentration of dopant atoms after LD was formed by the PSG film with the larger amount of dopant atoms. These results clearly showed that the reflectance of PSG film impacts on the doping profile of after LD.

3.5.2 CW Laser with 532 nm Wavelength

Fig. 3.7 shows the surface image after CW-laser with 532 nm wavelength irradiation to different reflectance of PSG film. Fig. 3.7 (a) and (b) show the surface morphology after LD at the reflectance of 37.0 % with 190 nm-thickness and 30.0 % with 330 nm-thickness at 532 nm wavelength, respectively. These images showed that there were no laser traces after LD in both case of reflectance of PSG film. However, different doping profile, especially different doping depth was confirmed as shown in Fig 3.8. The doping depth in the case of lower reflectance of PSG film was around 1000 nm. By contrast, the doping depth in the case of higher reflectance of PSG film was around 100 nm. These are due to high laser fluence on the surface in the case of lower reflectance of PSG film. Thus, high laser fluence on the surface induced deep melting depth. Consequently, doping depth in the case of lower reflectance of PSG film was deeper than that of higher reflectance of PSG film. On the other hand, in the case of higher reflectance of PSG film, the concentration of doping atoms after LD from the surface to 50 nm in doping depth was higher than that of lower reflectance of PSG film. This can be explained by the mechanism of doping in the case of a limited dopant source.18) Therefore, the doping process in this condition can be given by the Gaussian function:

$$C(\mathrm{x},\mathrm{t}) = \frac{S}{\sqrt{\pi D t}}\left(-\frac{x^2}{4Dt}\right) \tag{3.1}$$

Where *S*, *D*, *x*, and *t* are the total amount of dopant atoms [cm^{-3}], diffusivity [cm^2/s], distance [cm], and diffusing time [s], respectively.

Assuming the limited dopant atoms in the PSG film, in both case of reflectance, the concentration of dopant atoms near surface could depend on the depth of melting. Moreover, the surface images of after LD as shown in Fig. 3.7 suggested that there is no ablation of materials in both case of reflectance. Thus, in the case of low reflectance of PSG film, the reason of low concentration of doping near surface is the deep depth of melting due to high laser fluence on the surface. These results showed that the reflectance of PSG film influences to doping profile, especially depth of doing strongly depends.

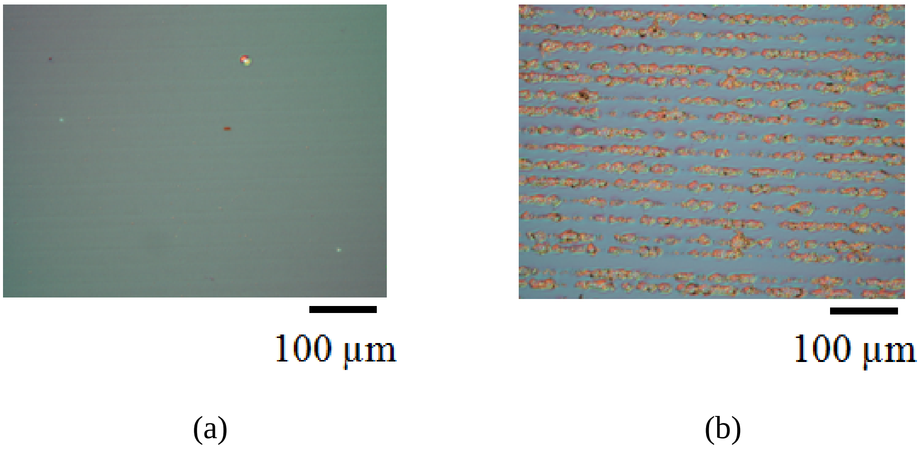

Figure 3.5: Surface image after pulsed-laser with 355 nm wavelength irradiation to different reflectance of PSG film. (Before PSG removal)
(a) Reflectance of 58.0 % with 240 nm-thickness
(b) Reflectance of 30.0 % with 180 nm-thickness

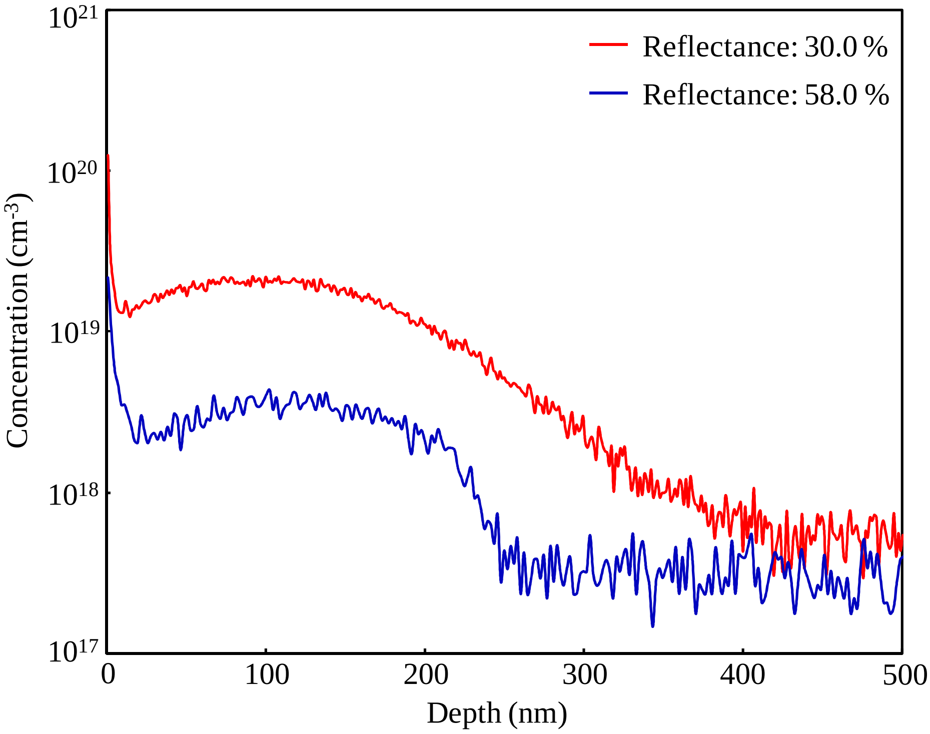

Figure 3.6: Doping profile of after LD with different reflectance of PSG films. (Pulsed-laser with 355 nm wavelength)

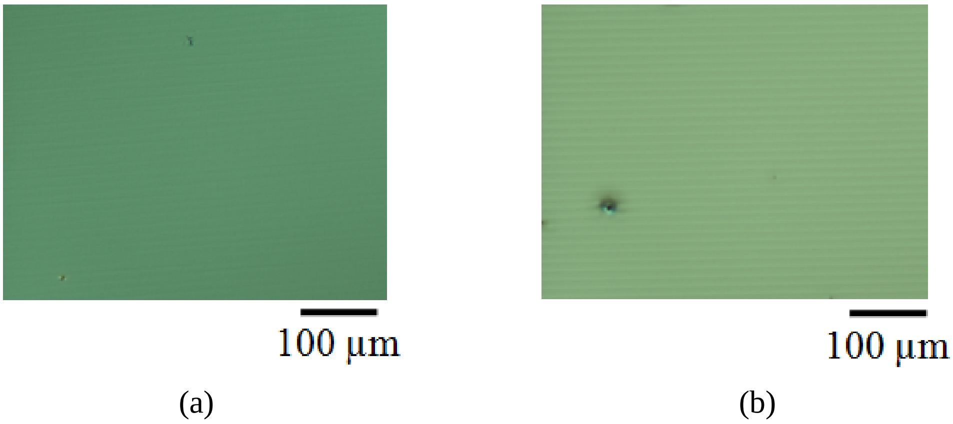

(a) (b)

Figure 3.7: Surface image after CW-laser with 532 nm wavelength irradiation to different reflectance of PSG films. (Before PSG removal)

(a) Reflectance of 37.0 % with 190 nm-thickness

(b) Reflectance of 30.0 % with 330 nm-thickness

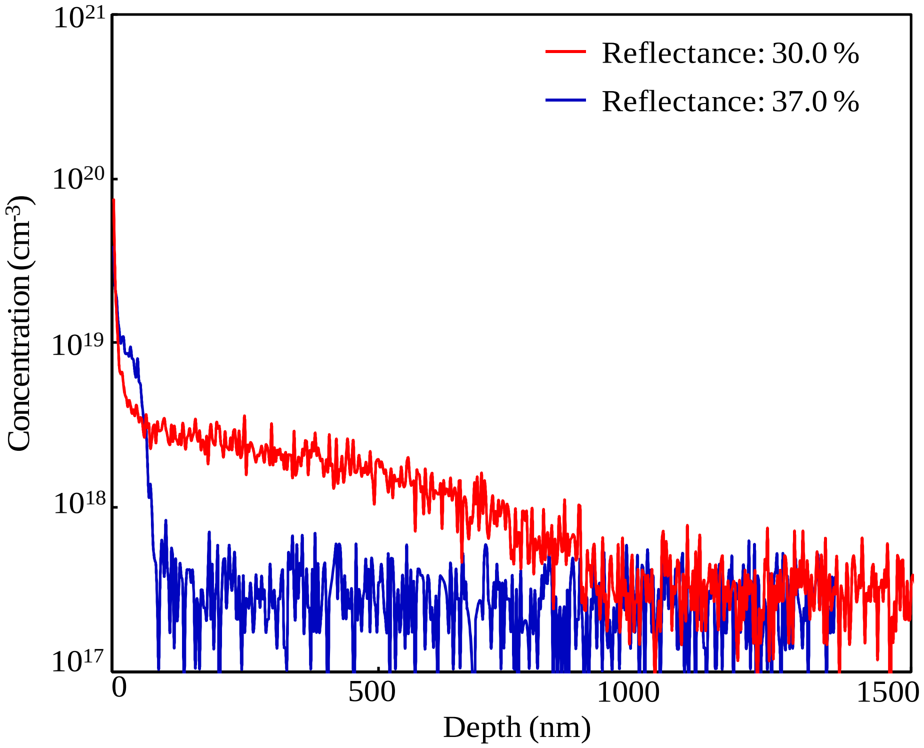

Figure 3.8: Doping profile of after LD with different reflectance of PSG films. (CW-laser with 532 nm wavelength)

3.6 Summary

The investigation of dopant precursor film for optimization of LD, especially focused on reflectance of dopant precursor film, was carried out. The dopant precursor film, namely PSG film was formed by the sputtering proposed as a new method for uniform film formation. A calculation of reflectance of PSG film at a specific wavelength which is laser wavelength predicted that the reflectance of PSG film is depended on PSG film thickness. The reflectance of PSG film formed by the sputtering method agreed well with calculations in the margin of error within 1.5 %. This indicated that various reflectance of PSG film can be formed and controlled by the sputtering method.

The controlled reflectance of PSG film, in the case of pulsed-laser with 355 nm wavelength, impacted on doping profile not only for the depth of doping, but also the concentration. These related to laser fluence due to reflectance of dopant precursor film. In the case of CW-laser with 532 nm wavelength, also influenced to doping profile. In particular, the depth of doping strongly depended on the reflectance of PSG film.

Further progress, the influence of reflectance of PSG film to LD has to investigate more detail. The results in this study do not enough to reveal the correlation between the reflectance of PSG film and LD. Because the doping profile which is doped by LD has a threshold for melting of silicon. More detail experiments will be clearly shown about correlations of optical properties on LD.

References of Chapter 3.

1) T. Sameshima, S. Usui, and M. Sekiya: J. Appl. Phys. **62(2)** (1987) 711.
2) C. Carlsson, A. Esturo-Breton, M. Ametowobla, J. R. Kohler, and J. H. Werner: Proc. of 21st European Photovoltaic Solar Energy Conf., 2006, p.938
3) T. C. Röder, S. J. Eisele, P. Grabitz, C. Wagner, C. Kulushich, J. R. Köhler, and J. H. Werner: Prog. Photovoltaics: Res Appl. **18**, (2010) 505.
4) B. S. Tjahjono, J. H. Guo, Z. Hameiri, L. Mai, A. Sugianto, S. Wang, S. R. Wenham: Proc. of Proc. 22nd European Photovoltaic Solar Energy Conf., 2006, p.938
5) A. Sugianto, B. S. Tjahjono, J. H. Guo, and S. R. Wenham: Proc. of Proc. 22nd European Photovoltaic Solar Energy Conf., 2007, p.1759
6) S. Hopman, A. Fell, K. Mayer, M. Aleman, M. Mesec, R. Müller, D. Kray, G. P. Willeke: Proc. of 22nd European Photovoltaic Solar Energy Conf., 2007, p.1261
7) A. Rodofili, A. Fell, S. Hopman, K. Mayer, G. P. Willeke, D. Kray, S. W. Glunz: Proc. of Proc. 23rd European Photovoltaic Solar Energy Conf., 2008, p.1808
8) H. Masuhara, et al.: *Handbook of Application of Laser Processing*, p.27 (in Japanese)
9) S. Eisele, G. Bilger, M. Ametowobla, J. R. Köhler, and J. H. Werner: Tech. Dig. of 17th Int'l Photovoltaic Solar Energy Conf., 2007, p.716
10) S. J. Eisele, M. Sämann and G. Bilger: Surf. Interface Anal. **42**(2010) 1573.
11) K. Wada et al, "Sputtering Technology" (in Japanese)
12) T. Funatani, NAIST Master Thesis (in Japanese)

13) A. Ogane, K. Hirata, K. Horiuchi, Y. Nishihara, Y. Takahashi, A. Kitiyanan, and T. Fuyuki: Jpn. J. Appl. Phys. **48** (2009) 071201.

14) A. Grohe, T. Wütherich, A. Knorz, J. Nekarda, N. Mingirulli, C. Harmel, R. Preu, S. Glunz: Proc. of Proc. 22st European Photovoltaic Solar Energy Conf., 2006, p.1751

15) M. A. Green: *SILICON SOLAR CELLS Advanced Principles & Practice* (University of New South Wales, Sydney, 1995), p. 334

16) S. Hermann, N-P. Harder, R. Brendel, D. Herzog, H. Haferkamp: Appl. Phys. A., **99** (2010) 151.

17) J. R. Köhler and S. Eisele: Prog. Photovoltaics: Res Appl. **18** (2010) 334.

18) S. M. Sze: *Physics of Semiconductor Devices* (Wiley, New York, 1981) 2nd ed., p.67

Chapter 4

Application of Laser Doping to Silicon Solar Cell Emitter

4.1 Introduction

The conventional silicon solar cell process in formation of pn junction method is a thermal diffusion. This method operates at high temperature and needs long time for forming a pn junction. This is caused by the diffusivity in solid silicon approximately 1.0×10^{-14} cm^2/s.(1) The typical pn junction formation in silicon solar cells takes for 30 min.(2,3) LD is an attractive method as an alternative to the conventional c-Si solar cell fabrication process. LD achieved the impurity doping in very short time at room temperature and in air ambience. Because, LD induces silicon melting and, the impurity is incorporated during re-crystallization after laser irradiation.(4) In addition, LD can widely control the doping depth depended on the laser irradiation conditions as revealed in chapter 2.

In this chapter, LD was applied to the fabrication of c-Si solar cells. LD can form a doping layer at room temperature and in air ambience. Thus, the doping layer which is formed LD becomes an emitter in the c-Si solar cells. A laser-doped emitter was optimized for the c-Si solar cell emitter. For optimization of the c-Si solar cell emitter formed by LD, the laser irradiation conditions were investigated. The optimum condition of laser irradiation for emitters was investigated to the c-Si solar cell fabrication process as an alternative to the conventional method.

4.2 Optimization of Laser Doping for Crystalline Silicon Solar Cell Emitter

For an application of LD to the c-Si solar cell emitter, LD needs to optimize the irradiation condition. The laser irradiation conditions are its output power, focus and scanning speed, respectively. The doping profile was verified in chapter 2 that the doping depth depended on the laser irradiation condition. In particular, the laser output power strongly gave a dependency of doping depth. The doping depth was widely controlled by the laser output power from around 0.5 µm to 4.0 µm as revealed in chapter 2.

In the experiment, the substrate, 0.1-2 Ωcm 300-µm-thick, p-type, Cz, (100)-orientation substrate was used as the base silicon substrate. The procedures for the fabrication of c-Si solar cells with LD were carried out as shown in Fig. 4.1. For the LD process, the laser irradiated on the PSG coated surface. The doped area was accomplished by moving the stage on which a sample was mounted during laser irradiation; an xy-translation stage was moved from edge to edge of sample surface. These operations were repeated to complete for full surface doping. The completed samples with full surface LD were dipped into HF solution to remove the residual PSG after LD. To form contact electrodes, the electrodes were evaporated using silver (Ag), titanium (Ti) on the front, and aluminum (Al) on the rear side. The space between front side electrodes was 650 µm. The rear side electrodes were 800 µm to cover full surface. The completed c-Si solar cells fabricated by LD were measured by the solar simulator which has the intensity of illumination at 100 mW/cm^2. Usually, this measurement is carried out in air mass (A.M.) 1.5.5) The evaluation method of solar cell properties was shown in Appendix B. No other techniques to improve the c-Si solar cell performance, such as texturization, passivation or antireflective coating (ARC), were applied. The reason why no other techniques were carried out this section tries to optimize LD for the fabrication of c-Si solar cells independently.

4.2.1 Laser Output Power

Fig. 4.2 shows the characteristics of illuminated solar cell with laser-doped emitter which formed at different laser output powers. The laser output power for LD was controlled in the range from 1.0 W to 5.0 W. Note in this experiment, the laser irradiation condition of focus and scanning speed were at approximately – 80 µm and 6.0 cm/s, respectively. The results demonstrated all of samples with laser-doped emitter excluding at 1.0 W operated as solar cells. It is considerable that the sample fabricated by LD at 1.0 W had insufficient

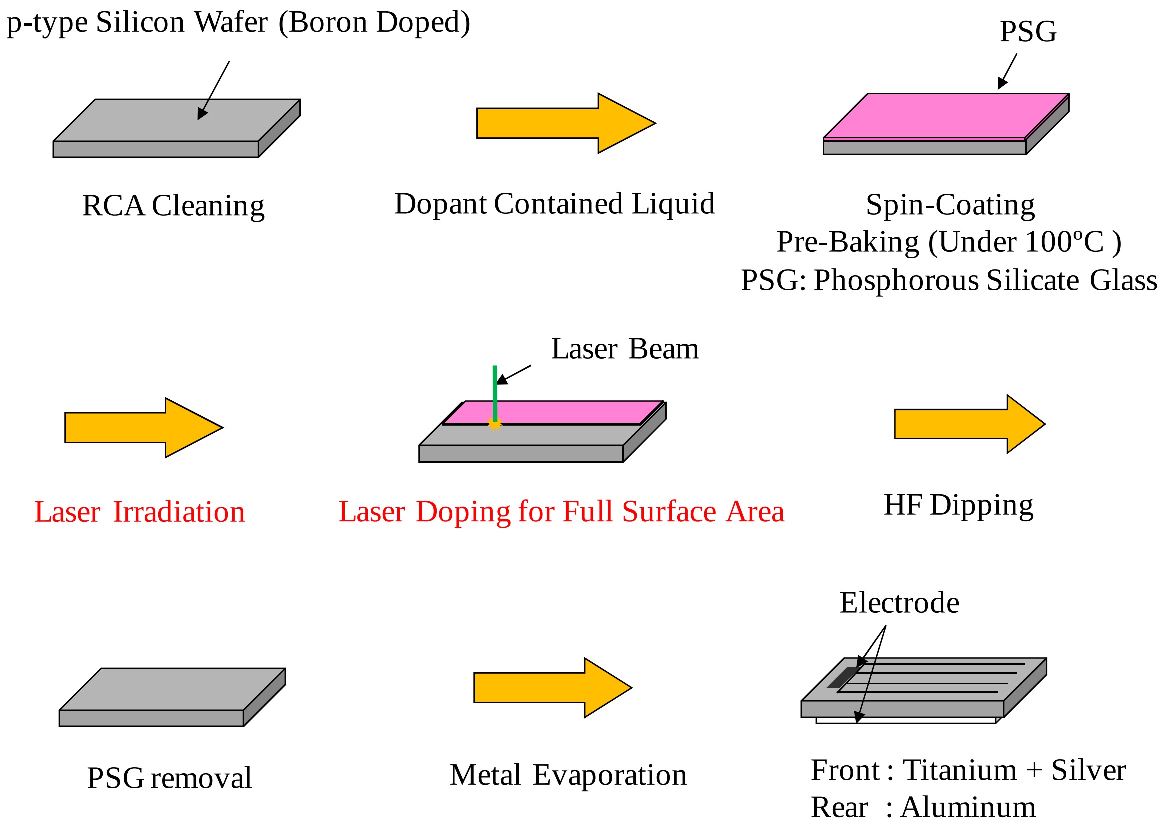

Figure 4.1: Procedures for fabrication of c-Si solar cells with LD.

doping impurity in emitter to be operated as solar cells. The photovoltaic properties were summarized in Table 4.1. In comparison of photovoltaic properties, the short current density (J_{sc}) of the samples with laser-doped emitter at 2.0 W and 3.0 W was higher than at 4.0 W and 5.0 W. By contrast, the open circuit voltage (V_{oc}) of the samples with laser-doped emitter at 2.0 W and 3.0 W was lower than at 4.0 W and 5.0 W. These are due to the formation of shallower depth of pn junction at 2.0 W and 3.0 W than at 4.0 W and 5.0 W as confirmed in Fig. 2.5. For fill factor (F.F.), the F.F. increased with the laser output power excluding at 4.0 W. The reason of the low F.F. value at 4.0 W was probably creating a defect with discontinuous recrystallization during laser irradiation.6) The highest F.F. obtained up to 64.6 % at 5.0 W in the samples with laser-doped emitter. Eventually, the highest efficiency of fabricated solar cells with laser-doped emitter which formed at different laser output powers resulted in up to 4.2 % at 5.0 W. Thus, the optimum irradiation condition of laser output power should be at 5.0 W in this thesis.

4.2.2 Laser Focus

Fig. 4.3 shows the characteristics of illuminated solar cell with laser-doped emitter which formed at different laser focus distances. The laser focus distance was changed in the range from 0 µm (focal point of objective lens) to – 100 µm. Note in this experiment, the laser irradiation condition of laser output power and scanning speed were at 5.0 W and 6.0

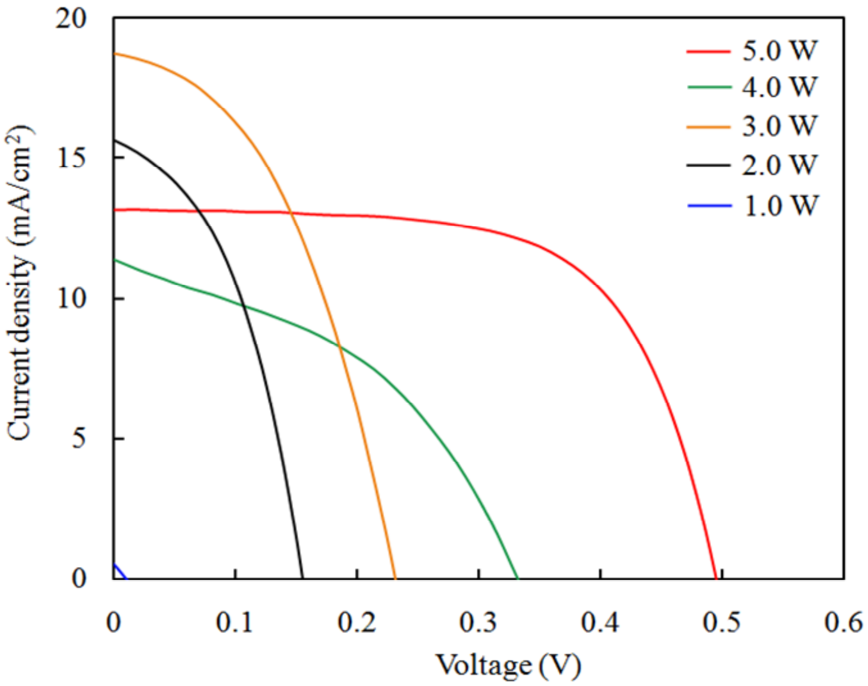

Figure 4.2: Characteristics of illuminated solar cell with laser-doped emitter which formed at different laser output powers.

Table 4.1: Properties of illuminated solar cell with laser-doped emitter formed at different laser output powers.

Laser output power	V_{oc} (mV)	J_{sc} (mA/cm^2)	F.F. (%)	Eff. （%）
1.0 W	1	0.5	25.1	0
2.0 W	155	15.7	43.5	1.1
3.0 W	231	18.7	43.7	1.9
4.0 W	332	11.4	42.3	1.6
5.0 W	495	13.1	64.6	4.2

cm/s, respectively. The results demonstrated that the characteristics depended on the laser focus condition. This is due to the dependence of doping profile on the laser focus as shown in Fig. 2.6. The photovoltaic properties were summarized in Table 4.2. In comparison of photovoltaic properties, the J_{sc}, V_{oc}, and F.F. of the samples increased with the outer focus condition. In particular, the F.F. at – 100 µm drastically increased. This strongly relates to state of silicon after laser irradiation as shown in Fig. 2.7 and 2.8. The obtained highest efficiency of laser-doped emitter which formed at different focus distances resulted in up to 4.0 % at - 100 µm. Thus, the optimum irradiation condition of focus should be at – 100 µm in this thesis.

4.2.3 Laser Scanning Speed

Fig. 4.4 shows the characteristics of illuminated solar cell with laser-doped emitter which formed at different laser focus distances. The laser focus distance was changed in the range from 0 µm (focal point of objective lens) to – 100 µm. Note in this experiment, the laser irradiation condition of laser output power and scanning speed were at 5.0 W and 6.0 cm/s, respectively. The results demonstrated that the characteristics depended on the laser scanning speed. The photovoltaic properties were summarized in Table 4.3. Especially, F.F. strongly depended on the laser scanning speed. In the case of 1.0 cm/s, it is considered that silicon is slowly recrystalization. However, other photovoltaic properties were the lowest at

1.0 cm/s. This is due to the deepest doping depth compared with other scanning speed as shown in Fig. 2.12. By contrast, the fastest scanning speed at 10.0 cm/s resulted in lowest F.F.. It is considered that a defect or dislocation probably created during recrystallization because of rapid cooling of molten silicon. The obtained highest efficiency of laser-doped emitter which formed at different laser scanning speeds resulted in up to 2.7 % at 6.0 cm/s. Thus, the optimum laser irradiation condition of scanning speed should be at 6.0 cm/s in this thesis.

4.3 Electrical Properties of Optimum Laser Doped Emitter

The optimum irradiation conditions for the fabrication of c-Si solar cells were summarized in Table 4.4. In this section, the electrical properties were investigated about the laser-doped emitter using optimum condition in focus and scanning speed. Only laser output power was controlled in the range from 2.0 W to 5.0 W again to investigate the effect of LD with optimum irradiation conditions. For the investigation of the optimum laser-doped emitter, the four-point probe method and the dark current-voltage measurement were performed to reveal the sheet resistance and pn junction diode characteristics, respectively. As a reference sample, c-Si solar cells were fabricated by a conventional solid phase thermal diffusion method. In condition of the conventional thermal diffusion, time of diffusion, temperature, and ambient gas were for 30 min, at 900ºC, and in N_2, respectively. Comparing with the reference sample is to find out a potential of LD for c-Si solar cells.

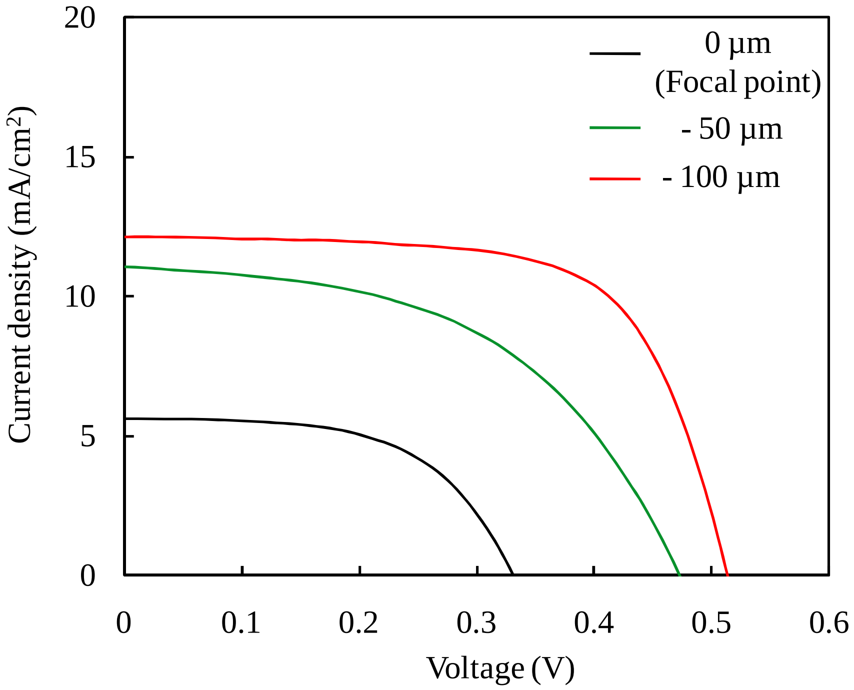

Figure 4.3: Characteristics of illuminated solar cell with laser-doped emitter formed at different laser focus distances.

Table 4.2: Properties of illuminated solar cell with laser-doped emitter formed at different laser focus distances.

Focus distance	V_{oc} (mV)	J_{sc} (mA/cm^2)	F.F. (%)	Eff. （%）
0 µm (Focal point)	330	5.6	57.4	1.1
- 50 µm	478	10.7	58.9	3.0
- 100 µm	531	11.5	67.7	4.0

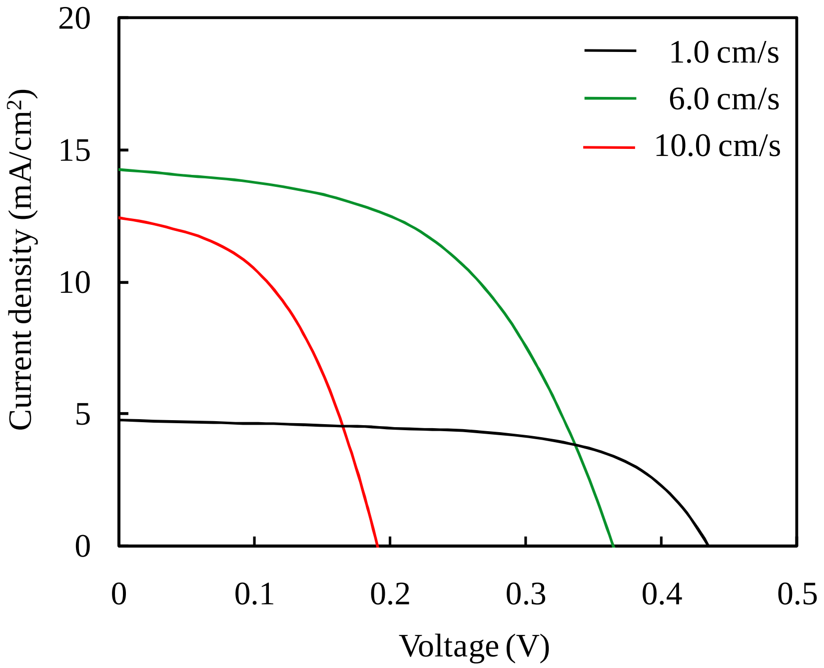

Figure 4.4: Characteristics of illuminated solar cell with laser-doped emitter formed at different laser scanning speeds.

Table 4.3: Properties of illuminated solar cell with laser-doped emitter formed at different laser scanning speeds.

Scanning speed	V_{oc} (mV)	J_{sc} (mA/cm^2)	F.F. (%)	Eff. （%）
1.0 cm/s	435	4.8	62.1	1.1
6.0 cm/s	364	14.2	52.0	2.7
10.0 cm/s	191	12.4	47.4	1.3

Table 4.4: Optimum conditions of laser irradiation for fabrication of c-Si solar cells.

Laser output power	Focus (direction)	Scanning speed
5.0 W	- 100 µm	6.0 cm/s

4.3.1 Dark Current-Voltage Characteristics of Laser-Doped Emitter

Fig. 4.5 shows the dark current-voltage characteristics of pn junctions of c-Si solar cells formed by LD, compared with p-n junctions formed by the thermal diffusion. The dark current-voltage characteristics were measured by using the semiconductor parameter analyzer (Precision Semiconductor Parameter Analyzer, Agilent). The samples for dark current-voltage characterization were measured current results at every 0.02 V when voltage was changing from – 0.6 V to + 0.6 V. As all of the laser-doped samples certainly showed the diode characteristics, the formation of p-n junction by LD at room temperature and in air ambience was verified. However, while the thermal diffused sample gave the clear 2-step slope (recombination current region and diffusion current region) and enough low reverse current, laser-doped samples showed higher reverse current and recombination current at low forward voltage.7) In addition, the slope angles of laser-doped samples at high forward voltage were lower than that of thermal diffusion except for the case of laser output power at 5.0 W, indicating higher series resistance.7) Because the minority carrier moved horizontal to the junction in the emitter layer due to the finger electrodes, this high series resistance was caused by the high sheet resistance. As laser output power dependence, lines became closer to the case of thermal diffusion with increasing of laser output power. This indicates there should be optimum laser output power at 5.0 W for pn junction formation by LD.

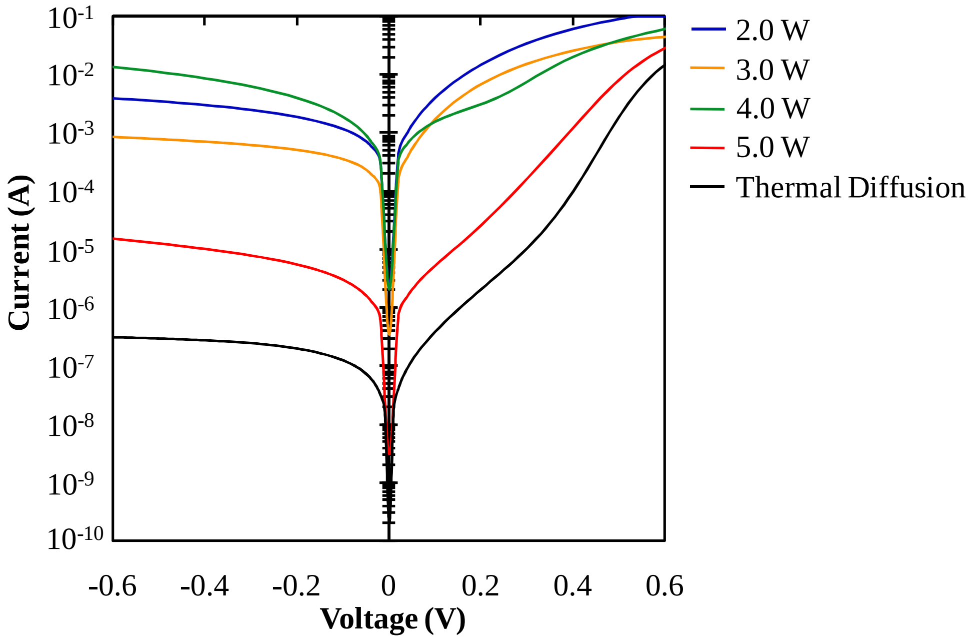

Figure 4.5: The dark current-voltage characteristics of pn junctions of c-Si solar cells formed by LD, compared with p-n junctions formed by the thermal diffusion.

4.4 Crystalline Silicon Solar Cells Fabricated by Laser Doping

The optimum conditions for the fabrication of c-Si solar cells were verified as shown in Table. 4.2. The dark current-voltage characteristics of pn junctions of c-Si solar cells formed by LD at room temperature and in air ambience were performed sufficiently. In this section, c-Si solar cells were fabricated by LD with passivation and ARC. The reason why other technique to improve c-Si solar cells were not performed is to reveal the potential of complete c-Si solar cells with LD. The ARC was deposited on the front surface of samples by Plasma Enhanced Chemical Vapor Deposition (PE-CVD) method. The film material of passivation and ARC is SiN_x. The SiN_x film deposited approximately 75 nm measured by ellipsometer. The NH_3 treatment and deposition of SiN_x film in PE-CVD chamber was taken for 5 min, respectively.

Table 4.5 shows the condition of deposition of SiN_x films. Prior to the deposition of SiN_x films, the NH_3 plasma treatment was carried out. Because, this treatment can expect that the effective surface passivation for c-Si solar cells is obtainable even if treated at quite low temperature below 300°C.[8)] As a reference, the samples were fabricated by thermal diffusion. The conditions of thermal diffusion were same as section 4.3.

For the investigation of laser-doped c-Si solar cells, current-voltage characteristics under illuminated, internal quantum efficiency (IQE), and electroluminescence (EL) were measured, respectively.

4.4.1 Characteristics of Illuminated Laser-Doped Crystalline Silicon Solar Cells

Fig. 4.5 shows the characteristics of illuminated laser-doped crystalline silicon solar cells. These solar cells were fabricated by LD with the output power in the range from 2.0 W to 5.0 W. The photovoltaic properties of laser-doped c-Si solar cells were summarized in Table 4.6. These results indicated that the optimum laser irradiation condition for the fabrication of c-Si solar cells with ARC film was at 5.0 W of laser output power. In addition, all of properties depended on the laser output power. In the case of 5.0 W, the properties were mostly similar to the reference that was fabricated by the conventional thermal diffusion. Especially, V_{oc} was almost same value. However, J_{sc} and F.F. resulted in poorer than that of reference. Being lower J_{sc} in laser-doped cells is due to deeper doping depth than the reference.6) Thus, the photo-active (light-absorption) area between fingers had heavy recombination compared with the reference. Being low F.F. in laser-doped cells is probably due to the inhomogeneous doping by LD.

Table 4.5: Conditions of deposition of SiNx films by PE-CVD.

Gas	NH_3 plasma treatment	SiNx deposition
SiH_4 (sccm)	0	50
NH_3 (sccm)	200	80
N_2 (sccm)	0	100
RF (W)	40	40
Pressure (Pa)	80	80
Temperature (°C)	300	300

sccm: standard cc/min

RF: Radiofrequency

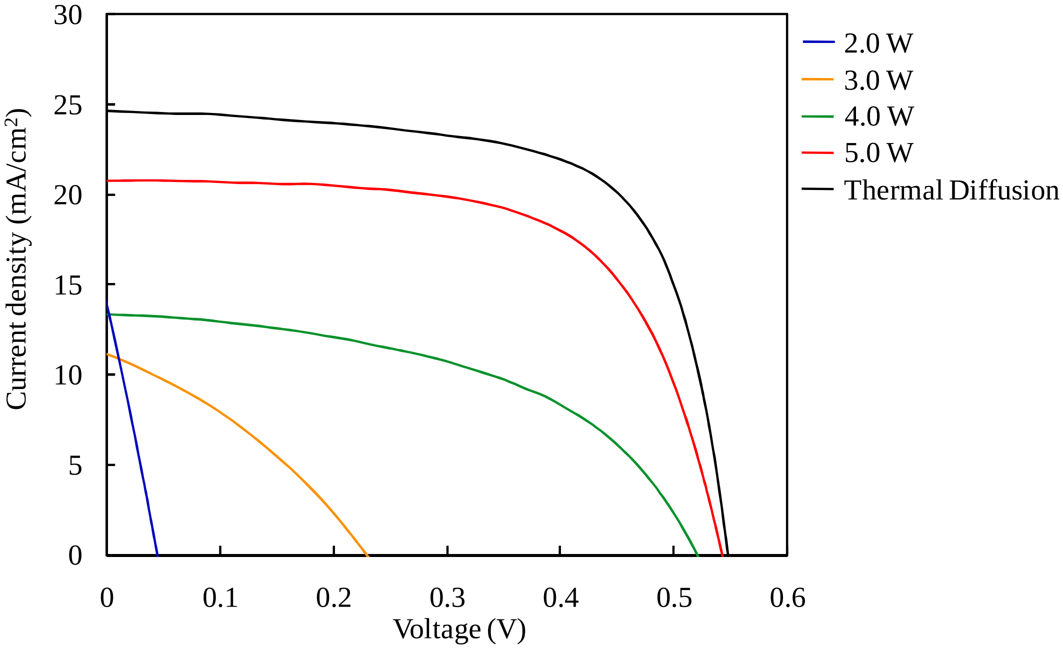

Figure 4.6: Characteristics of illuminated laser-doped c-Si solar cells with ARC.

Table 4.6: The solar cell properties of laser-doped c-Si solar cells with ARC.

Laser output power	V_{oc} (mV)	J_{sc} (mA/cm^2)	F.F. (%)	Eff. (%)
2.0 W	45	14.1	26.6	0.2
3.0 W	230	11.2	33.2	0.9
4.0 W	520	13.4	49.1	3.4
5.0 W	543	20.8	64.2	7.3
Thermal Diffusion	547	24.6	67.3	9.1

Table 4.7 shows the solar cell properties of illuminated laser-doped c-Si solar cells before or after deposition of SiN_x film. These results indicated that the deposition of SiN_x film improved the laser-doped c-Si solar cells. In particular, the V_{oc} was considerably improved compared with the reference. In the case of reference, the decrease of V_{oc} is due to the damage induced plasma. By contrast, in the case of laser-doped c-Si solar cell, the increase of V_{oc} is probably due to the improvement of surface statement. Thus, the laser-doped surface was cleaned by NH_3 plasma treatment.8) Indeed, the LD incorporates not only a dopant but also other impurities simultaneously because of the performance in air ambience.9) The other impurities, especially carbon which is a contamination to silicon reduces the minority carrier lifetime which affects to the solar cell performances. An original surface treatment toward LD should be developed in further progress.

4.4.2 Internal Quantum Efficiency of Laser-Doped Crystalline Silicon Solar Cells

Fig. 4.7 shows the internal quantum efficiency (IQE) of laser-doped c-Si solar cells against the reference. The laser-doped cells only at 4.0 W and 5.0 W samples demonstrated in IQE measurement. The results of IQE were shown that the laser-doped c-Si solar cells were the lower response in the short wavelength region in the range from 400 nm to 600 nm, compared with the reference. Thus, this indicated that the pn junction of LD formed deeper depth than the reference. In further progress, the LD depth should be shallower to improve the short wavelength response as the reference or applied to other type of c-Si cell structures, particularly back-junction type of solar cells.10, 11)

4.4.3 Electroluminescence of Laser-Doped Crystalline Silicon Solar Cells

Fig. 4.8 shows the electroluminescence (EL) of laser-doped c-Si solar cells. Fig. 4.9 shows the line profile of EL intensity between indicated points. The image was taken by the cooled (at -55°C) silicon charge-coupled device infrared camera with 2 sec of exposure time, applying a 200 mA/cm^2 forward current. EL intensity reflects the total number of radiative recombination which is proportional to the total number of minority carriers (electrons) in p-type base layer.12) The total number of electron in base is determined by the injected carrier density from junction and the effective diffusion length of electron and then, EL intensity indicates the emitter or junction condition, assuming there is no distribution of effective diffusion length in mono-crystalline materials.12) The no uniformity of EL intensity between A and B showed the less injection of electron to base due to the voltage drop by series resistance which is caused by inhomogeneous doping. Thus, the EL intensity's decreasing explained the higher series resistance in emitter by LD.13) This result suggested that the F.F. could be increased with more uniform doping by LD in future progress.

Table 4.7: The solar cells properties of laser-doped c-Si solar cells before/after SiN_x film deposition, compared with the reference.

Laser output power	V_{oc} (mV)	J_{sc} (mA/cm^2)	F.F. (%)	Eff. (%)
LD before SiN_x depsition	495	13.1	64.1	4.2
LD after SiN_x deposition	543	20.8	64.2	7.3
Thermal Diffusion before SiN_x depsition	566	19.3	68.5	7.5
Thermal Diffusion after SiN_x deposition	547	24.6	67.3	9.1

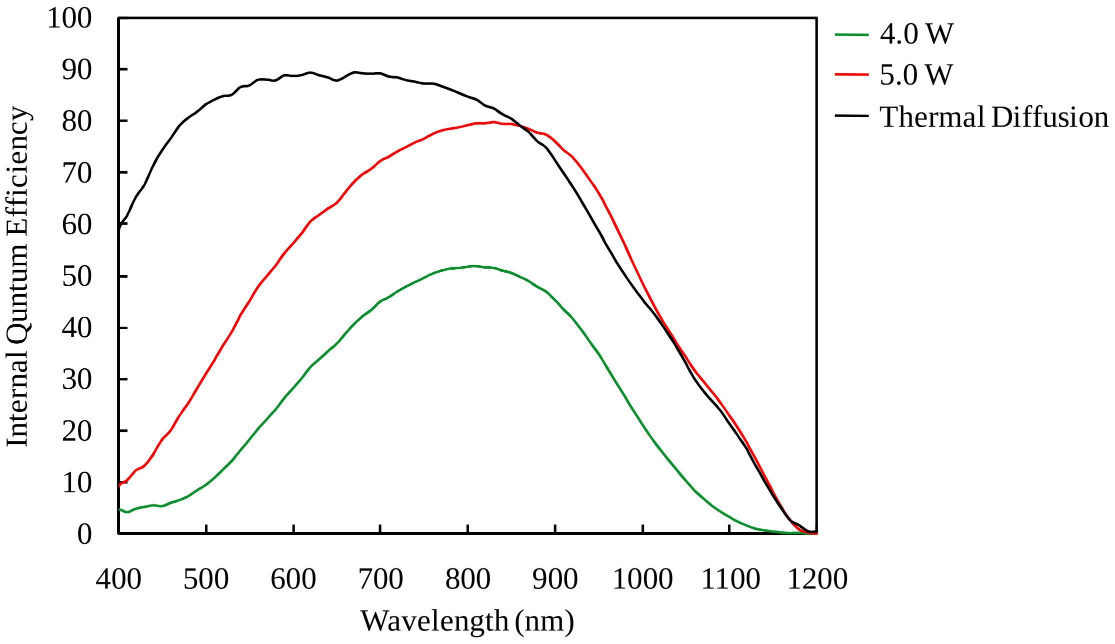

Figure 4.7: Internal Quantum Efficiency of laser-doped c-Si solar cells.

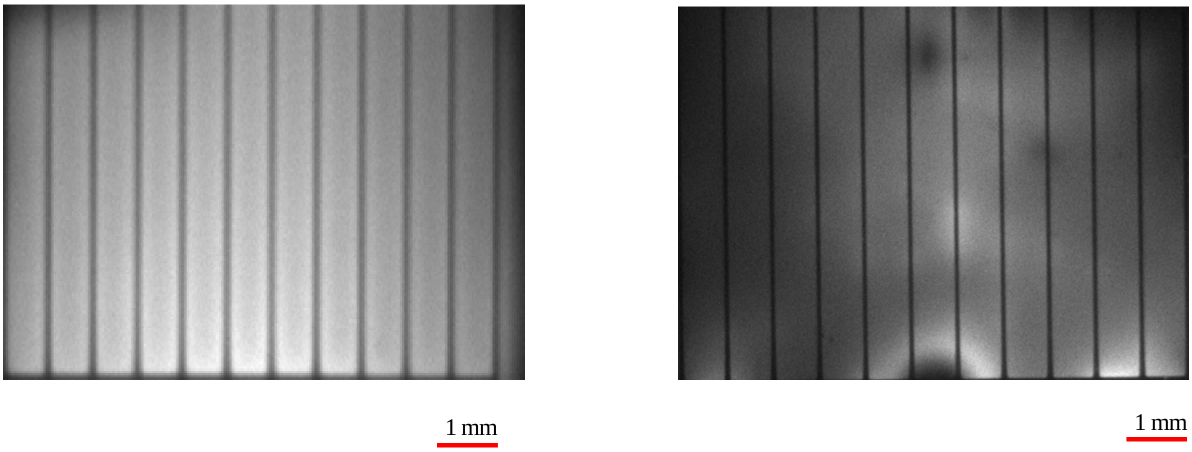

(a) (b)

Figure 4.8: Electroluminescence of c-Si solar cells. The image was taken by the cooled (at -55°C) Si CCD camera with 2 sec of exposure time, applying a 200 mA/cm^2 forward current. (Laser output power at 5.0 W)
(a) Thermal diffused sample (conventional method), (b) Laser doped sample

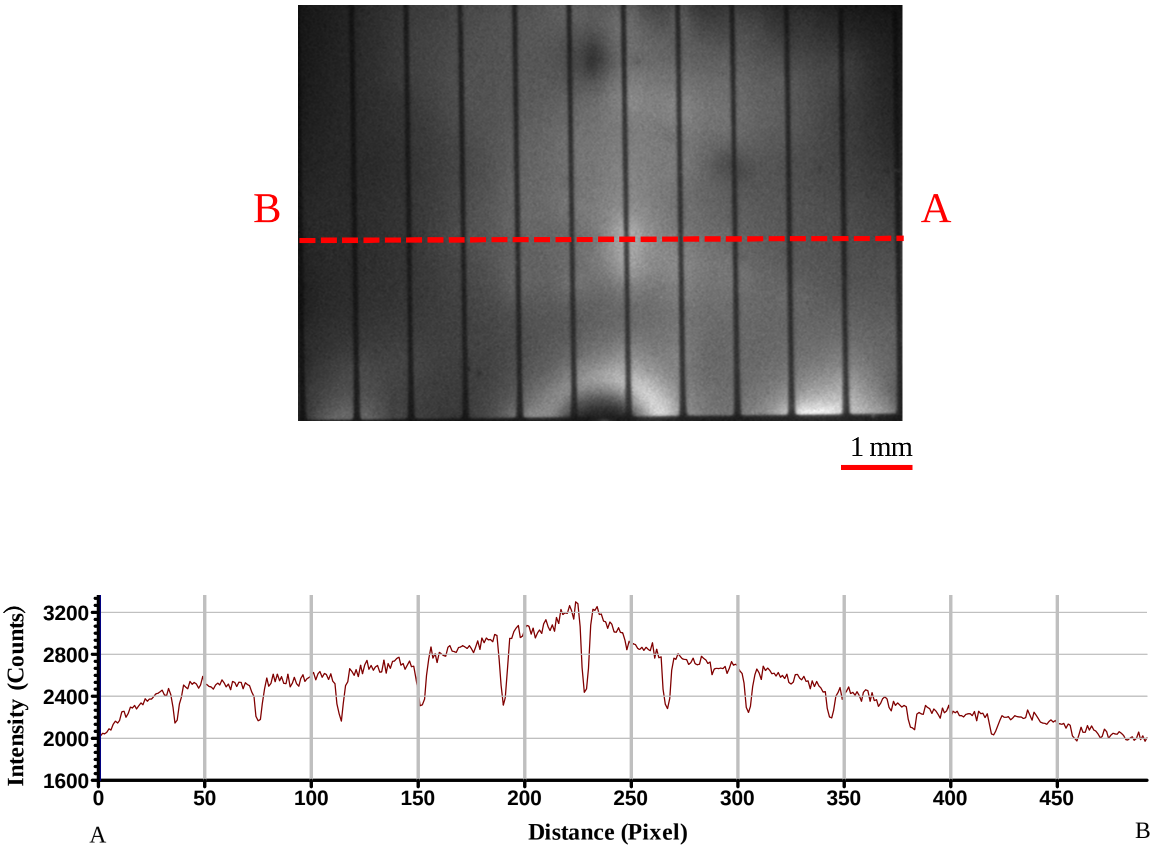

Figure 4.9: Line profile of EL intensity between A and B.

4.5 Summary

LD was applied to the fabrication of c-Si solar cells at room temperature and in air ambience. The conditions of laser irradiation in LD were optimized for the c-Si solar cell emitters. The optimum laser irradiation conditions for c-Si solar cell emitter were confirmed in this chapter. The formation of pn junction formed by LD was revealed to become similar characteristics to it formed by the conventional solid phase thermal diffusion.

The obtained results demonstrated that c-Si solar cells fabricated by LD in condition of optimum laser irradiation gave relatively similar photovoltaic properties to one fabricated by the conventional method. In particular, V_{oc} of laser-doped c-Si solar cells deposited with SiN_x film was considerably improved than thermal diffused c-Si solar cells. It is considered that surface of LD cleaned due to the effect of surface cleaning by NH_3 plasma. Thus, this indicated that development of surface treatment after LD for realizing the high conversion efficiency c-Si solar cells is important. The results of IQE indicated that laser-doped c-Si solar cells formed deeper pn junction than that of thermal diffused. Finally, EL was revealed that laser-doped c-Si solar cells emitted the inhomogeneous EL in 2 dimensions, probably due to the un-uniformity of doping by LD. The efficiency of laser-doped c-Si solar cells deposited with SiN_x film as ARC eventually obtained 7.3 %.

References of Chapter 4.

1) S. M. Sze: *Physics of Semiconductor Devices* (Wiley, New York, 1981) 2nd ed., p.68
2) M. A. Green: *SILICON SOLAR CELLS Advanced Principles & Practice* (University of New South Wales, Sydney, 1995), p.108
3) A. Ogane: NAIST PhD Thesis, p.106
4) T. Sameshima, S. Usui and M. Sekiya: J. Appl. Phys. **62(2)** (1987) 711.
5) A. Goetzberger and V. U. Hoffman: *Photovoltaic Solar Energy Generation* (Springer, Germany, 2005), p.88
6) Z. Hameiri, T. Puzzer, L. Mai, A. B. Sproul, and S. R. Wenham: Prog. Photovoltaics: Res. Appl. **19** (2011) 391.
7) S. M. Sze: *Physics of Semiconductor Devices* (Wiley, New York, 1981) 2nd ed., p.91
8) Y. Takahashi: NAIST PhD Thesis, p.64
9) A. Ogane, K. Hirata, K. Horiuchi, Y. Nishihara, Y. Takahashi, A. Kitiyanan, and T. Fuyuki: Jpn. J. Appl. Phys. **48** (2009) 071201.
10) K. R. McIntosh, M. J. Cudzinovic, D. D. Smith, W. P. Mulligan, R. M. Swanson: Proc. of 3rd World Conf. on Photovoltaic Energy Conversion, 2003, p. 971
11) F. Granek, M. Hermle, D.M. Huljic, O. Sultz-Wittmann, and S.W. Glunz1: Prog. Photovoltaics: Res. Appl. **17** (2009) 47.
12) T. Fuyuki, H. Kondo, T. Yamazaki, Y. Takahashi, and Y. Uraoka: Appl. Phys. Lett. **86**, (2005) 262108.

13) K. Bothe, P. Oohl, J. Schmidt, T. Weber, P. Altermatt, B. Fischer, and R. Brendel: Proc. of 2^{1st} European Photovoltaic Solar Energy Conf., 2006, p.597

Chapter 5

Crystalline Silicon Solar Cell with Selective Emitter Structured by Laser Doping

5.1 Introduction

In the fabrication of c-Si solar cells process, doping process is indispensable to form junctions. Now, instead of the conventional thermal diffusion method, laser doping (LD) technique is noticed as alternative.1-4) LD can easily control the doping depth of impurity in silicon by changing the laser power, pulse duration, or number of laser pulses.5-7) In addition, LD induces silicon melting and forms a doping layer in a short time, since the diffusivity in liquid silicon is up to 10 orders of magnitude greater than that in solid silicon.8,9) Thus, this is a simple and easy method for fabrication of low-cost and high-conversion-efficiency c-Si solar cells. These advantages can improve the fabrication yield, especially in the case of silicon substrates of less than 100 μm thickness, which lead to low-cost and high-conversion-efficiency c-Si solar cells. The application of LD to full surface doping for pn junction of solar cells has achieved efficiencies of up to 18.7%.10) Selective emitter formation for c-Si solar cells is very important to increase efficiency η.11, 12) Typical processes for the selective emitter formation require extra diffusion in the furnace and photolithography.13, 14) These can apply to form the selective emitter for c-Si solar cells. However, c-Si solar cells require additional treatment at these processes. For example, it needs deposition step of masks to become diffusion barriers, furnace diffusions, chemical etching and cleaning. C-Si solar cells are subjected to stress at each process step. These steps are time-consuming and result in additional costs.

In this chapter, the formation of selective emitter using LD at room temperature in air ambience was carried out. Moreover, the formation of selective emitter using LD was applied to the new-type of silicon substrate which is expected for realizing the stable high-conversion-efficiency c-Si solar cell. Therefore, the aim of this chapter is to reveal the effect of laser-doped selective emitter for solar cell performance and the feasibility of the selective emitter using LD for the high-conversion-efficiency c-Si solar cells.

5.2 Selective Emitter Features in c-Si Solar Cells

The selective emitter is very important to increase efficiency η of c-Si solar cells. The selective emitter gives improvement of c-Si solar cell properties with the features. The features of selective emitter were described as below, and the structure was shown in Fig.5.1.

1. Heavily doping underneath finger electrodes

2. Lower doping level between fingers
3. Deep depth of doping underneath fingers

The first feature gives less contact resistance between contact metal and semiconductor interface.15) Therefore, F.F. improves in solar cell properties. The second feature gives less Auger reconbination in photo active areas.16) Therefore, the spectra responce in the short wavelength is better as well as improved emitter passivation.16,17) The third feature gives the wider process window at contact firing process , thus avoiding metal spikes indued by co-firing step.15,18)

5.3 Selective Emitter Formation by Laser Doping to Furnace Diffused Emitter

The selective emitter was formed by laser irradiation to the furnace diffused emitter surface at room temperature. In particular, we tried to control the selective emitter depth in various pn junction depths to investigate the correlation between the diffused emitter and the selective emitter.

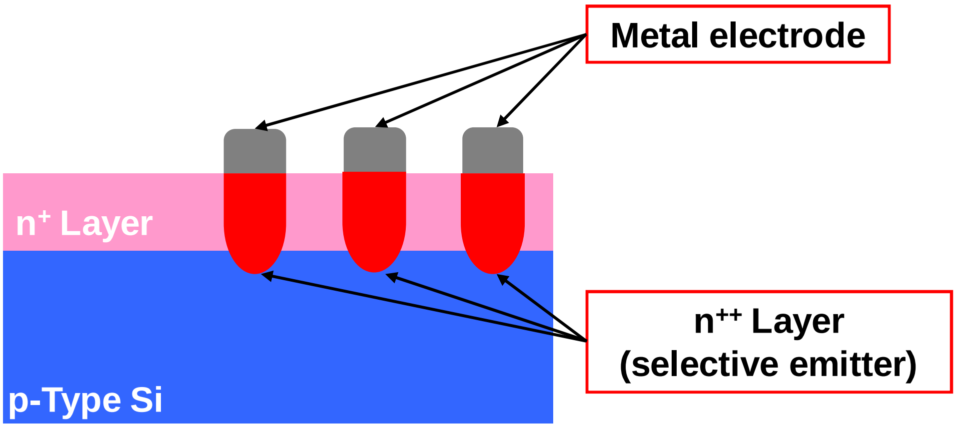

Figure 5.1: Structure of selective emitter in c-Si solar cells

5.3.1 Experiment

As the silicon substrate, 0.1-2 Ωcm 300 μm thick p-type Czochralski substrate was used. After RCA cleaning, phosphorous contained liquid was spun onto the substrate and baked on the hotplate at 100°C to obtain the solid phase doping precursor (PSG). The first step to form the pn junction for the carrier collection was performed by thermal solid phase diffusion at 900ºC in N_2 amibient for 30 and 90 minutes. And then, the selective emitter was formed underneath the finger electrode pattern by controlling the laser irradiation as shown in Fig. 5.2. The laser irradiated to residual PSG after thermal diffusion. A used laser to form the selective emitter was Nd: YVO_4 CW laser with 532 nm wavelength. The laser spot diameter on the sample surface, laser power and scanning speed were 6 μm, 5.0 W (maximum power) and 6 cm/s (then shifted 6 μm in y-direction), respectively. Doped area was accomplished by moving the stage on which a sample was mounted during laser irradiation; the selective emitter like the finger electrode pattern was formed by controlled xy-translation. After the irradiation of laser to form the selective emitter in c-Si solar cells, the residual PSG on the laser-irradiated surface was removed by HF dipping. Electrodes were evaporated using silver (Ag), titanium (Ti) on the front, and aluminum (Al) on the rear side. The space between front side electrodes was 650 μm. The selective emitter and front side electrode width were 250 μm and 50 μm, respectively. Fig. 5.3 shows the process sequence for the selective emitter formation in this section.

Evaluating the sheet resistance, the four-point probe measurement was performed. The secondary ion mass spectrometry (SIMS) measurement was performed to investigate the depth profile and dopant concentration. The doping depth and dopant concentration were compared in this measurement. No other techniques to improve the solar cell performance, such as texturization, passivation or antireflection coating (ARC), were applied to analyze the effect of selective doping independently.

5.3.2 Evolution of Sheet Resistance with Laser Doping

The results of sheet resistance measurement after laser irradiation were shown in Fig. 5.4. The pn junction was formed at different diffusing time to form deeper diffusion depth and reveal the sheet resistance dependence of laser power. The solid lines are given as a guide to the eyes about the evolution of sheet resistance at each measured data. The sheet resistance decreased at higher laser power in thermal diffusion for 30 min. However, this dependence slightly decreased at longer diffusing time for 90 min. This result indicated that there is probably the limitation of impurity doping in diffused layer.[19)]

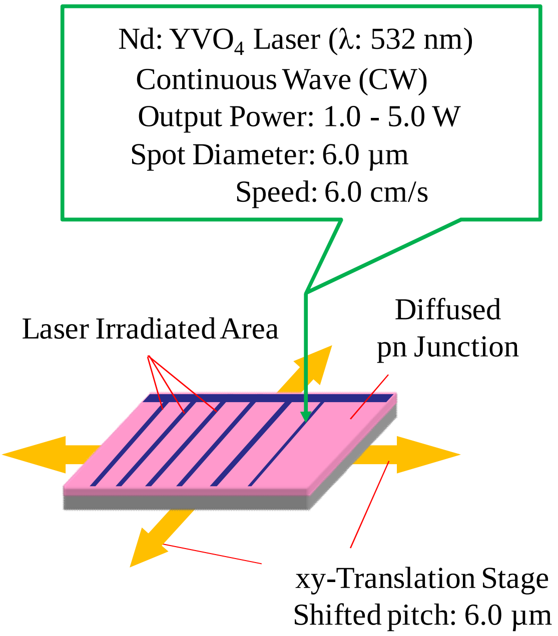

Figure 5.2: Schematic model of LD with 532 nm CW laser including parameters

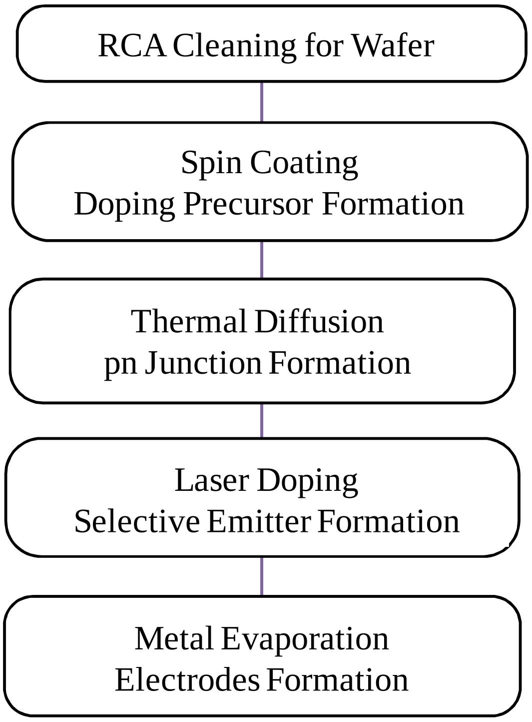

Figure 5.3: Process sequence of selective emitter formation by laser irradiation to residual dopant film after thermal diffusion

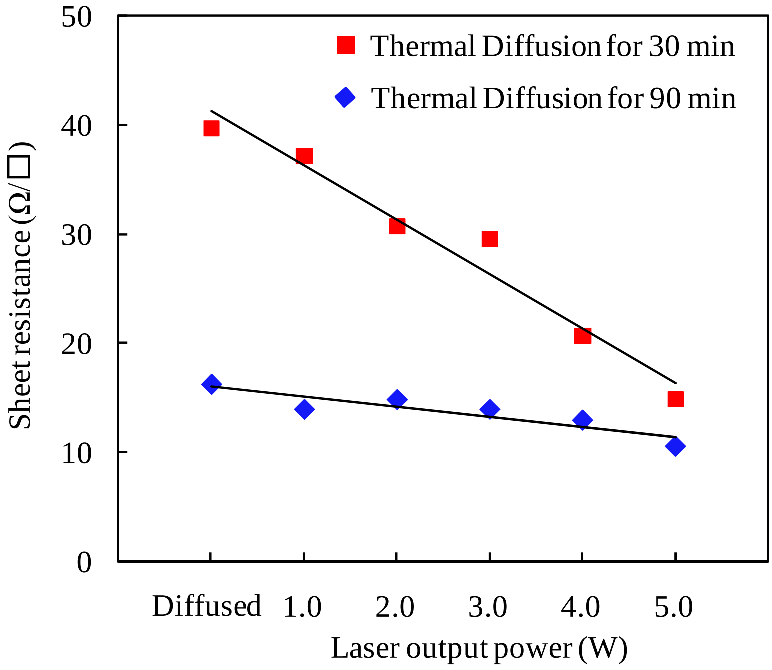

Figure 5.4: Evolution of sheet resistance with increase of laser output power.

5.3.3 Doping Profile after Laser Doping Evaluated by SIMS

The SIMS results which indicate the concentration of phosphorous atom doped into p-type silicon substrate comparing with every laser power were shown in Fig. 5.5. Fig. 5.5 (a) and (b) show the thermal diffusion to form the pn junction for 30 min and 90 min, respectively. In the case of thermal diffusion for 30 min, phosphorous atom near 400 nm was confirmed. Additional doping atom by laser irradiation into diffused emitter for selective emitter formation confirmed deeper depth which was laser-doped at the middle and high laser power (3.0 W and 5.0 W) than diffused emitter. However, the similar to the doping profile of diffused emitter was confirmed at low laser power (1.0 W). On the other hand, thermal diffusion for 90 min, phosphorous atom near 700 nm was confirmed. Additional doping atom by laser irradiation into diffused emitter for selective emitter formation confirmed deeper depth which was laser-doped at only high laser power (5.0 W) than diffused emitter. In the case of low and middle laser power (1.0 W and 3.0 W), the doping profile was similar to diffused emitter. These results indicate that there is melting threshold or silicon was melted at very near surface at low laser power (1.0 W). In the case of 90 min at middle laser power, the doping profile was similar to diffused emitter. This result is considered that melting region by laser was not affected by diffused atom (melting region around 500 nm); also high laser power was the same behavior in both cases (melting region between 600 to 700 nm). In spite of impurity was diffused in silicon, LD which induced melting of silicon is no effect to the doping profile. By contrast, doping concentration was reduced at high laser power. In particular, the doping concentration on surface in the case of 90 min was strongly decreased than that of 30 min. This is due to the limitation of dopant atoms in the precursor film formed surface.(20, 21) The dopant atoms in the precursor film diffused into silicon at the first step like thermal diffusion. Therefore, the poor atoms in the dopant precursor film were formed at the second step. Indeed, the dopant precursor film to form the selective emitter used the residual dopant after thermal diffusion in this study.

5.3.4 I-V Characteristics of Illuminated Solar Cell with Different Selective Emitter Profiles

It was shown in subsection 5.2.3 that the sheet resistance was reduced by laser irradiation and the evolution of sheet resistance depended on laser power. Moreover, additional doping by laser to form the selective emitter could be formed in the deeper depth Thus, formation of a different selective emitter profile through junction or not through junction was verified.

We investigated the correlation between the diffused emitter profile and selective emitter in the solar cell performance. The samples were prepared by the thermal diffusion to form pn junction. Subsequently, the laser irradiated to residual dopant film after thermal diffusion. Diffused emitters prepared two kinds of diffusing time and conditions of laser irradiation were same as the previous section. The fabricated c-Si solar cells were measured by the solar simulator to investigate the illuminated IV characteristics. Fig. 5.6 shows the IV characteristics of illuminated solar cells with various selective emitters. Fig. 5.6 (a) and (b) are the diffusion time to form the pn junction for 30 min and 90 min, respectively. The values of solar cell properties of illuminated solar cells were summarized in Table 5.1. Table 5.1 (a) and (b) are the diffusion time to form the pn junction for 30 min and 90 min, respectively. In the case of diffusion time for 30 min as shown in Fig. 5.6 (a), the characteristics of all samples were decreased by laser-doped selective emitter. In this case, the laser-doped selective emitter formed through pn junction except for LD at low laser power (1.0 W) but it was formed nearby pn junction. On the other hand, in the case of diffusion time for 90 min as shown in Fig. 5.6 (b), the characteristics of samples with selective emitters doped at low and middle laser power (1.0 W and 3.0 W) were improved. These laser-doped selective emitters formed far from the depth of pn junction. The reason of V_{oc} increasing is probably induction of heat by the laser near surface for incorporating additional dopant atoms underneath fingers. Thus, it reduced doping level between fingers resulted in improvement of J_0 inside emitter.12) The reason of J_{sc} increasing is the improvement of blue response in the solar cell. However, characteristics were reduced at high laser power (5.0 W). This laser-doped selective emitter was formed nearby pn junction. Consequently, if the selective emitter reached nearby and through pn junction, the solar cell properties would be decreased. By contrast, if the selective emitter existed far from pn junction, namely near surface, they would be improved. These results indicated that selective emitter using LD need to optimize its depth. The F.F., in the case of diffusion time for 30 min, laser output power at 1.0 W and 3.0 W was improved. This is due to the reduction of series resistance (R_s) in c-Si solar cells as verified in Table 5.1 (a). By contrast, laser output power at 5.0 W was resulted in the decrease of F.F., in spite of the reduction of series resistance. This is probably due to the creation of shunts by high density of dopant in emitter or break of diffused pn junction. In addition, the shunts might be also created by laser induced damage.23) On the other hand, in the case of diffusion time for 90 min, all samples were resulted in the decrease of F.F.. This is also the same reason with that of diffusion time for 30 min.

Fig. 5.7 shows the dependence of series resistance of c-Si solar cells on laser output power. The solid lines are given as a guide to the eyes about the evolution of series resistance at each measured data. As shown in Fig. 5.7, the series resistance of c-Si solar cells reduced by LD, in other words, the laser-doped selective emitter gave to improve the series resistance. Thus, these results indicated that laser-doped selective emitter can improve the series resistance in any case.

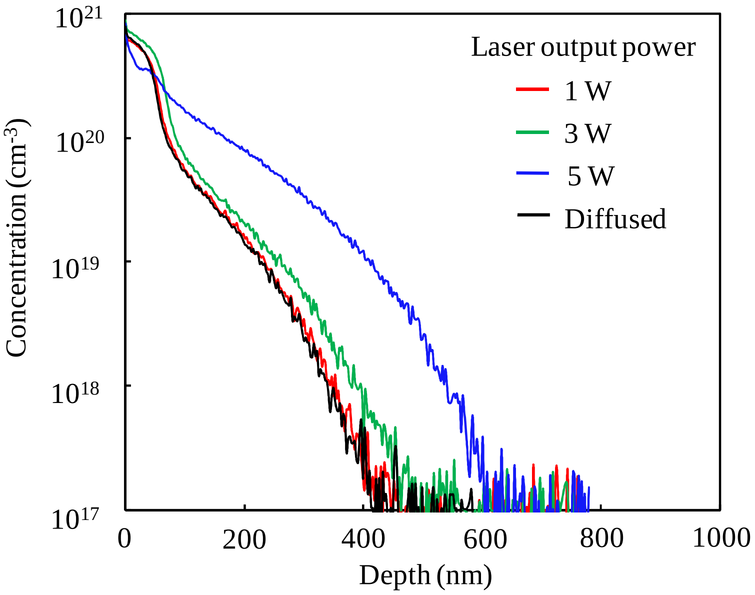

(a)

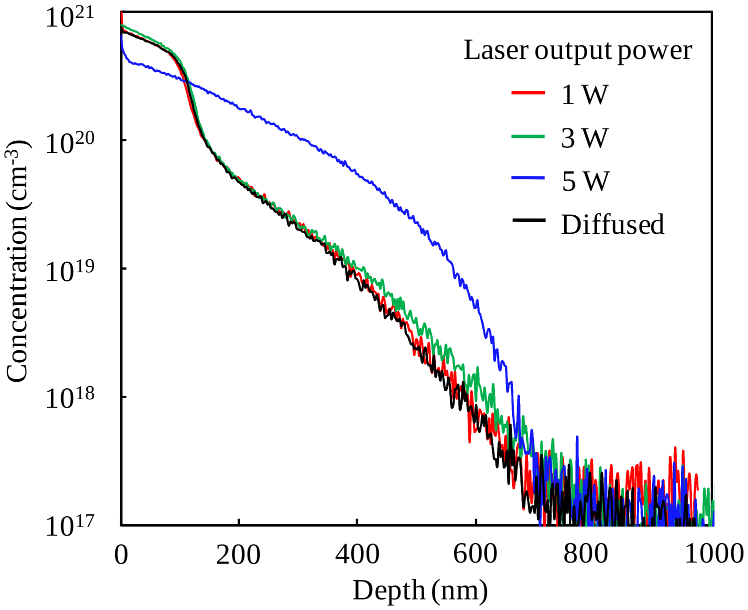

(b)

Figure 5.5: Doping profile of laser-doped emitter formed into thermal diffused emitter. (a) diffusion time for 30 min, (b) diffusion time for 90 min.

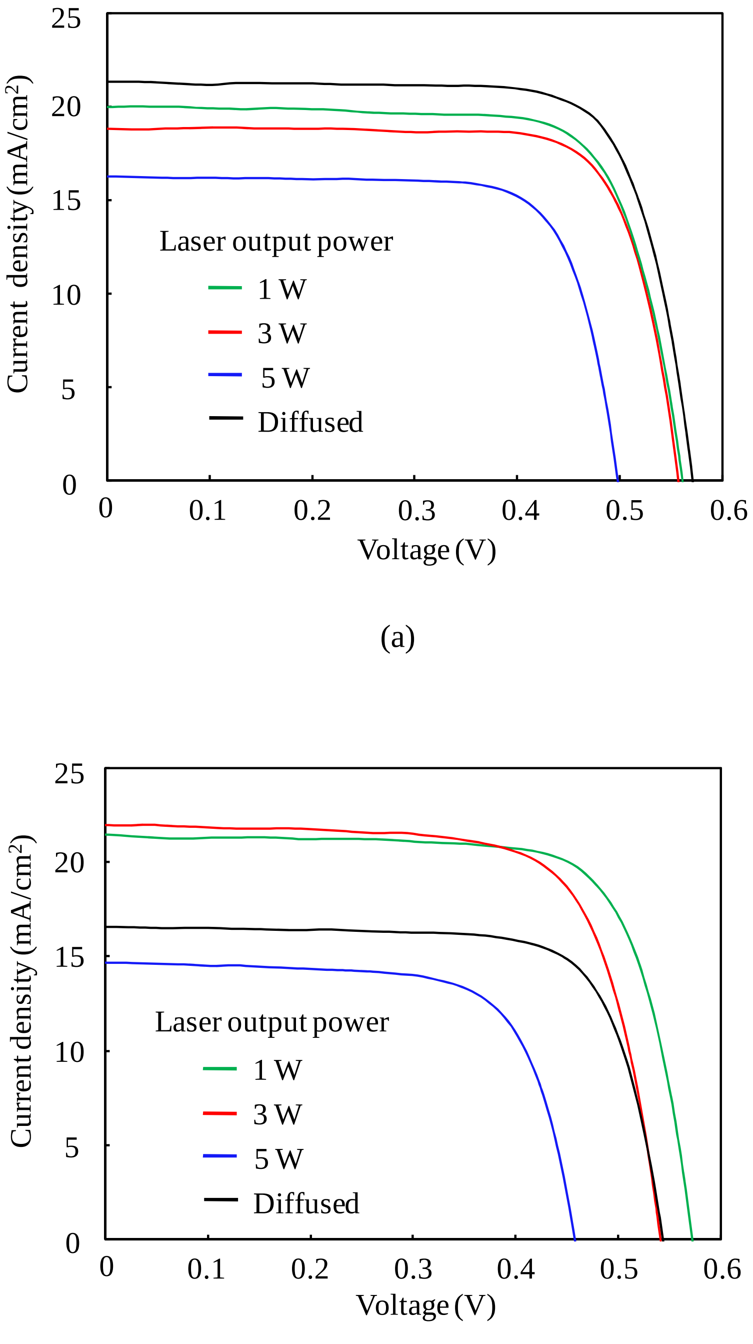

(a)

(b)

Figure 5.6: IV characteristics of illuminated solar cells with laser-doped selective emitter formed into different thermal diffused emitter.
(a) diffusion time for 30 min, (b) diffusion time for 90 min

Table 5.1: The solar cell properties of laser-doped selective emitter formed into different thermal diffused emitter.
(a) diffusion time for 30 min, (b) diffusion time for 90 min

(a)

Sample	V_{oc} (mV)	J_{sc} (mA/cm^2)	F.F. (%)	R_s (Ω)	E_{ff} (%)
No SE	571	21.1	75.9	2.0	7.7
SE by LD at 1.0 W	555	17.9	76.0	1.8	6.3
SE by LD at 3.0 W	556	18.7	76.7	1.7	6.6
SE by LD at 5.0 W	497	16.1	75.3	1.6	5.0

SE: Selective emitter
R_s: Series resistance

(b)

Sample	V_{oc} (mV)	J_{sc} (mA/cm^2)	F.F. (%)	R_s (Ω)	E_{ff} (%)
No SE	544	16.4	74.3	1.9	5.6
SE by LD at 1.0 W	579	23.5	72.5	1.8	8.2
SE by LD at 3.0 W	542	21.8	71.3	1.8	7.0
SE by LD at 5.0 W	458	14.5	70.2	1.6	3.9

SE: Selective emitter
R_s: Series resistance

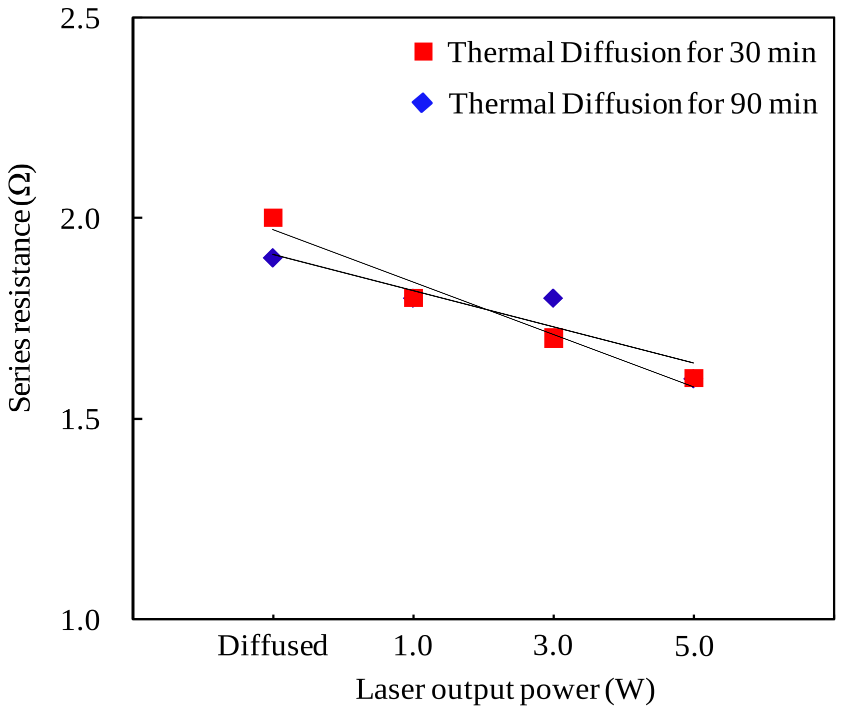

Figure 5.7: Dependence of series resistance on laser output power.

5.4 Selective Emitter Formation by Laser Doping to Laser-Doped Emitter

The formation of the selective emitter using LD into diffused emitter pn junction was able to reduce the series resistance of c-Si solar cells as indicated in section 5.3. In this section, we tried to fabricate the c-Si solar cells with high efficiency only by LD at room temperature and in air ambience. Indeed, Ogane *et al.* reported that LD for full surface doping to form pn junction resulted in low F.F. of c-Si solar cells due to the high sheet resistance on laser-doped surface.5) In this study, LD for the formation of selective emitter was carried out to improve the F.F. of laser-doped c-Si solar cells.

5.4.1 Experiment

The procedures of sample preparation until dopant film formation were same as subsection 5.3.1. At the first step to form a pn junction formation of solar cells for the carrier collection, Nd^{3+}:YAG Pulsed laser with 355 nm wavelength was irradiated to the full-surface area of the precursor coated sample at room temperature and in air ambient as shown in Fig. 5.8. The laser spot diameter on the sample surface was adjusted to 50 μm. After formed the pn junction by the laser with 355 nm wavelength, the sample was cleaned by HF dipping (Fig. 5.8 (a)). After this cleaning, the sample was re-coated by the dopant contained liquid and re-dried on a hotplate at 100°C and PSG was obtained on the surface. Subsequently, Nd: YVO_4 CW laser with 532 nm wavelength was irradiated to form a selective emitter underneath the finger electrodes. The irradiated areas were controlled to become electrode pattern (Fig. 5.8 (b)). The laser spot diameter on the sample surface was adjusted to 6.0 μm. These steps were faster than the conventional process as use of thermal diffusion and photolithography. Before forming a selective emitter, the samples were irradiated on the whole area by the laser with 532 nm wavelength for the sheet resistance measurement on the sample surface.

For the investigation of doping condition, the secondary ion mass spectrometry (SIMS) measurement to evaluate the depth profile and the dopant concentration was performed. The doping depth and the dopant concentration were compared in this measurement.

After the formation of pn junction and selective emitter on the front surface, front (Ti/Ag) and back (Al) side electrodes were evaporated. In this section, any further techniques to improve the photovoltaic properties were also not applied.

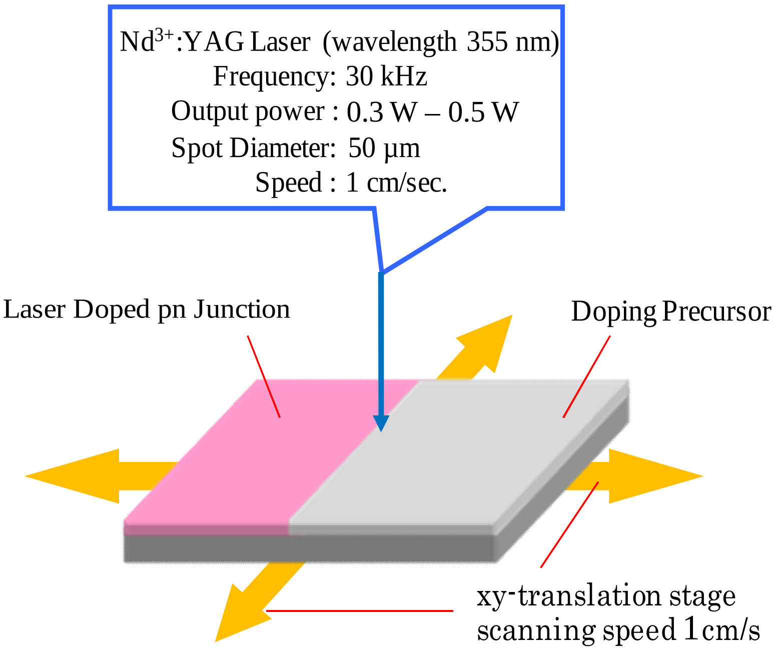

(a)

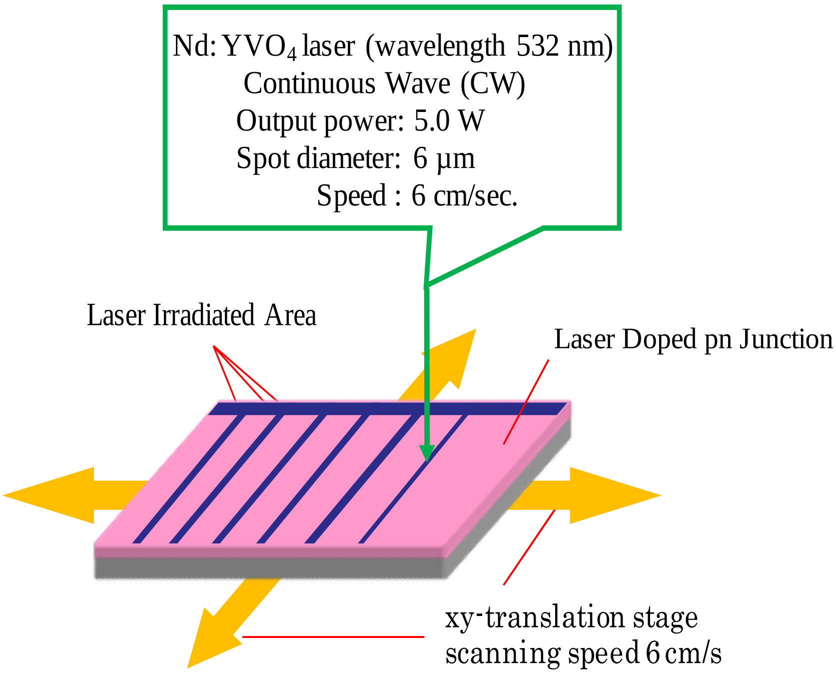

(b)

Figure 5.8: Schematic model of sample procedures using LD
(a) Formation of pn junction,
(b) Formation of selective emitter

5.4.2 Evaluation of Doping Profile after Laser Doping

The SIMS result which indicates the concentration of phosphorous atoms doped into p-type silicon substrate comparing with after each irradiation was shown in Fig. 5.9. Fig. 5.9 showed that the second irradiation by the laser with 532 nm wavelength was confirmed to form a deeper and higher doped area than the first irradiation by the laser with 355 nm wavelength. A reason of this doping profile would be explained as follows.9) To become the deeper doping depth is due to the effect of penetration depth of light into silicon substrate. It is around 1 μm from surface at 532 nm wavelength into silicon.24) Additionally, the reason why higher doping concentration on near surface was became, the dopant precursor film did not use residual dopant precursor film as section 5.3, but the precursor film with the large amount of dopant atoms was formed by re-coating process prior to the second irradiation. Consequently, deeper melting of silicon depth which is induced by the laser with 532 nm wavelength formed the deeply and highly doped layer. Moreover, their sheet resistances were measured, as shown in Table 5.2. The sheet resistance value was confirmed to be less than half by the second irradiation. Basically, the second irradiation improved the sheet resistance in silicon solar cells.

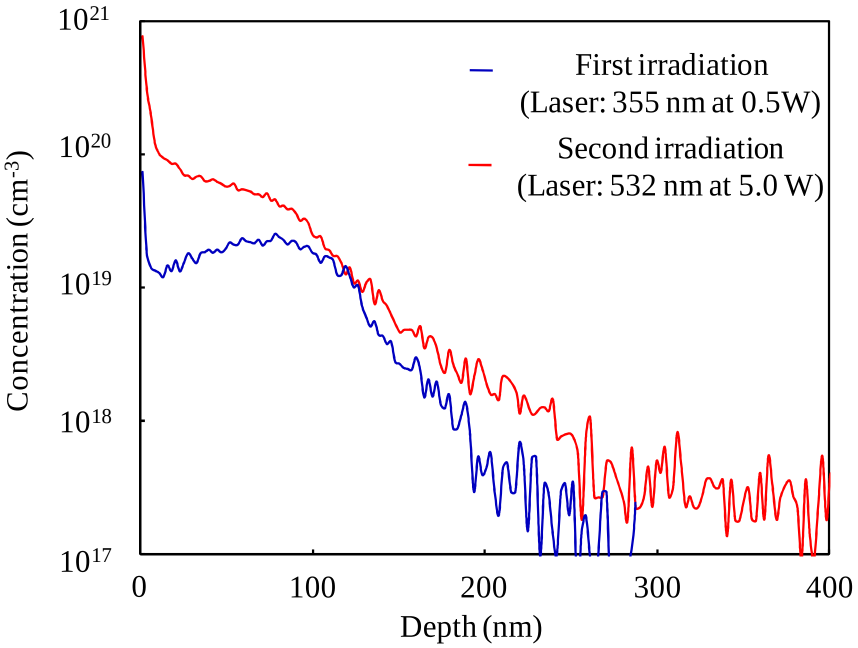

Figure 5.9: The SIMS results of phosphorous atoms doped into p-type silicon substrate compared with after each irradiation.

Table 5.2: Sheet resistance after laser irradiation on each doping step

Doping step	First irradiation with 355 nm laser	Second irradiation with 532 nm laser
Sheet resistance	265 Ω/☐	101 Ω/☐

5.4.3 I-V Characteristics of Illuminated Solar Cells with Different Laser-Doped Emitters

It was verified as above that a deeply and highly doped layer could be formed and the sheet resistance was decreased after the second irradiation by laser with 532 nm wavelength. This LD was tried to apply and optimize to form a selective emitter into different laser-doped emitters. The samples with various doping depth on the first irradiation step by laser with 355 nm wavelength for pn junction were prepared. In this preparation, the laser output power was controlled from 0.3 W to 0.5 W. Subsequently, laser with 532 nm wavelength was irradiated on these samples, and laser output power was fixed at 5.0 W.

These doping depth profiles which measured with SIMS were shown in Fig. 5.10. These results demonstrated that the doping depth was controlled from around 100 nm to 200 nm by the first irradiation for a laser-doped emitter. Thus, the different laser-doped emitters were formed. Furthermore, a deeply and highly doping layer was formed by the second irradiation for a selective emitter. The sheet resistance with its emitter was probably improved.

The fabricated solar cells with the different laser-doped emitters by laser with 355 nm wavelength changed the output power from 0.3 W to 0.5 W. The selective emitter was formed by laser with 532 nm wavelength at 5.0 W. Those were measured for I-V characteristics of illuminated solar cells as shown in Fig. 5.11. The conversion efficiency of all fabricated solar cells with the selective emitter improved. Especially, F.F. was considerably improved for all samples. This is due to the lower resistance underneath finger electrodes by laser with 532 nm wavelength on the selective emitter, and it is possible that the second irradiation made higher crystallinity than that of the first irradiation.

The solar cell properties of different laser-doped emitters formed by 355 nm laser with or without selective emitters formed by 532 nm were summarized in Table 5.3. On the condition of laser output power at 0.5 W, F.F. was increased from 50.6% to 64.8% even though any further techniques were not applied. This is due to the reduction of series resistance (R_s) in the solar cell as shown in Table 5.4. However, other properties for the samples such as V_{oc} and J_{sc} did not relatively improve; especially J_{sc} for all samples was decreased. V_{oc} was improved with laser-doped selective emitter on the lower output power at the first irradiation This is probably due to improvement of the surface recombination. On the other hand, V_{oc} was decreased at the higher output power (0.5 W). This is guessed that the emitter saturation current density increased in the selective emitter. Thus, this behavior is related to the increase Auger recombination inside the emitter.10) J_{sc} for all samples was decreased on all conditions. This is due to the wider selective emitter width than the front side electrode. It is necessary to optimize the selective emitter width for improvement of J_{sc}.

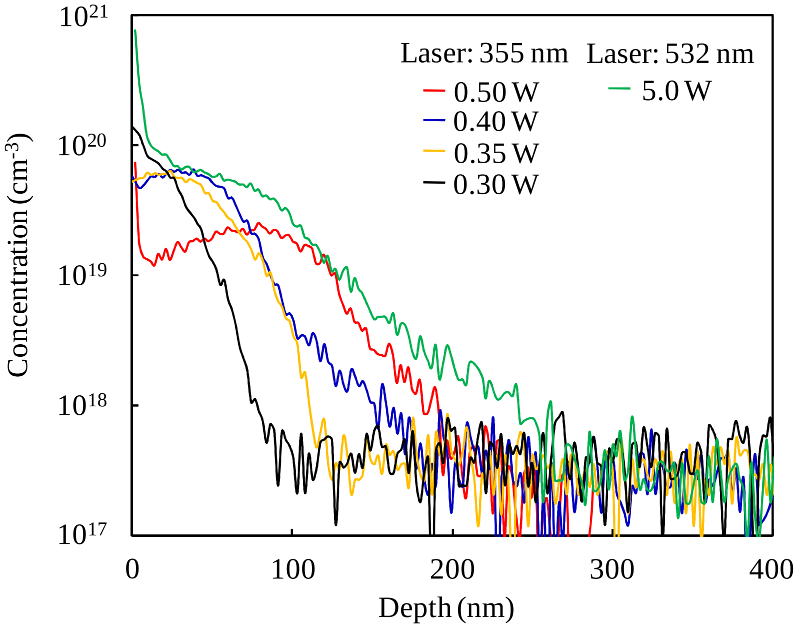

Figure 5.10: Doping profile of different laser-doped emitters and laser doped selective emitter.

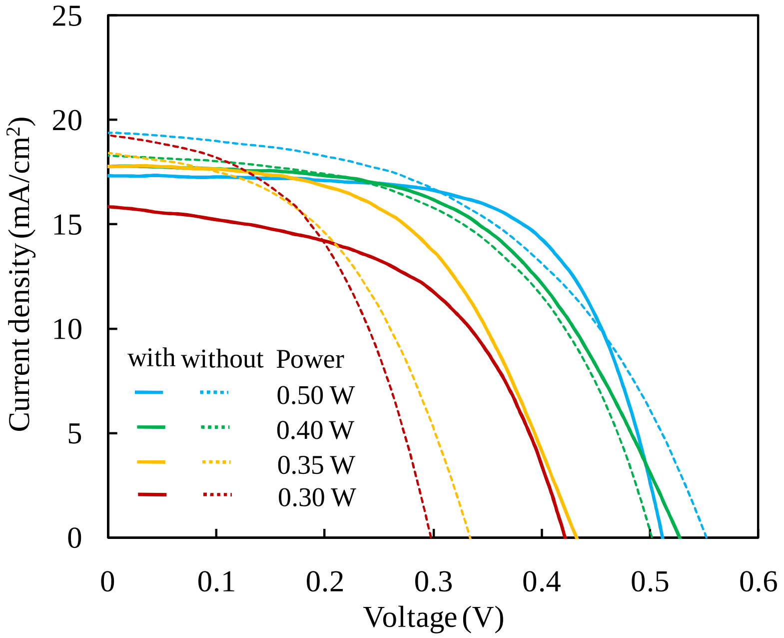

Figure 5.11: I-V characteristics of illuminated solar cells of different laser-doped emitters formed by 355 nm laser with or without selective emitter formed by 532 nm laser at 5.0 W

Table 5.3: The solar cell properties of different laser-doped emitters formed by 355 nm laser with or without selective emitter formed by 532 nm laser at 5.0 W.

	V_{oc} (mV)		J_{sc} (mA/cm^2)		F.F. (%)		E_{ff} (%)	
Laser output power	without SE	with SE	without SE	with SE	without SE	with SE	without SE	with SE
0.50 W	552	511	19.4	17.3	50.6	64.8	5.4	5.8
0.40 W	502	527	18.3	17.7	54.3	55.0	5.0	5.1
0.35 W	334	432	18.4	17.8	48.3	53.8	3.0	4.1
0.30 W	298	421	19.3	15.8	49.4	52.9	2.9	3.5

SE: Selective Emitter

Table 5.4: Comparison of solar cell properties with the series resistance in laser-doped emitter formed by 355 nm laser at 0.5 W with or without selective emitter formed by 532 nm laser at 5.0 W.

Sample	V_{oc} (mV)	J_{sc} (mA/cm^2)	F.F. (%)	R_s (Ω)	E_{ff} (%)
Without selective emitter	552	19.4	50.6	6.2	5.4
With selective emitter	511	17.3	64.8	2.8	5.8

R_s: Series resistance

5.5 Selective Emitter Formation by Laser Doping to Phosphorous-Doped n-Type Silicon

C-Si solar cells usually use boron-doped p-type silicon as base substrate. However, the boron-doped p-type silicon has the problem that the boron and oxygen complex acts as a carrier recombination center.25) Thus, n-type silicon-based solar cells become very important for realizing stable high conversion efficiency. P-type doping in n-type silicon substrates by LD has not yet been reported so far.

In this section, LD was applied to form a p-type selective emitter in n-type c-Si solar cells.

5.5.1 Experiment

1×1 cm^2, 1-5 Ωcm 280-μm-thick, phosphorous-doped n-type Cz silicon was used as the base substrate. In the first step, the emitter (p-n junction) was formed by the thermal solid-phase diffusion of boron atoms at 900 °C, for 30 min, in N_2 ambient. The doping precursor was coated and prebaked to form boron silicate glass (BSG) on the surface. After the thermal solid-phase diffusion, laser irradiation was applied to the diffused emitter surface at room temperature and in air ambient as shown in Fig. 5.12. The wavelength, pulse duration, and output power of used laser were 355 nm (UV), 15 ns, and 0.5 W, respectively. The laser spot diameter on the sample surface was adjusted to 50 μm. The doped area was accomplished by moving the stage on which a sample was mounted during laser irradiation; an xy-translation stage was moved and controlled by a controller that was connected to a computer (scanning speed of 1.0 cm/s). Secondary ion mass spectrometry (SIMS) measurement was carried out to investigate the doping profile after laser irradiation. The surface image after laser irradiation was observed using an optical microscope. After the irradiation of laser to form the selective emitter in silicon solar cells, the residual BSG on the laser-irradiated surface was removed by HF dipping. Electrode materials and space between front side fingers were same as the previous section. This process sequence is same as Fig. 5.3 This section also was not applied further techniques to improve the solar cell performance.

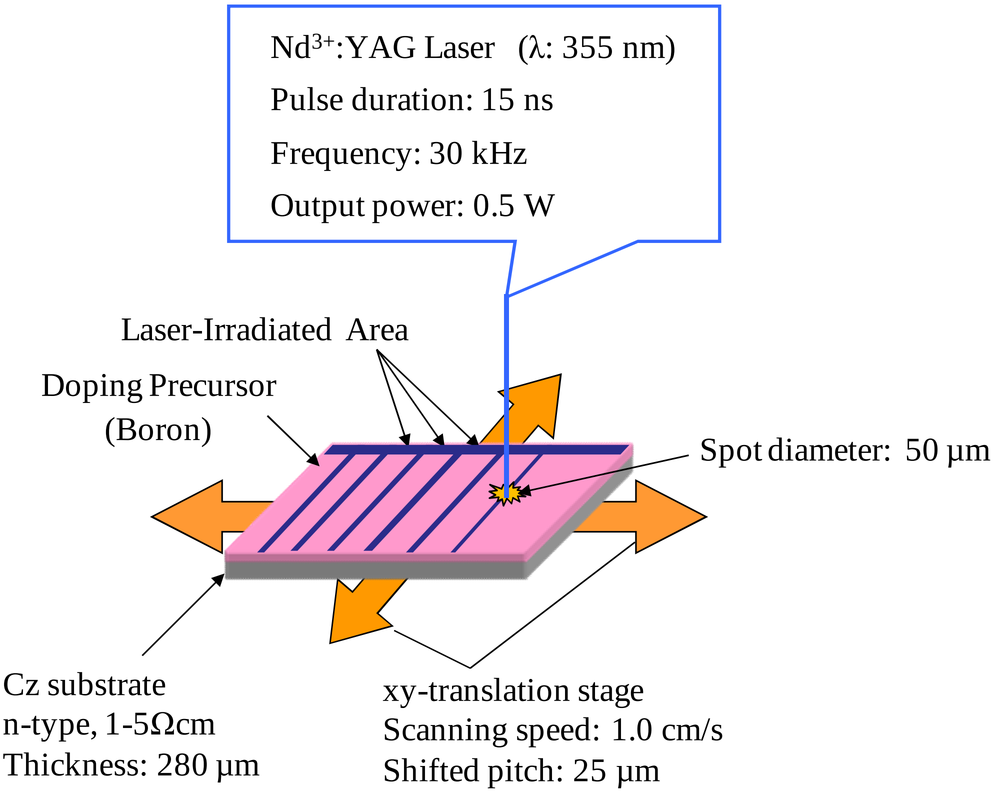

Figure 5.12: Schematic model of LD with 355 nm pulsed laser including parameters

5.5.2 Results and Discussion

A surface image indicating the laser-irradiated area for the formation of a selective emitter is shown in Fig. 5.13. We confirmed that the surface appearance had changed in the laser-irradiated area. These different appearances related to the mechanism of LD are explained as follows. Laser irradiation causes the melting of silicon and simultaneously creates dopant atoms by heat induction to the solid-phase doping precursor. Then, dopant atoms are incorporated into the molten silicon region by the liquid-phase diffusion during the melt recrystallization of silicon.9) Therefore, the surface appearance was changed by laser irradiation, which induced the melting of silicon. Thus, the selective emitter was formed only in laser-irradiated areas.

Fig. 5.14 shows the depth profiles of boron atoms for the unirradiated and laser-irradiated areas. We confirmed the unirradiated area had boron atoms forming pn junctions. For the irradiated area, the depth profile of boron atoms maintained a high doping concentration at a deeper depth. In particular, the dopant concentration in the irradiated area was over 10^{19} cm^{-3} at a depth of 100 nm. The dopant concentration in unirradiated areas was less than 10^{19} cm^{-3} at a depth of 100 nm. LD achieved both high doping concentration and deeper doping depth for the selective emitter, and this probably led to a reduction of its sheet resistance on the silicon surface.26) Doping of boron atoms into n-type silicon substrate by LD gave the same result as doping of phosphorous atoms into p-type silicon substrate.5)

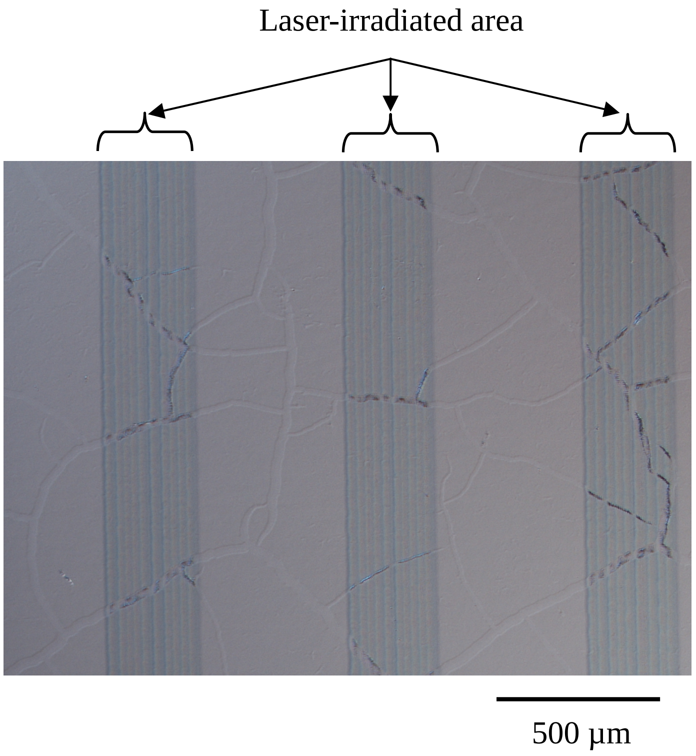

Figure 5.13: Surface image after laser irradiation observed using microscope.

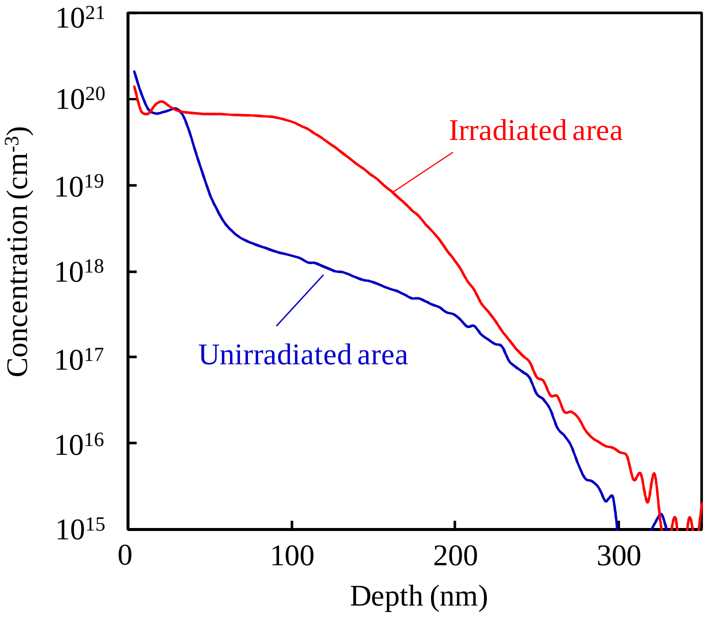

Figure 5.14: Doping profiles of boron atoms in phosphorous-doped silicon substrate before/after LD.

Fig. 5.15 shows the IV characteristics of illuminated solar cells with the laser-doped selective emitter. As a reference, the solar cell was fabricated by solid-phase thermal diffusion without the selective emitter. Our results demonstrated the influence of the selective emitter formed by LD. As shown in Fig. 5.15, compared with the sample without the selective emitter, the solar cell with the selective emitter increased both V_{oc} and J_{sc}. The solar cell peformances of the samples with and without the selective emitter are summarized in Table 5.5. V_{oc} was slightly increased from 569 to 573 mV. J_{sc} was increased considerably by the selective emitter formation from 19.4 to 24.0 mA/cm^2. This is due to the improvement of the

current collection characteristic in the shallow pn junction by the deeply selective emitter formation, as shown in Fig. 5.15. It will be investigated by spectra response measurement in the future. However, the fill factor was slightly decreased by the selective emitter formation. The series and shunt resistances of the samples were evaluated at the high- and low-voltage regions in the illuminated IV curve. The series resistance of the samples was found to be reduced from 3.8 to 1.9 Ω by the selective emitter formation. By contrast, the shunt resistance of the samples was found to be reduced from 1.6 to 0.6 kΩ by the selective emitter formation. This is probably due to the defects induced by laser irradiation being shorted between the front surface electrode and base silicon substrate.23)

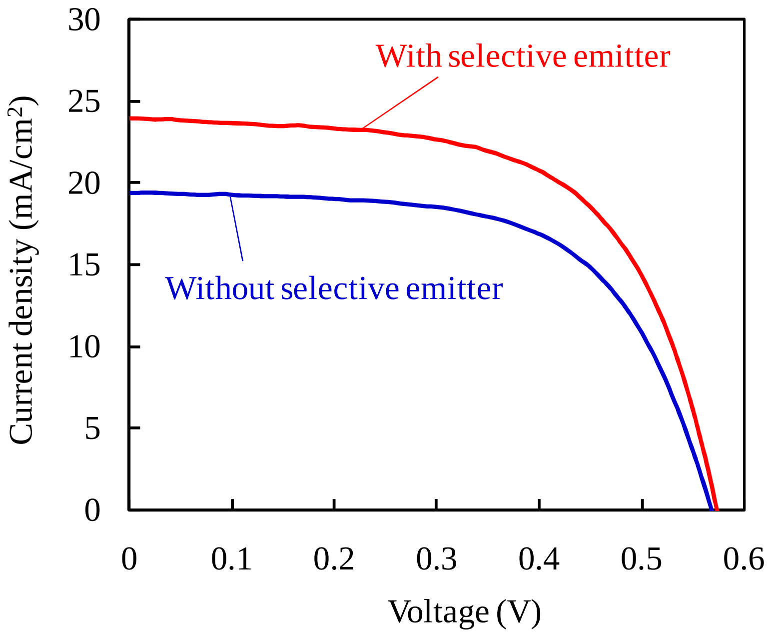

Figure 5.15: I-V characteristics of Illuminated solar cells with a selective emitter formed by LD, compared with those a selective emitter.

Table 5.5. Solar cell properties of sample with and without selective emitter.

Sample	J_{sc} (mA/cm^2)	V_{oc} (mV)	F.F. (%)	R_s (Ω)	R_{sh} (kΩ)	Eff (%)
Without selective emitter	19.4	569	61.8	3.8	1.6	6.8
With selective emitter	24.0	573	61.4	1.9	0.6	8.4

5.6 Summary

In this chapter, we tried to form and optimize the selective emitter using laser doping. It was confirmed that a selective emitter formed by LD at room temperature and in air ambient was realized to fabricate the high-conversion-efficiency of c-Si solar cells.

Firstly, we investigated the correlation between the diffused emitter and the selective emitter for the solar cells. The sheet resistance decreased by laser doping depending on laser power in thermal diffusion for 30 min. However, this dependence did not confirm at longer diffusing time for 90 min. There is probably the limitation of impurity doping in the diffused layer. The doping profile using SIMS was confirmed to form various selective emitters which doped at different laser powers and whether laser-doped emitter formed through or unthrough pn junction. The highest laser power formed the deepest depth but reduced surface concentration. This is probably due to the limitation of dopant source in dopant film. The illuminated IV characteristics were measured for two kinds of diffused emitter with various selective emitters. The results of solar cell properties with selective emitter which passed through pn junction were reduced compared to without selective emitter. On the other hand, properties with selective emitter which unpassed through pn junction were improved. These results indicated that selective emitter depth needs to optimize. Our results demonstrated that the selective emitter depth affects to the solar cell properties. Eventually, laser-doped selective emitter was resulted in improvement of the F.F. around 1 % in maximum, and gave the improvement of series resistance in any case.

Secondly, we tried to apply only LD method to the fabrication process of c-Si solar cells at room temperature and verified the effect in silicon solar cells for the different laser-doped emitters which were formed by the laser (λ= 355 nm) with a selective emitter which was formed by the laser (λ= 532 nm). The emitter doped by second laser irradiation with 532 nm wavelength into laser-doped which formed by first laser irradiation with 355 nm wavelength was verified to become a deeply and highly region. The sheet resistance for its emitter was decreased to less half comparing with the first irradiation. Moreover, it was applied to a selective emitter in c-Si solar cells and optimized for the different laser-doped emitters that controlled the depth by the first irradiation. The fabricated solar cells with a selective emitter improved the conversion efficiency. In particular, F.F. was considerably improved by laser-doped selective emitter into laser-doped emitter at 0.5 W from 50.6% to 64.8% due to the reduction of series resistance from 6.2 Ω to 2.8 Ω.

Finally, we tried to apply the LD method to form a selective emitter in phosphorous-doped n-type c-Si solar cells using a pulsed UV laser at room temperature and in air ambient. The dopant concentration increased and the doping depth became deeper in the selective emitter formed by LD as determined by SIMS measurement. Therefore, the characteristics of the solar cell with the selective emitter improved in this study. The selective emitter formed by UV LD increased not only V_{oc} but also J_{sc}. In particular, J_{sc} was considerably increased by the selective emitter formation. The efficiency of fabricated n-type c-Si solar cells was increased from 6.8 % to 8.4 %.

References of Chapter 5.

1) C. Carlsson, A. Esturo-Breton, M. Ametowobla, J. R. Kohler, and J. H. Werner: Proc. of 21st European Photovoltaic Solar Energy Conf., 2006, p. 938

2) M. Ametowobla, A. Esturo-Breton, J. R. Kohler, and J.H. Werner: Proc. of 31st IEEE Photovoltaic Specialist Conf., 2005, p. 1277

3) C. Carlsson, A. Esturo-Breton, M. Ametowobla, J. R. Kohler, and J. H. Werner: Proc. of 22nd European Photovoltaic Solar Energy Conf., 2007, p. 1593

4) K. Horiuchi, Y. Nishihara, A. Ogane, Y. Takahashi, A. Kitiyanan, Y. Uraoka, and T. Fuyuki: Proc. of 22nd European Photovoltaic Solar Energy Conf., 2007, p. 1423

5) A. Ogane, K. Hirata, K. Horiuchi, Y. Nishihara, Y. Takahashi, A. Kitiyanan, and T. Fuyuki: Jpn. J. Appl. Phys. **48** (2009) 071201.

6) U. Jäger, S. Mack, A. Kimmerle, A. Wolf, and R. Preu: Proc. of 35th IEEE Photovoltaic Specialist Conf., 2010, p.3185.

7) T. Akane, T. Nii, and S. Matumoto: Jpn. J. Appl. Phys. **31** (1992) 4437.

8) H. Kodera: Jpn. J. Appl. Phys. **2** (1963) 212.

9) T. Sameshima, S. Usui and M. Sekiya: J. Appl. Phys. **62(2)** (1987) 711.

10) S. J. Eisele, T. C. Röder, J. R. Köhler, and J. H. Werner: Appl. Phys. Lett. **95** (2009) 133501.

11) J. Szlufcik, S. Sivoththaman, J. Nijs, R. P. Mertens, and R. Van Overstraeten: in *Practical Handbook of Photovoltaics: Fundamentals and Applications,* ed. T. Markvart and L.

Castañer (Elsevier, Oxford, 2003), p. 137.

12) S. Wenham: Prog. Photovoltaics: Res. Appl., **1** (1993) 3.
13) A. W. Blakers, A. Wang, A. M. Milne, J. Zhao, and M. A. Green: Appl. Phys. Lett. **55** (1989) 1363.
14) P. Engelhart, S. Hermann, T. Neubert, H. Plagwitz, R. Grischke, R. Meyer, U. Klug, A. Schoonderbeek, U. Stute, R. Brendel: Prog. Photovoltaics: Res. Appl., **15** (2007) 521.
15) G. Hahn: Proc. of 5th World Conf. on Photovoltaic Energy Conversion, 2010, p.1091.
16) M. J. Kerr, and A. Cuevas: Appl. Phy. Lett. **91** (2002) 2473.
17) J. Zhao, A. Wang, and M. A. Green: Prog. Photovoltaics: Res. Appl., **7** (1999) 471.
18) T. C. Röder, S. J. Eisele, P. Grabitz, C. Wagner, C. Kulushich, J. R. Köhler, and J. H. Werner: Prog. Photovoltaics: Res. Appl., **18**, (2010) 505.
19) S. Solmi, A. Parisini, R. Angelucci, and A. Armigliato: Phys. Rev. B., **53** (1996) 7836.
20) S. M. Sze: *Physics of Semiconductor Devices* (Wiley, New York, 1981) 2nd ed., p.67
21) U. Jäger, D. Suwito, J. Benick, S. Janz, M. Hermle, S. W. Glunz, and R. Preu: Proc. of 5th World Conf. on Photovoltaic Energy Conversion, 2010, p.1386.
22) A. Cuevas and D. Macdonald: Solar Energy, **76** (2004) 255.
23) A. Sugianto, B. S. Tjahjono, L. Mai, S. R. Wenham: Sol. Energy Mater. Sol. Cells **93** (2009) 1986.
24) M. A. Green: *SILICON SOLAR CELLS Advanced Principles & Practice* (University of New South Wales, Sydney, 1995), p.334

25) S. W. Glunz: Sol. Energy Mater. Sol. Cells **90** (2006) 3276.

26) S. M. Sze: *Physics of Semiconductor Devices* (Wiley, New York, 1981) 2nd ed., p.7.

Chapter 6

Conclusions

6.1 Summary

The purpose of this research is the development of LD at room temperature for c-Si solar cell fabrication process. Especially, LD has the potential of fabricating the low-cost and high efficiency c-Si solar cells. In order to achieve this goal, the investigation of LD at room temperature from fundamental characteristics of LD to not only for applying to the fabrication of c-Si solar cells but also for applying to the formation of selective emitter for realizing the high-conversion-efficiency c-Si solar cells has been carried out experimentally.

In Chapter 2, in order to reveal the principle of LD, a dependency of laser irradiation condition for the doping profile was investigated in detail. It was found out that the laser irradiation conditions influenced to not only the doping profile, but also the surface appearance after laser irradiation. The doping depth was able to control depending on laser output power, focus condition and scanning speed. In particular, laser output power could control the doping depth in range from 1.0 µm to 5.0 µm. Furthermore, LD mechanism was discussed to reveal the principle of LD. The LD induces the silicon melting, and then the impurity doping into silicon during solidification of silicon. Thus, the LD has the transient mechanism related to melting and solidification of silicon. From a point of view of a doping layer formation, the laser doped layer could be formed at a few second due to higher diffusivity than that of the conventional solid phase thermal diffusion. In particular, it was found that LD gave higher diffusivity of impurity than that of melting point of silicon ($D=1.0\times10^{-10}$ cm^2/s). Therefore, LD can form a doping layer in silicon at very short time compared with conventional thermal diffusion. Furthermore, laser output power at 5.0 W and 4.0 W were the diffusivity of liquid silicon ($D=5.1\times10^{-4}$ cm^2/s). Thus, a deep doping depth within a few second can be formed, since the diffusivity in liquid silicon is up to 10 orders of magnitude greater than that in solid silicon.

In Chapter 3, dopant precursor film, namely PSG film, for optimization of LD was investigated. In particular, the investigation of PSG film focused on reflectance of PSG film. A new method for uniform PSG film formation was proposed. A calculation of reflectance of PSG film at a specific wavelength which is laser wavelength indicated that the reflectance of PSG film is depended on PSG film thickness. The reflectance of PSG film formed by the sputtering method agreed well with calculations in the margin of error within 1.5 %. This indicated that various reflectance of PSG film can be formed and controlled by the sputtering method.

The controlled reflectance of PSG film, in the case of pulsed-laser with 355 nm wavelength, impacted on the doping profile not only for the depth of doping, but also the concentration. These related to laser fluence due to reflectance of dopant precursor film. In the case of CW-laser with 532 nm wavelength, also influenced to doping profile. In particular, the depth of doping strongly depended on the reflectance of PSG film.

In Chapter 4, LD was applied to the fabrication of c-Si solar cells at room temperature and in air ambience. The conditions of laser irradiation in LD were optimized for the c-Si solar cell emitters. The formation of pn junction formed by LD was revealed to become similar characteristics to it formed by the conventional solid phase thermal diffusion.

The obtained results demonstrated that c-Si solar cells fabricated by LD in condition of optimum laser irradiation gave relatively similar photovoltaic properties to one fabricated by the conventional method. In particular, V_{oc} of laser-doped c-Si solar cells deposited with SiN_x film was considerably improved than thermal diffused c-Si solar cells. It is considered that surface of LD cleaned due to the effect of surface cleaning by NH_3 plasma. Furthermore, the results of IQE indicated that laser-doped c-Si solar cells formed deeper pn junction than that of thermal diffused. Finally, EL was revealed that laser-doped c-Si solar cells emitted the inhomogeneous EL in 2 dimensions, probably due to the un-uniformity of doping by LD. The efficiency of laser-doped c-Si solar cells deposited with SiN_x film as ARC eventually obtained 7.39 %.

In Chapter 5, LD applied to form and optimize the selective emitter. It was confirmed that a selective emitter formed by LD at room temperature and in air ambient was realized to fabricate the high-conversion-efficiency of c-Si solar cells.

Firstly, we investigated the correlation between the diffused emitter and the selective emitter for the solar cells. The evolution of sheet resistance was verified in different diffused emitter profile. The doping profile using SIMS was confirmed to form various selective emitters which doped at different laser output powers, and whether the laser-doped emitter formed through or unthrough pn junction. The highest laser output power formed the deepest depth but reduced surface concentration. This is probably due to the limitation of dopant source in dopant film. The illuminated IV characteristics were measured for different diffused emitter with various selective emitters. The solar cell properties with selective emitter which passed through pn junction were reduced compared to without selective emitter. On the other hand, properties with selective emitter which unpassed through pn junction were improved. These results indicated that selective emitter depth needs to optimize. Our results demonstrated that the selective emitter depth affects to the solar cell properties. Eventually, laser-doped selective emitter was resulted in improvement of the F.F. around 1 % in maximum, and gave the improvement of series resistance in any case.

Secondly, only LD applied to fabricate c-Si solar cells at room temperature and in air ambience, and verify the effect in silicon solar cells for the different laser-doped emitters which were formed by the laser (λ= 355 nm) with a selective emitter which was formed by the laser (λ= 532 nm). The emitter doped by the second laser irradiation with 532 nm wavelength into laser-doped which formed by the first laser irradiation with 355 nm wavelength was verified to become a deep depth and heavy doping concentration region. The sheet resistance for its emitter was decreased to less half comparing with the first irradiation. Moreover, it was applied to a selective emitter in c-Si solar cells and optimized for the different laser-doped emitters that controlled the depth by the first irradiation. The fabricated solar cells with a selective emitter improved the conversion efficiency. In particular, F.F. was considerably improved by forming the selective emitter. Basically, F.F. was considerably improved by laser-doped selective emitter into laser-doped emitter at 0.5 W from 50.6% to 64.8% due to the reduction of series resistance from 6.2 Ω to 2.8 Ω.

Finally, LD was applied to the formation of a selective emitter in phosphorous-doped n-type c-Si solar cells using a pulsed UV laser at room temperature and in air ambient. The dopant concentration increased and the doping depth became deeper in the selective emitter formed by LD as determined by SIMS measurement. Therefore, the characteristics of the solar cell with the selective emitter improved in this study. The selective emitter formed by UV LD increased not only V_{oc} but also J_{sc}. In particular, J_{sc} was considerably increased by the selective emitter formation, and eventually, the efficiency of fabricated n-type c-Si solar cells was increased from 6.8 % to 8.4 %.

6.2 Outlooks

In order to realize not only high-efficiency c-Si solar cells fabricated by LD, but also transfer LD to industrial c-Si solar cell fabrication process, there are many issues to study as followings:

1. The doping profile has to be investigated with conditions of laser irradiation in more detail. Actually, a little bit rough conditions to investigate the doping profile in LD have carried out in this thesis. Especially, influence of ablated material could give directly dependency of doping concentration. Thus, the laser scan pitch has to change.

2. The reflectance of dopant precursor film with more detail has to form to find out a threshold of melting induced by laser irradiation. This is very important for revealing clearly correlation between LD and dopant precursor film.

3. The doping profile has to be revealed the uniformity of three dimensions. In addition, the establishment of optics system to form Top-Hat energy distribution of laser is necessary for uniform doping. Used laser in this thesis did not shape the laser energy distribution. Thus, laser energy distribution in this thesis was Gaussian. To change distribution from Gaussian to Top-hat will be able to form the homogeneous doping. In particular, CW

laser with Top-Hat energy distribution has a potential of homogeneous doping due to having the high stable laser beam.

4. Laser doping layer should investigate the crystallinity. In addition, surface direction after LD should be investigated because LD induces melting and recrystallizaiton of silicon.

5. The transient thermal analysis of LD should be introduced to investigate LD profiles. The diffusivity of LD in this thesis was found out the between melting point and liquid of silicon. The transient thermal analysis of LD will be helpful for investigation of LD mechanism. Furthermore, the thermal of LD will be able to be controlled by the introduction of transient thermal analysis into LD.

6. For applying to c-Si solar cell fabrication process, the LD should apply to the textured surface. The c-Si solar cells generally have a texture on the surface due to light trapping for improving the efficiency. Furthermore, minority carrier lifetime after LD, especially surface recombination has to be investigated.

7. For the selective emitter formation, more and more optimization of LD is necessary for improvement. Especially, the metal contact method should change to the other precise alignment method contacted onto selective emitter. Also, selective emitter width has to be

narrower. Furthermore, for transferring laser-doped selective emitter into industrial c-Si fabrication process, it is necessary that LD is matched into the c-Si solar cell process; in particular contact firing process optimizes for laser-doped selective emitter. Because, the obtained sheet resistance on laser-doped selective emitter in this research has demonstrated quite low less than 20 Ω/□.

Appendix A

Equations for Calculation of Film Reflectance$^{1)}$

It is expected that the reflectance of samples with PSG film deposited on silicon base substrate used in this thesis is changed by PSG film thickness due to the interference of incident light in film which is different from the reflectance of bare silicon surface. Therefore, the optical calculation of reflectance on Air/PSG/Si can be carried out to reveal the correlation between the PSG film thickness and reflectance.

The conditions for optical calculation of reflectance are assumed as followings.

- Single layer of PSG (SiO_2) film depositing on silicon base substrate
- Incident light through air ambience and vertically against sample
- Absorption into silicon base substrate, No absorption into PSG and air

The refractive index, attenuation coefficient, complex refractive index of PSG are expressed in n, k, $N = n - ik$, respectively. Similarly, the refractive index, attenuation coefficient, complex refractive index of silicon are expressed in n_m, k_m, $N_m = n_m - ik_m$, respectively.

ρ_0 is amplitude reflectance coefficient of Fresnel which means amplitude reflectance of electric filed on front surface of thin film. τ_0 is amplitude absorption coefficient of Fresnel which means amplitude absorption of electric filed on front surface of thin film. ρ_1 and τ_1 are amplitude reflectance coefficient and amplitude absorption coefficient between rear surface of thin film and substrate, respectively. From this point forward, these coefficients are rewritten to Fresnel coefficient. The refractive index and attenuation coefficient referred to literature.[2)] Fig. A.1 shows the schematic model of Air/PSG/Si. The reflectance R was calculated by following equations.

The Fresnel coefficient on front surface of thin film is:

$$\rho_0 = \frac{n_0 - N}{n_0 + N} = \frac{n_0 - n + ik}{n_0 + n - ik} \qquad \tau_0 = \frac{2n_0}{n_0 + N} = \frac{2n_0}{n_0 + n - ik} \tag{A-1}$$

The Fresnel coefficient between rear surface of thin film and substrate:

$$\rho_1 = \frac{N - N_m}{N + N_m} = \frac{n - n_m - i(k - k_m)}{n + n_m - i(k + k_m)} \qquad \tau_1 = \frac{2N}{N + N_m} = \frac{2(n - ik)}{n + n_m - i(k + k_m)} \tag{A-2}$$

In addition, the incident light through PSG film once is:

$$\Delta = \frac{2\pi}{\lambda} Nd = \frac{2\pi}{\lambda}(n - ik)d = \frac{2\pi}{\lambda} nd - i\frac{2\pi}{\lambda} kd = \delta - i\gamma \tag{A-3}$$

Here,

$$\delta = \frac{2\pi}{\lambda} nd \qquad \gamma = \frac{2\pi}{\lambda} kd \tag{A-4}$$

Only change the phase of incident light through PSG film. δ is the phase changes in case of no absorption. γ is the coefficient regarding amplitude by absorption. Thus, whole Fresnel coefficient is:

$$\rho = \frac{\rho_0 + \rho_1 e^{-i2\Delta}}{1 + \rho_0 \rho_1 e^{-i2\Delta}} = \frac{\dfrac{n_0 - n + ik}{n_0 + n - ik} + \dfrac{n - n_m - i(k - k_m)}{n + n_m - i(k + k_m)} e^{-i2\delta} e^{-2\gamma}}{1 + \dfrac{n_0 - n + ik}{n_0 + n - ik} \cdot \dfrac{n - n_m - i(k - k_m)}{n + n_m - i(k + k_m)} e^{-i2\delta} e^{-2\gamma}} \tag{A-5}$$

$$= \frac{A - iB}{C - iD} = \frac{AC + BD + i(AD - BC)}{C^2 + D^2} \tag{A-6}$$

Here, A, B, C, and D are expressed by:

$$\begin{aligned} A &= (n_0 - n)(n + n_m) + k(k + k_m) \\ &+ [\{(n_0 + n)(n - n_m) - k(k - k_m)\} cos\, 2\delta - \{(n_0 + n)(k - k_m) + (n - n_m)k\} sin\, 2\delta] e^{-2\gamma} \end{aligned} \tag{A-7}$$

$$\begin{aligned} B &= (n_0 - n)(k + k_m) - k(n + n_m) \\ &+ [\{(n_0 + n)(k - k_m) + k(n - n_m)\} cos\, 2\delta + \{(n_0 + n)(n - n_m) + (k - k_m)k\} sin\, 2\delta] e^{-2\gamma} \end{aligned} \tag{A-8}$$

$$\begin{aligned} C &= (n_0 - n)(n + n_m) - k(k + k_m) \\ &+ \left[\{(n_0 - n)(n - n_m) + k(k - k_m)\} cos\, 2\delta - \{(n_0 - n)(k - k_m) - (n - n_m)k\} sin\, 2\delta\right] e^{-2\gamma} \end{aligned} \tag{A-9}$$

$$\begin{aligned} D &= (n_0 + n)(k + k_m) + k(n + n_m) \\ &+ \left[\{(n_0 - n)(k - k_m) - k(n - n_m)\} cos\, 2\delta + \{(n_0 - n)(n - n_m) + (k - k_m)k\} sin\, 2\delta\right] e^{-2\gamma} \end{aligned} \tag{A-10}$$

Hence, the reflectance *R* is:

$$R = |\rho|^2 = \left(A^2 + B^2\right) / \left(C^2 + D^2\right) \tag{A-11}$$

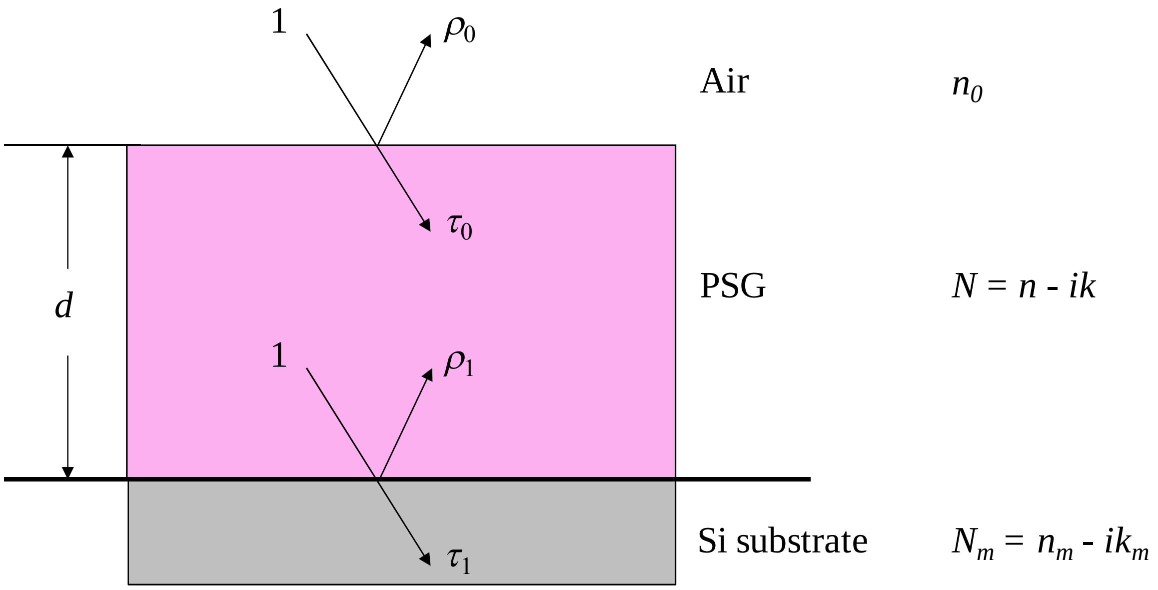

Figure A.1: Schematic model for the optical calculation of film reflectance.

References of Appendix A.

1) T. Funatani, Master thesis, Nara Institute of Science and Technology (in Japanese)

2) M. Kohiyama, *Fundamental theory of optical thin film* (Optronics, Tokyo, 2006), p.65 (in Japanese)

Appendix B

Evaluation of Solar Cell Property[1, 2)]

Irradiation spectrum was AM 1.5 with the total power intensity of 100 mW/cm^2 in the wavelength in region from 200 to 1500 nm. The light was illuminated vertically onto the solar cell. The illuminated light was refracted and reflected on the basis of continuous boundary condition. Some of incident light were absorbed in the solar cell and the other permeated the solar cell. The unabsorbed light was reflected totally at the Back Surface Reflector (BSR), and reflected light was returned, and then was absorbed in the solar cell.

In order to investigate the solar cell performance, the current-voltage characteristics were calculated. A typical current density-voltage and power-voltage curve of a solar cell under illumination is shown in Fig. B.1. The short circuit current density (J_{sc}), the open circuit voltage (V_{oc}) and the maximum power point P_{max} (V_{m}, J_{m}) were indicated in the figure. The conversion efficiency η is the ratio of the incident power P_{in} and P_{max}, and given by,

$$\eta = \frac{P_{\max}}{P_{in}} \times 100 = \frac{J_{sc} \cdot V_{oc} \cdot FF}{P_{in}} \times 100 \quad (\%) \qquad \text{(B-1)}$$

where *FF* is the fill factor and defined by $FF = (J_{\mathrm{m}} \cdot V_{\mathrm{m}})/(J_{\mathrm{sc}} \cdot V_{\mathrm{oc}})$.

.

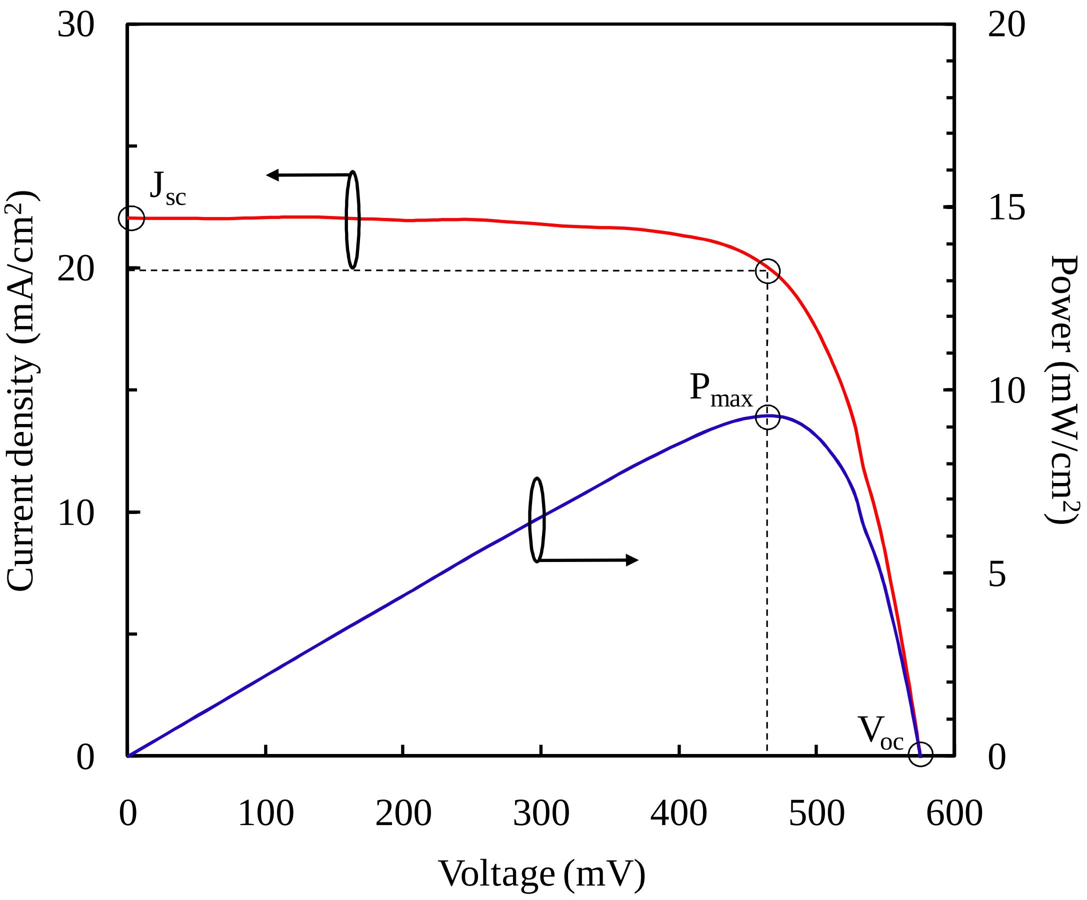

Figure B.1: Current density-voltage and power-voltage curves of a solar cell under illumination condition. (A.M. 1.5, 100 mW/cm^2)

References of Appendix B.

1) K. Takahashi, et al., *Handbook of Photovoltaics*, (Institute of Electrical Engineers of Japan, Tokyo, 1985) p. 198. (in Japanese)

2) Y. Takahashi: PhD thesis NAIST, Japan, (2008)

Appendix C

Advantage and Suitability of Diode Pumped Solid State Laser for Crystalline Silicon Solar Cell Fabrication Process

This thesis used two kinds of diode pumped solid state (DPSS) lasers for investigation of LD and c-Si solar cell fabrication at room temperature. One used and another laser are CW and pulsed, respectively. These lasers can fabricate c-Si solar cells at room temperature, in air ambience, as shown in this thesis. In addition, these lasers have a potential for realizing a low-cost and high- efficiency c-Si solar cells. Thus, these lasers can apply to c-Si solar cell fabrication process. To clarify laser of ability with pulse or CW, the advantages and suitability of each lasers for c-Si solar cell fabrication process were summarized in table C.1. As a note to read table C.1, the wavelength of lasers are 532 nm.

Table C.1. Summary of advantages and suitability of pulsed and CW DPSS laser with 532 nm wavelength for c-Si solar cells fabrication process.1-4)

	Pulsed Laser	CW Laser
Power	< 5.0 W	< 15.0 W
Peak Power	◎ (ex. Q switch)	× (Need of light focusing)
Optics	△	◎
Lifetime (Stability)	×	◎
Size	○	○
Controllability	◎	○
Doping	Liquid phase	Liquid phase (Solid phase)
Throughput	△ (Dependence on pulse duration)	◎ (> 10m/s)
Cost	△	◎

References of Appendix C.

1) F. Colville: "Laser-assisted selective emitters and the role of laser doping", *Photovolt. Int.***5**, 2009.

2) R. S. Patel, J, Bovatsek, A. Sugianto, B. Hallam, B. Tijahjono, S. Wenham: presented at World Conference on Photovoltaic Energy Conversion, (Valencia, Spain), 2010, 2CV.1.82.

3) COHERENT, Inc.: http://www.coherent.com/

4) Newport Corporation: http://www.newport.com/

List of Publications

Academic journals

[1] "Selective Emitter Formation by Laser Doping for Phosphorous-Doped N-Type Silicon Solar Cells"

Kenji Hirata, Takashi Saitoh, Akiyoshi Ogane, Emi Sugimura, and Takashi Fuyuki

Applied Physics Express, Vol. 5, No. 1, 016501 (2012)

[2] "Optimization of Selective Emitter Profiles by Laser Doping in Crystalline Silicon Solar Cells"

Kenji Hirata, Hideki Nishimura, Takuya Katagiri, Sohichiroh Takamoto, Emi Sugimura, and Takashi Fuyuki

Submitted to Japanese Journal of Applied Physics

[3] "Investigation of Dopant Film for Laser Doping in Crystalline Silicon Solar Cell Process"

Kenji Hirata, Tomohiro Funatani, Takuya Katagiri, and Takashi Fuyuki

Submitted to Japanese Journal of Applied Physics

International conferences

[1] "Novel Silicon Solar Cell Process by Laser Doping Technique"

Kenji Hirata, Akiyoshi Ogane, Takashi Saitoh, Athapol Kitiyanan, Yukiharu Uraoka, and Takashi Fuyuki

The 5th International Congress on Laser Advanced Materials Processing 2009, (Kobe, Japan), 2009

[2] "Optimization of CW Laser Doping in Crystalline Silicon Solar Cells"

Kenji Hirata, Akiyoshi Ogane, Takashi Saitoh, Athapol Kitiyanan, Emi Sugimura, and Takashi Fuyuki

24th European Photovoltaic Solar Energy Conference and Exhibition, (Hamburg, Germany), 2009

[3] "Improvement of J_{sc} with Selective Emitter Formed by Ultraviolet Laser Doping"

Kenji Hirata, Takashi Saitoh, Akiyoshi Ogane, Athapol Kitiyanan, Emi Sugimura, and Takashi Fuyuki

19th International Photovoltaic Science and Engineering Conference and Exhibition, (Jeju, Korea), 2009

[4] “Selective Emitter Formation in Crystalline Silicon Solar Cell by Laser Doping at Room Temperature”

Kenji Hirata, Takashi Saitoh, Tamaki Takayama, Mitsuhiro Hasegawa, Tomohiro Funatani, and Takashi Fuyuki

5th World Conference on Photovoltaic Energy Conversion, (Valencia, Spain), 2010

[5] “Application of Laser Doping to Form Selective Emitter in Silicon Solar Cells”

Kenji Hirata, Tamaki Takayama, Tomohiro Funatani, Mitsuhiro Hasegawa, and Takashi Fuyuki

2010 MRS Fall Meeting, (Boston, USA), 2010

[6] “OPTIMIZATION OF SELECTIVE EMITTER FORMATION USING LASER DOPING IN CRYSTALLINE SILICON SOLAR CELL”

Kenji Hirata, Tamaki Takayama, Mitsuhiro Hasegawa, Tomohiro Funatani, and Takashi Fuyuki

26th European Photovoltaic Solar Energy Conference and Exhibition,

(Hamburg, Germany), 2011

[7] “OPTIMIZATION OF SELECTIVE EMITTER PROFILES BY LASER DOPING IN CRYSTALLINE SILICON SOLAR CELLS”

Kenji Hirata, Hideki Nishimura, Takuya Katagiri, Sohichiroh Takamoto, Emi Sugimura, and Takashi Fuyuki

21st International Photovoltaic Science and Engineering Conference and Exhibition, (Fukuoka, Japan), 2011

Domestic conferences

[1] “Development of laser doping for silicon solar cells”

Kenji Hirata, Koyo Horiuchi, Akiyoshi Ogane, Yu Takahashi, Yukiharu Uraoka, and Takashi Fuyuki

Abstracts of the 55th Spring Meeting of the Japan Society of Applied Physics and Related Societies, (Funabashi), 2008, in Japanese

[2] “Development of laser doping process using green laser for silicon solar cell fabrication”

Kenji Hirata, Akiyoshi Ogane, Athapol Kitiyanan, Yukiharu Uraoka, and Takashi Fuyuki

Abstracts of 5th Next Generation Photovoltaic System Symposium, (Miyazaki), 2008 in Japanese

[3] “Fabrication of back-contact silicon solar cells by laser doping technique”

Kenji Hirata, Takashi Saitoh, Akiyoshi Ogane, Emi Sugimura, and Takashi Fuyuki

Abstracts of 6th Next Generation Photovoltaic System Symposium, (Niigata), 2009 in Japanese

[4] "Development of Laser Doping for Crystalline Silicon Solar Cell Process"

Kenji Hirata, Tamaki Takayama, Mitsuhiro Hasegawa, Tomohiro Funatani, Hideki Nishimura, and Takashi Fuyuki

Abstracts of the 58th Spring Meeting of the Japan Society of Applied Physics and Related Societies, (Kanagawa), 2011 in Japanese

[5] "Formation and Optimization of Selective Emitter Structure by Laser Doping in Crystalline Silicon Solar Cells"

Kenji Hirata, Tamaki Takayama, Hideki Nishimura, Takuya Katagiri, Sohichiroh Takamoto, Emi Sugimura, and Takashi Fuyuki

Abstracts of 7th Next Generation Photovoltaic System Symposium, (Gifu), 2011 in Japanese

Related academic journals

[1] "Rear side Passivated Monocrystalline Silicon Thin Film Solar Cells with Laser Fired

Contact Process"

Yu Takahashi, Kenji Hirata, Akiyoshi Ogane, Yukihar Uraoka, and Takashi Fuyuki

Applied Physics Express 1, 085002 (2008)

[2] "Laser-Doping Technique Using Ultraviolet Laser for Shallow Doping in Crystalline Silicon Solar Cell Fabrication"

Akiyoshi Ogane, Kenji Hirata, Koyo Horiuchi, Yoshiyuki Nishihara, Yu Takahashi, Athapol Kitiyanan, and Takashi Fuyuki

Jpn. J. Appl. Phys. 48, 071201 (2009)

[3] "Improved Inversion Channel Mobility in 4H-SiC MOSFETs on Si-face Utilizing Phosphorus-Doped Gate Oxide"

Dai Okamoto, Hiroshi Yano, Kenji Hirata, Tomoaki Hatayama, and Takashi Fuyuki

IEEE Electron Device Letters, Vol.31, No.7, 710 (2010)

Related international conferences

[1] "Application of laser doping technique to bulk and thin film multicrystalline silicon solar cells"

Akiyoshi Ogane, Kenji Hirata, Koyo Horiuchi, Athapol Kitiyanan, Yukiharu Uraoka, and

Takashi Fuyuki

23rd European Photovoltaic Solar Energy Conference, (Valencia Spain), 2008

[2] "Feasible control of laser doping profiles in silicon solar cell processing using multiple excitation wavelengths"

Akiyoshi Ogane, Kenji Hirata, Koyo Horiuchi, Athapol Kitiyanan, Yukiharu Uraoka, and Takashi Fuyuki

33rd IEEE Photovoltaic Specialists Conference, (San Diego USA), 2008

[3] "The Investigation of Multicrystalline Si Solar Cells by The Electroluminescence Imaging Techniqe with Different Wavelength Bandpass Filters"

Emi Sugimura, Athapol Kitiyanan, Akiyoshi Ogane, Ayumi Tani, Kenji Hirata, Takashi Saitoh, Tomoaki Hatayama, Hiroshi Yano, and Takashi Fuyuki.

24th European Photovoltaic Solar Energy Conference and Exhibition,

(Hamburg, Germany), 2009

[4] "Control of Doping Depth by Multiple Laser Irradiations for Low-temperature Process of Silicon Solar Cell"

Takashi Saitoh, Kenji Hirata, Akiyoshi Ogane, Athapol Kitiyanan, Emi Sugimura, and Takashi Fuyuki.

19th International Photovoltaic Science and Engineering Conference and Exhibition, (Jeju, Korea), 2009

[5] "Local Analysis of Multi-crystalline Silicon Solar Cells Using Electroluminescence"

Emi Sugimura, Athapol Kitiyanan, Akiyoshi Ogane, Kenji Hirata, Takashi Saitoh, Ayumi Tani, and Takashi Fuyuki

19th International Photovoltaic Science and Engineering Conference and Exhibition, (Jeju, Korea), 2009

[6] "Laser Doping Technique using Continuous Wave Laser in Multi-crystalline Silicon Solar Cell Process"

Mitsuhiro Hasegawa, Kenji Hirata, Takashi Saitoh, Tamaki Takayama, Tomohiro Funatani, Emi Sugimura, Shinichiro Tsujii, Ayumi Tani, Takashi Fuyuki

35th IEEE Photovoltaic Specialists Conference, (Hawai, USA), 2010

[7] "Classification of Defects in Polycrystalline Si by Temperature Dependence of Electroluminescence under Forward and Reverse-biases"

Shinichiro Tsujii, Emi Sugimura, Kenji Hirata, Takashi Saito, Ayumi Tani, Tomoaki Hatayama, Hiroshi Yano, Takashi Fuyuki

35th IEEE Photovoltaic Specialists Conference, (Hawai, USA), 2010

[8] "Laser doping for several types of emitter layer"

Takashi Saitoh, Kenji Hirata, Tamaki Takayama, Mitsuhiro Hasegawa, Tomohiro Funatani, Emi Sugimura, and Takashi Fuyuki

RENEWABLE ENERGY 2010, (Yokohama, Japan), 2010

[9] "The study of defects in multi-crystalline Si solar cells utilizing electroluminescence imaging combining forward and reverse bias conditions"

Emi Sugimura, Shinichiro Tsujii, Kenji Hirata, Takashi Saitoh, Ayumi Tani, and Takashi Fuyuki

RENEWABLE ENERGY 2010, (Yokohama, Japan), 2010

[10] "Distinction of Crystalline Defects by Temperature Dependence of Electroluminescence"

Emi Sugimura, Shinichiro Tsujii, Kenji Hirata, Ayumi Tani, and Takashi Fuyuki

5th World Conference on Photovoltaic Energy Conversion, (Valencia, Spain), 2010

[11] "MDECR Plasma Deposition of Microcrystalline Silicon as An Alternative to RF Capacitive Methods"

Samir Kasouit, Kenji Hirata, Lourent Kroely, Pere Roca i Cabarrocas

5th World Conference on Photovoltaic Energy Conversion, (Valencia, Spain), 2010

[12] "REVEALING SHUNT ORIGINS BY TEMPRERATURE DEPENDENCE OF ELCTROLUMINESCENCE UNDER REVERSE-BIAS"

Emi Sugimura, Shinichiro Tsujii, Souichirou Takamoto, Kenji Hirata, Ayumi Tani, and Takashi Fuyuki

37th IEEE Photovoltaic Specialists Conference, (Seattle, USA), 2011

[13] "Improvement of multi-crystalline silicon solar cell fabricated by Laser Doping Technique Using Continuous Wave Laser"

Hideki Nishimura, Kenji Hirata, Mitsuhiro Hasegawa, Tomohiro Funatani, Tamaki Takayama, and Takashi Fuyuki

37th IEEE Photovoltaic Specialists Conference, (Seattle, USA), 2011

[14] "Investigation of Precursor Layer for Laser Doping Technique in Crystalline Silicon Solar Cell Process"

Takuya Katagiri, Tomohiro Funatani, Kenji Hirata, Hideki Nishimura and Takashi Fuyuki

26th European Photovoltaic Solar Energy Conference and Exhibition, (Hamburg, Germany), 2011

[15] "PRESCRIPTION OF PRECURSOR FILM DEPOSITION FOR LASER DOPING IN CRYSTALLINE SILICON SOLAR CELL PROCESS"

Takuya Katagiri, Tomohiro Funatani, Kenji Hirata, Hideki Nishimura and Takashi Fuyuki

21st International Photovoltaic Science and Engineering Conference and Exhibition, (Fukuoka, Japan), 2011

[16] "IMPROVED ELECTRONIC PROPERTIES OF LASER DOPED EMITTERS BY REDUCING SURFACE ROUGHNESS"

Hideki Nishimura, Kenji Hirata, Mitsuhiro Hasegawa, Takuya Katagiri and Takashi Fuyuki

21st International Photovoltaic Science and Engineering Conference and Exhibition, (Fukuoka, Japan), 2011

[17] "SPATIALLY RESOLVED ELECTROLUMINESCENCE IMAGING OF SHUNT SOURCES IN CRYSTALLINE SILICON SOLAR CELLS"

Emi Sugimura, Sohichiroh Takamoto, Shinichiro Tsujii, Kenji Hirata, Ayumi Tani and Takashi Fuyuki

21st International Photovoltaic Science and Engineering Conference and Exhibition, (Fukuoka, Japan), 2011

[18] "EVALUATION OF SUBSTRATE DEFECTS BY TEMPERATURE DEPENDENCE

OF SPECTROSCOPIC ELECTROLUMINESCENCE"

Sohichiroh Takamoto, Emi Sugimura, Shinichiro Tsujii, Kenji Hirata, Ayumi Tani and Takashi Fuyuki

21st International Photovoltaic Science and Engineering Conference and Exhibition, (Fukuoka, Japan), 2011

[19] "Demonstration of High Channel Mobility in 4H-SiC MOSFETs by Utilizing Phosphorus-Doped Gate Oxide"

Dai Okamoto, Hiroshi Yano, Kenji Hirata, Shinya Kotake, Tomoaki Hatayama, and Takashi Fuyuki

The 2010 Int'l Meeting for Future Electron Devices Kansai, (Osaka, Japan), 2010

[20] "Improved Inversion Channel Mobility in Si-face 4H-SiC MOSFETs by Phosphorus In corporation Technique"

Dai Okamoto, Hiroshi Yano, Kenji Hirata, Shinya Kotake, Tomoaki Hatayama, and Takashi Fuyuki

2010 MRS Spring Meeting, (San Francisco, USA), 2010

Related domestic conferences

[1] "The Study of Defects in Crystalline Si Solar Cells by Electroluminescence Imaging under Reverse Bias Condition"

Athapol Kitiyanan, Marie Buffiere, Ayumi Kawakita, Akiyoshi Ogane, Kenji Hirata, and Takashi Fuyuki

Abstracts of 5th Next Generation Photovoltaic System Symposium, (Miyazaki), 2008

[2] "Crystalline Silicon Solar Cells Fabricated by Continuous Wave Nd:YVO_4 Laser "

Takashi Saitoh, Kenji Hirata, Akiyoshi Ogane, Yukiharu Uraoka, and Takashi Fuyuki

Abstracts of the 56th Spring Meeting of the Japan Society of Applied Physics and Related Societies, (Tsukuba), 2009, in Japanese

[3] "Spectroscopic Electroluminescence in Multicrystalline Silicon Solar Cells Characteristics"

Emi Sugimura, Athapol Kitiyanan, Kenji Hirata, Akiyoshi Ogane, Ayumi Tani, and Takashi Fuyuki

Abstracts of the 56th Spring Meeting of the Japan Society of Applied Physics and Related Societies, (Tsukuba), 2009, in Japanese

[4] "Impurity Doping by Multiple Irradiation with UV Laser in Crystalline Silicon Solar Cell Fabrication Process"

Takashi Saitoh, Kenji Hirata, Akiyoshi Ogane, Athapol Kitiyanan, and Takashi Fuyuki

Abstracts of 6th Next Generation Photovoltaic System Symposium, (Niigata), 2009

in Japanese

[5] "Depth Analysis by Electroluminescence for Crystalline Silicon Solar Cells"

Emi Sugimura, Athapol Kitiyanan, Takashi Saitoh, Kenji Hirata, Akiyoshi Ogane, Ayumi Tani, and Takashi Fuyuki

Abstracts of 6th Next Generation Photovoltaic System Symposium, (Niigata), 2009

in Japanese

[6] "Decrease of Interface Trap Density by Phosphorous Introduced into 4H-SiC MOS Interface"

Dai Okamoto, Hiroshi Yano, Kenji Hirata, Tomoaki Hatayama, and Takashi Fuyuki

Proceedings of IEICE SDM, (Ikoma), 2009 in Japanese

[7] "Fabrication of 4H-SiC MOSFET with Improved Channel Mobility by phosphorous introduced into SiO_2/SiC Interface"

Dai Okamoto, Hiroshi Yano, Kenji Hirata, Shinya Kotake, Tomoaki Htayama, and Takashi Fuyuki

18th Professional Group of SiC and Related Wide Bandgap Semiconductors Annual

Meeting, (Kobe), 2009 in Japanese

[8] "Comparison of Electroluminescence image under Forward and Reverse Biases in Crystalline Silicon Solar Cells"

Emi Sugimura, Shinichiro Tsujii, Kenji Hirata, Takashi Saitoh, Ayumi Tani, and Takashi Fuyuki

Abstracts of the 57th Spring Meeting of the Japan Society of Applied Physics and Related Societies, (Hiratsuka), 2010, in Japanese

[9] "Evaluation of Defects by Temperature Dependence of Electroluminescence under Reverse Bias"

Shinichiro Tsujii, Emi Sugimura, Kenji Hirata, Ayumi Tani, and Takashi Fuyuki

Abstracts of 7th Next Generation Photovoltaic System Symposium, (Kitakyusyu), 2010 in Japanese

[10] "Formation and Optimization of Selective Emitter Structure using UV Laser"

Tamaki Takayama, Kenji Hirata, Takashi Saitoh, Mitsuhiro Hasegawa, Tomohiro Funatani, and Takashi Fuyuki

Abstracts of 7th Next Generation Photovoltaic System Symposium, (Kitakyusyu), 2010 in Japanese

[11] "Optimization of Laser Doping Technique by Dopant Film Control"

Tomohiro Funatani, Kenji Hirata, Takashi Saitoh, Tamaki Takayama, Mitsuhiro Hasegawa, and Takashi Fuyuki

Abstracts of 7th Next Generation Photovoltaic System Symposium, (Kitakyusyu), 2010 in Japanese

[12] "Development of Laser Doping Technique for Multicrystalline Silicon Solar Cell Fabrication Process"

Mitsuhiro Hasegawa, Kenji Hirata, Takashi Saitoh, Tamaki Takayama, Tomohiro Funatani, and Takashi Fuyuki

Abstracts of 7th Next Generation Photovoltaic System Symposium, (Kitakyusyu), 2010 in Japanese

[13] "Laser Doping in Room Temperature for Multicrystalline Silicon Solar Cells Fabrication"

Mitsuhiro Hasegawa, Kenji Hirata, Tamaki Takayama, Tomohiro Funatani, and Takashi Fuyuki

Proceedings of IEICE SDM, (Kyoto), 2009 in Japanese

[14] “Optimization of Laser Doping Technique by Dopant Film Control in Crystalline Silicon Solar Cells”

Tomohiro Funatani, Kenji Hirata, Tamaki Takayama, Mitsuhiro Hasegawa, and Takashi Fuyuki

Proceedings of IEICE SDM, (Kyoto), 2009 in Japanese

[15] “Laser doping process in multi-crystalline silicon solar cells”

Hideki Nishimura, Kenji Hirata, Mitsuhiro Hasegawa, Tomohiro Funatani, Tamaki Takayama, and Takashi Fuyuki

Abstracts of the 58th Spring Meeting of the Japan Society of Applied Physics and Related Societies, (Kanagawa), 2011 in Japanese

[16] “Correlation between Surface Roughness and Electrical Properties of Laser Doped Emitter in Multicrystalline Silicon Solar Cells”

Hideki Nishimura, Kenji Hirata, Mitsuhiro Hasegawa, Takuya Katagiri, and Takashi Fuyuki

Abstracts of 8th Next Generation Photovoltaic System Symposium, (Gifu), 2010 in Japanese

[17] “Influence of Phosphorous Concentration in PSG Film for Laser Doped Emitter”

Takuya Katagiri, Tomohiro Funatani, Kenji Hirata, Hideki Nishimura, and Takashi Fuyuki

Abstracts of 8th Next Generation Photovoltaic System Symposium, (Gifu), 2010

in Japanese

[18] "Evaluation of Defects in Poly Crystalline Silicon by Temperature Dependence of Spectroscopic Electroluminescence"

Sohichiroh Talamoto, Shinichiro Tsujii, Emi Sugimura, Kenji Hirata, Ayumi Tani, and Takashi Fuyuki

Abstracts of 8th Next Generation Photovoltaic System Symposium, (Gifu), 2010

in Japanese

[19] "Local Laser Doping into Silicon at Room Temprature and Application to Solar Cells"

Takashi Fuyuki and Kenji Hirata

76th Annual Meeting of Japan Laser Processing Society, (Tokyo), 2011 in Japanese (Invited)

About the Author

Personal Data

Name: Kenji Hirata

Data of birth: August 30th in 1984, Ikoma city in Nara prefecture, Japan

Nationality: Japan

E-mail: hi-kenji@ms.naist.jp

Education

2000-2005	Associate course study at Department of Electrical Engineering in Nara National Collage of Technology Associate thesis on ***Development of Lithium-ion Secondary Battery using High Ionic Conducting Gel Electrolytes***
2005-2007	Bachelor course study at Advanced course of Electronic and Information Engineering in Nara National collage of Technology Bachelor thesis on ***Application to the Dye-sensitized Solar Cells using High Ionic Conducting Gel Electrolytes***
2007-2009	Master course study at Graduate school of Materials Science in Nara Institute of Science and Technology (NAIST) Master thesis on ***Development of Laser Doping Technique in Crystalline Silicon Solar Cell Process***

2009-2012	Doctor course study at Graduate School of Materials Science in Nara Institute of Science and Technology (NAIST) Ph. D. thesis on ***Development of Laser Doping at Room Temperature for Crystalline Silicon Solar Cell Fabrication Process***
2009-2010	Overseas study at Laboratoire de Physique des Interfaces et Couches Minces (LPICM), École Polytechnique, France

Research Interests

- Technologies and electronic properties of laser doping for crystalline silicon solar cell application
- Technologies for the improvement of photovoltaic properties of crystalline silicon solar cells
- Laser processing for micro and nano device fabrication

Language

Japanese (Native), English (Limited working proficiency)

Financial Support Acquirement

- Exemption from returning of scholarship during master course from Japan Student Services Organization (Half) (2009)
- International research activity support by Foundation of Nara Institute of Science and Technology (2010), (2011)
- International research activity support by Kansai Research Foundation for Technology Promotion (2010)